# FACILITATORY NEURAL DYNAMICS FOR PREDICTIVE EXTRAPOLATION

A Dissertation

by

HEE JIN LIM

Submitted to the Office of Graduate Studies of
Texas A&M University
in partial fulfillment of the requirements for the degree of

DOCTOR OF PHILOSOPHY

August 2006

Major Subject: Computer Science

# FACILITATORY NEURAL DYNAMICS FOR PREDICTIVE EXTRAPOLATION

A Dissertation

by

HEE JIN LIM

Submitted to Texas A&M University
in partial fulfillment of the requirements
for the degree of

DOCTOR OF PHILOSOPHY

Approved as to style and content by:

| | |
|---|---|
| Yoonsuck Choe<br>(Chair of Committee) | Nancy M. Amato<br>(Member) |
| Dezhen Song<br>(Member) | Takashi Yamauchi<br>(Member) |
| Won-jong Kim<br>(Member) | Hank Walker<br>(Head of Department) |

August 2006

Major Subject: Computer Science

# ABSTRACT

Facilitatory Neural Dynamics for
Predictive Extrapolation. (August 2006)
Heejin Lim, B.S., Keimyung University;
M.S., Keimyung University
Chair of Advisory Committee: Yoonsuck Choe

Neural conduction delay is a serious issue for organisms that need to act in real time. Perceptual phenomena such as the flash-lag effect (FLE) suggest that the nervous system may have mechanisms to compensate for delay. In motion FLE, the position of a moving object is perceived to be ahead of a brief flash when they are actually co-localized. Motion extrapolation hypothesis suggests that FLE may be due to an extrapolation process in the nervous system that counters the effects of neural conduction delay. However, the precise neural mechanism for extrapolation has not been fully investigated.

One potential neural mechanism for delay compensation can be found in dynamic synapses. Dynamic synapses, facilitating or depressing, have drawn much attention due to their implicated functional role in memory and temporal information processing. The main hypothesis of this dissertation is that facilitating synapses, with their dynamic sensitivity to the rate of change in input, may also play an important role in compensating for neural delay. To test this hypothesis, I developed the Facilitatory Activation Model (FAM), a model based on firing rate neurons, and tested it in motion FLE. The computational results were consistent with human data. The model was further extended to account for a peculiar behavior not fully explainable by extrapolation alone: the lack of FLE at motion termination or motion reversal points.

I adopted the idea of Kalman smoothing, which resulted in an accurate match with human data, while preserving the delay compensation property (which is not the case for original Kalman smoothing).

In order to ground the computational model on firm neurophysiological ground, I extended FAM by incorporating a spike-based model of facilitating synapses by Markram and colleagues. The new model was tested in the luminance FLE domain. Unlike the Markram et al.'s model, the spike-based FAM was able to model extrapolation in both increasing and decreasing luminance conditions. The model also included an analog of smoothing, in the form of backward masking, where an on-going facilitation (or extrapolation) process can be abruptly terminated by a stimulus offset signal. To model more complex FLEs such as orientation FLE, I extended the model to include facilitation across multiple neurons. For this to be successful, the connection weights need to be setup so that facilitation can reach only a small number of specific target neurons. Spike-timing-dependent plasticity (STDP) is ideal for this task, so it was used to learn the appropriate connections weights. The resulting multi-neuron FAM was able to express behavior consistent with orientation FLE.

The idea was further tested in an engineering control task. The firing-rate FAM was tested in a 2D pole-balancing problem, modified to include delay in the sensory input. A recurrent neural network with facilitatory neural dynamics was trained via neuroevolution. The results were compared against a network without any single-neuron dynamic, and another one with decaying dynamic. The results suggested that facilitating activity greatly enhances control performance under various forms of input delay. The experimental framework was used to test the robustness of the model under increasing delay, and also under input blank-out conditions, showing consistent results with the original experiment.

The main contribution of this dissertation is that it showed an interesting link

between (1) the organism-level problem of delay compensation, (2) perceptual phenomenon of FLE, (3) computational function of extrapolation, and (4) neurophysiological mechanisms of facilitating synapses (and STDP). The results are expected to shed new light on real-time processing in the brain, and help better understand specific neural processes (such as facilitating synapses). Broader implications of the work include clinical applications such as early detection of autism and dyslexia, where motion-related perceptual deficits are found.

To my parents, Kwangkil Lim and Haeja Lee, and my husband

Page

## ACKNOWLEDGMENTS

First of all, I would like to thank my advisor Yoonsuck Choe for his continuous interest, support, and encouragement throughout this research. His advice on research and writing was essential to the completion of this dissertation and has taught me innumerable lessons and insights on the workings of academic research. I would also like to thank my committee members Dr. Nancy M. Amato, Dr. Dezhen Song, Dr. Takashi Yamauchi, and Dr. Wong-jong Kim for their keen interest, suggestions, and encouragement. I am grateful of Yingwei Yu for the numerous discussion and suggestions to my research and for his friendship as a lab colleague. I am also grateful of Dr. Paul D. Lyons for his suggestion in clinical perspective of my research. I would like to thank Dr. Faustino Gomez and Dr. Risto Miikkulainen for making their ESP implementation available to me. Without which, my research would not have been possible. I would also like to thank David Mayerich and Andrew Jones for initial implementation of the STDP model. I would also like to thank the members of Neural Intelligence Lab for the intriguing discussions which help broaden my research perspective. I am also grateful of the Department of Computer Science at Texas A&M for providing me teaching assistantship and scholarship through which I could get invaluable experience as well as financial support during my study. The scholarship was awarded in honor of Dr. Ronnie Ward, a distinguished former student of our department, to whom I am grateful. My sincerest thanks go to my parents, who have been loving, patient, and supportive throughout my life, and to my husband Sangeun Kim for his love, patience, and continuous encouragement. Without his sacrificing love, I could not have accomplished this work. I would like to thank my brothers, Hoeun Lim and Hoyoung Lim, and their families, for their brotherly affection, support, and absolute confidence in me, and the rest of my (extended) family

Page

for their love and support. Also, I am thankful to my kids, Chaeyoung, Sungtaek, and Sunghyun for their love and cheer.

TABLE OF CONTENTS

CHAPTER Page

# LIST OF TABLES

# LIST OF FIGURES

FIGURE Page

FIGURE Page

FIGURE Page

FIGURE Page

FIGURE Page

FIGURE Page

FIGURE Page

FIGURE Page

FIGURE Page

FIGURE Page

FIGURE Page

FIGURE Page

FIGURE Page

FIGURE Page

FIGURE Page

FIGURE Page

FIGURE Page

# CHAPTER I

# INTRODUCTION

The temporal aspect of neuronal signaling has been studied widely. One important question is how the brain can overcome long neural transmission delay within various parts of its system. For example, in the macaque, the neural latency (from stimulus onset to the prefrontal cortex) ranges from 100 ms to 130 ms [1], thus putting the internal clock steadily behind the environmental clock. How can the brain function in real-time in spite of such delays? Investigation of delay compensation mechanism and its neural implementation may give us fundamental insights into the operations in the brain.

## I.1 Research problem: Delay in the neural system

Neuron is a primary computational unit in the nervous system. It generates and sends electronic signals to other neurons through axonal conduction. In such a signaling scheme in a living organisms, delay is unavoidable since there are physical limits in the speed of signal transmission. For example, experiments with macaque monkeys showed that the mean latency from the onset of visual stimulus to the spike arrival in the macaque's finger muscle can be as large as 260 ms (Fig. 1) [1]. Also, it takes at least 50 ms to 70 ms from the retina to the early cortical visual areas (for V1 and V4, respectively) for the first spike to arrive (Fig. 2) [2].

Such a delay can cause serious problems as shown in Fig. 3. During the time a signal travels from a peripheral sensor (such as the photoreceptor) to the central nervous system (e.g. the visual cortex), a moving object in the environment can cover

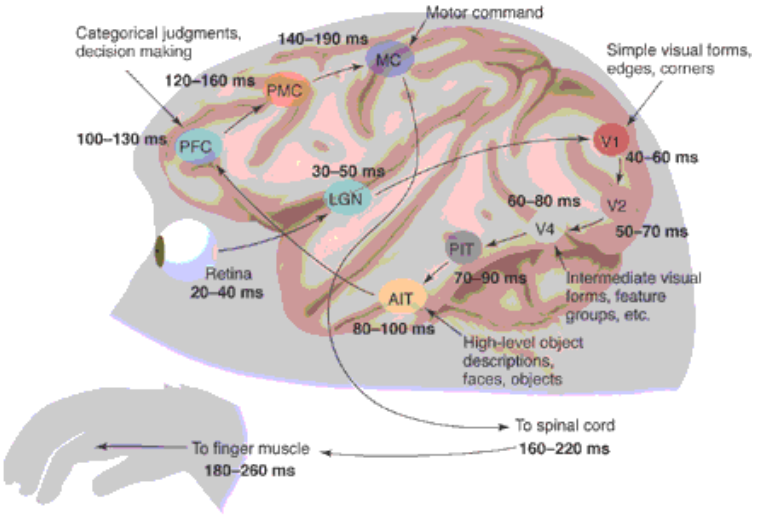


Fig. 1. **Delay in perception.** Neural latencies in various areas in the macaque's brain are shown. It depicts a plausible route between the retina and the muscles of the hand during a categorization task. Visual stimulus captured by the retina is transduced into neural spikes and relayed by the lateral geniculate nucleus of the thalamus (LGN) to V1 (the primary visual cortex). After processed in V2 and V4 of the ventral visual pathway, the neural signals are transferred to the posterior and anterior inferior temporal cortex (PIT and AIT), which contain neurons that respond specifically to certain objects. After some decision is made at the prefrontal cortex (PFC), the neural signals are passed to the pre-motor cortex (PMC) and primary motor cortex (MC). Finally, the motor neurons of the spinal cord receive signal from MC and stimulate the neurons in finger muscle for action. Two numbers (in milliseconds) are given for the earliest response time and mean latency respectively. (Adapted from [1].)

a significant distance, which can subsequently lead to critical errors in the motor output which was initially based on that input. For example, the neural latency between visual stimulus onset and the motor output can be no less than 100 ms up to a couple of hundred milliseconds [1]. At that rate, an object moving at 40 mph can cover about 9 m in 500 ms (Fig. 3*b*), a very large distance considering the size of most vertebrates.

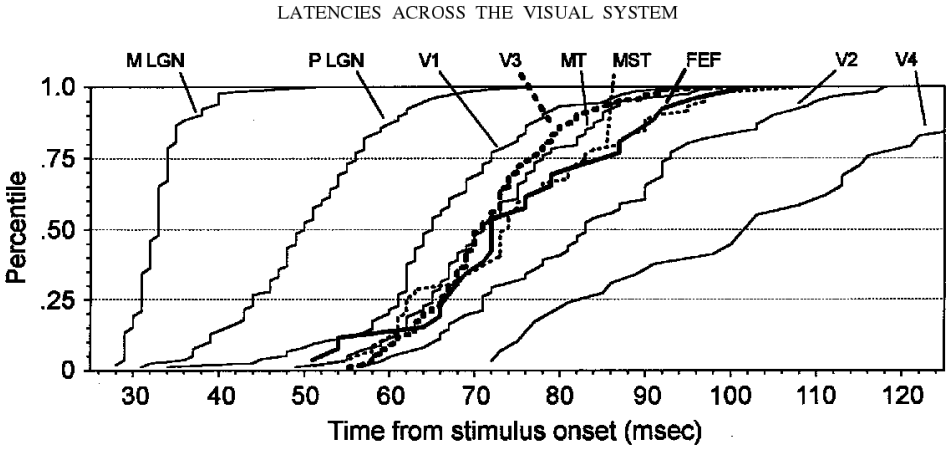


Fig. 2. **Time from stimulus onset.** Cumulative distributions of visually evoked onset response latencies are shown. The $x$-axis represents the time taken from the stimulus presentation and the $y$-axis the percentile of neurons that have begun to respond. For example, about 100 ms are needed for the 50 % of neurons in V4 to start to respond to visual stimulus. (Adapted from [2].)

However, the problem can be overcome if the central nervous system can take into account the neural transmission delay $\Delta t$ and generate action based on the estimated current state $S(t + \Delta t)$ at time $t + \Delta t$, rather than that in its periphery at time $t$, $S(t)$ (Fig. 3$c$). Such a compensatory mechanism can be built into the system at birth, but such a fixed solution is not feasible because the organism grows in size during development, resulting in a gradual increase in delay [11]: For example, consider that the axons are stretched to become longer during growth. How can the nervous system compensate for such a delay at the same time maintaining the internal state to be in synchrony with the present environmental state in real time? This is the main research question to be addressed in this dissertation.

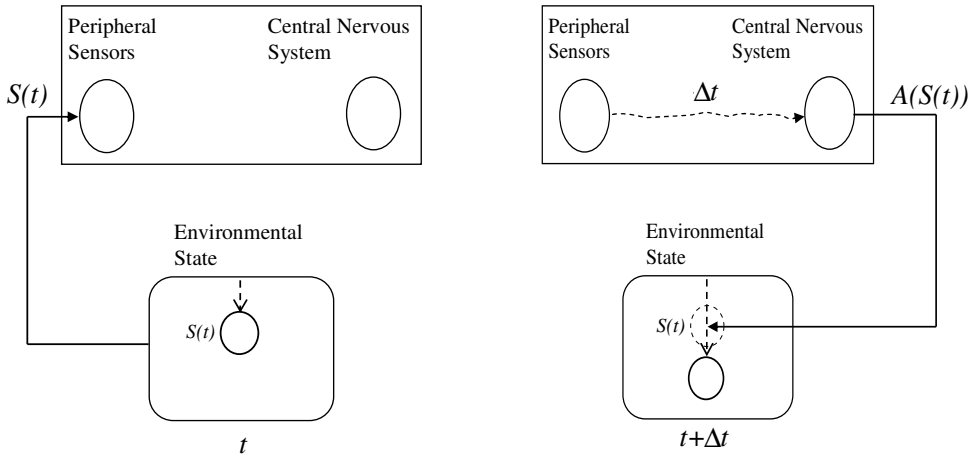


(*a*) Initial state (time $t$) (*b*) No extrapolation (time $t + \Delta t$)

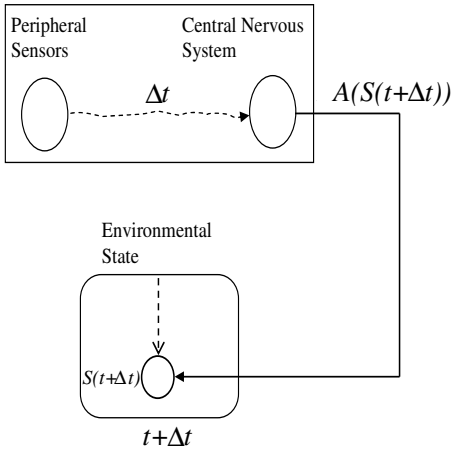


(*c*) With extrapolation (time $t + \Delta t$)

Fig. 3. **Interaction between agent and environment under internal delay.** (*a*) The state $S(t)$ of a moving object (circle) in the environment is received at the sensors in an agent (e.g., an animal) at time $t$. (*b*) Delay ($\Delta t$) in the central nervous system causes error in the resulting action $A(S(t))$, since state $S(t)$ is not extrapolated. (*c*) No error results if the action is based on a predicted (or extrapolated) state of the object, $S(t + \Delta t)$.

### I.2 Potential solution: Extrapolation

Psychophysical experiments with flash lag effect suggested that extrapolation may be in use in the nervous system. Flash-lag effect (FLE) refers to a visual phenomenon in which the position of a moving object is perceived to be ahead of a briefly flashed

object when they are actually co-localized [12, 13]. Fig. 4 and 5 illustrate examples of flash-lag effect. Flash-lag effect has been found in various sensorimotor modalities such as motor performance [14], auditory perception [15]; and in various visual modalities such as color, pattern entropy, and luminance [16]. The ubiquity of FLE suggests that the central nervous system may have a general mechanism to overcome the discrepancy between events in internal brain time and those in external world time, caused by delay in neural signal transmission [17].

A potential explanation for FLE is the motion extrapolation model [13, 18, 19]. (More details are to be found in Sec. II.1.) Given that nervous systems have conduction delay, delayed object's location data have to be extrapolated so that the perceived location of the object at a given moment is close to that in the environment, at that same instant. According to the motion extrapolation hypothesis, FLE is caused by such a delay compensation mechanism implemented in our nervous system. In spite of the limitation of extrapolation model addressed in [3], the model has more desirable properties, such as: (1) without an accompanying flash, a clear localization error in the direction of movement is observed [20, 21], which can be interpreted as some neural mechanisms being used for the perception of the moving object itself; (2) with a blurned moving object, humans observe overshoot (i.e., object appears ahead of its physical location) at the motion terminating point [22]. Thus, the limitation of extrapolation can be weaker than initially thought; and (3) through extrapolation, accuracy of perception is increased. With such a mechanism, the living organism can live in the present not in the past [23]. The limitation can be overcome computationally and neurophysiologically as well [24] (Sec. III.3 and Sec. IV.3 will discuss in detail). A potential answer to the main research question is that the nervous system employs extrapolative mechanisms to overcome problems associated with delay. So far, the precise neural mechanism of such an extrapolative process has not been fully

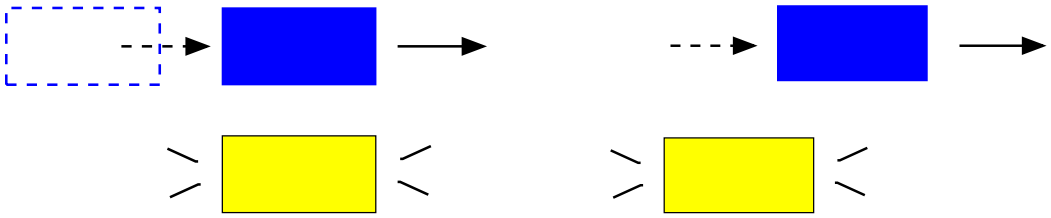

(*a*) Physical (*b*) Perceived

Fig. 4. **Motion flash-lag effect.** Motion flash-lag effect is illustrated. (*a*) A moving object (blue rectangle) is physically aligned with a flashed object (yellow rectangle) at the moment of flash. (*b*) The flashed object appears to be lagging behind the moving object at the time of perception.

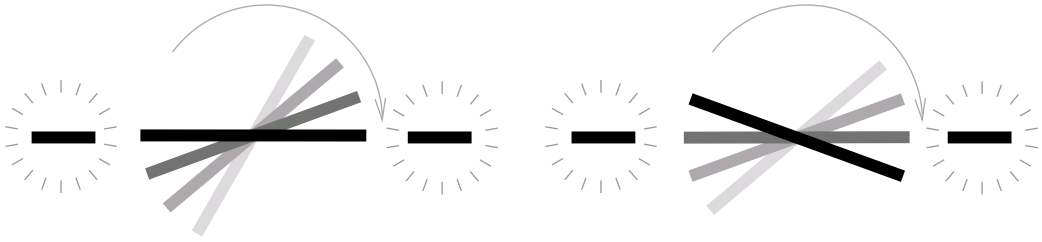

(*a*) Physical (*b*) Perceived

Fig. 5. **Orientation flash-lag effect.** Orientation flash-lag effect is illustrated. (*a*) Gray scale indicates bar orientation over time (black = present, lighter = farther into the past). The two short flanking bars are flashed when the rotating bar is horizontal. (*b*) The rotating bar is perceived to be tilted in the direction of motion.

investigated, which will be the main focus of this dissertation.

## I.3 Approach

What could be the neural basis of extrapolation? It is possible that recurrently connected networks of neurons in the brain can carry out extrapolation, since recurrence makes available the history of previous activations [25, 26], based on which extrapolated activation can be generated. However, such an approach alone may not be sufficient to effectively compensate for neural delay since the evolving dynamics of the recurrent neural network may not be fast enough. The recurrent connections themselves may introduce further delay.

For fast extrapolation, the mechanism may have to be implemented at a single-neuron level. One possible mechanism for such a neuron-level extrapolation is that of facilitating synapses. Facilitating synapses have been found at a single neuron level, where membrane potential dynamics show a dynamic sensitivity to the changing input. Previously, facilitating (or depressing) synapses have been studied in the context of memory (e.g., sensitization and habituation) [27, 28] or temporal information processing [29, 4, 30, 31, 32]. The main hypothesis of this dissertation is that such facilitatory neural activities can play an important role in delay compensation by serving an extrapolatory function.

My research aims at building a biologically plausible neural model for the compensation of neural transmission delay. To test how facilitatory neural activity in single neurons can ensure real-time processing under internal and external delay conditions, I derived neuron models from two perspectives: (1) computational and (2) biological.

From the computational perspective, *facilitatory activation model* (FAM) was developed. With that, facilitatory neural activity can be represented by real-valued firing rate, where extrapolation can be analyzed in formal terms. The model was

extended to FAM with smoothing, to address the shortcoming of the extrapolation model, and was tested in the motion reversal flash-lag paradigm [3, 5], showing that various flash-lag effects can be explained in terms of delay compensation.

From the biological perspective, a spiking neuron model was developed to ground the computational model on a biological foundation. For this task, I extended the dynamic facilitating synapse model by Markram and colleagues [4, 29] and evaluated the model in the luminance flash-lag effect domain [16].

Facilitatory neural activity at a single-neuron level alone cannot explain other flash-lag illusions such as orientation FLE, where a single neuron cannot represent the full range of feature dimensions. To address this issue, I extended the spike-based facilitation model to include multiple neurons, and allowed facilitation to go across neurons. I tested cross-neuron facilitation combined with spike-timing dependent synaptic plasticity (STDP) and evaluated the model in the orientation flash-lag effect domain. Neurophysiological experiments have shown that STDP changes the synaptic weight between two neurons when they fire together within a small time interval [33, 34]. Such a basic principle forced initially symmetric weights to evolve to have directionality, and facilitating dynamics provided extra influence in the direction of input rotation. With these mechanisms, the model was able to implement an extrapolative function that requires multiple neurons.

It is an interesting question whether the approach outlined above can be applied in tough real-world control applications. To test this, the *facilitatory activation model* was applied to a modified 2D pole-balancing problem which included sensory delays. In this domain, I tested the behavior of recurrent neural networks with facilitatory neural dynamics, trained via neuroevolution. Analysis of the performance and the evolved network parameters showed that, under various forms of delay, networks utilizing extrapolatory dynamics are at a significant competitive advantage compared

to networks without such dynamics. It turned out that a proper amount of extrapolation based on the facilitating activation (a form of memory) can significantly help overcome delay while decaying activity (another form of memory) does not contribute to delay compensation.

Another question that is relevant to biology is, how can the nervous system cope with the increase in neural delay. Although certain tasks such as synchronization over a delay line can be achieved via Hebbian learning [35], little is known about how information content can be delivered over different delay lines in a timely manner. To test whether facilitatory activity can help counteract increasing neural delay, I tested the *facilitatory activation network* under increasing delay. The network with facilitatory dynamics showed a slower degradation in performance compared to other controllers as the delay is increased. Also, to test the ability of facilitatory dynamics to deal with uncertainty in the external environment, I conducted blank-out test where the input signals were blocked for a certain time period. Input blank-out experiments in pole-balancing tasks suggested that the delay compensation mechanisms that have evolved to deal with internal delay can be directed outward to handle environmental uncertainty.

In sum, facilitatory (or extrapolatory) dynamics in a single-neuron (or multiple-neuron) level serves as the main approach in this dissertation. With this mechanism, the brain can function in real time, and, at the same time, cause visual illusions such as the flash-lag effect. Furthermore, the biologically inspired delay compensation model can be applied to engineering domains where sensory delays in the system can be overcome by recurrent neural networks with facilitatory activity.

## I.4 Outline of the dissertation

This dissertation is organized into four parts:

- Introduction and Background
  - **Chapter I** and **Chapter II**
- Models and Results
  - Computational Model and Results: **Chapter III**
  - Spike-Based Single-Neuron Model and Results: **Chapter IV**
  - Spike-Based Multi-Neuron Model and Results: **Chapter V**
- Application to Real-Time Control
  - **Chapter VI**
- Discussion and Conclusion
  - **Chapter VII** and **Chapter VIII**

In **Chapter II**, I will give a review of the flash-lag effect; the merits and limitations of the extrapolation model; and facilitating synapses.

In **Chapter III**, I will suggest *facilitatory activation model*, a biologically plausible extrapolation model, and test the model in the motion flash-lag effect domain.

In **Chapter IV**, I will extend the facilitatory activation model into a spike-based facilitating-synapse model and test it in the luminance flash-lag effect domain. Also, to explain the absence of flash-lag effect in motion termination (or change) condition, backward masking mechanism will be applied to the facilitatory activation model.

In **Chapter V**, I will extend the spike-based facilitation model into a cross-neuronal facilitation model. With this, we can explain flash-lag effects which include

spatial changes in the stimulus properties that are not representable by a single neuron. I will provide details of the model and how cross-neuronal facilitation can be implemented by combining it with spike-timing-dependent plasticity (STDP), and present experimental results with orientation flash-lag effect.

In **Chapter VI**, I will apply the facilitatory activation model to real time control. The model will be tested in a modified 2D pole-balancing problem which includes sensory delays. Within this domain, I will test the behavior of recurrent neural networks with facilitatory neural dynamics, trained via neuroevolution. I will examine the capability of the facilitatory activation model under increasing neural delay and in input blank-out test; and evaluate the possibility of predictive ability emerging from delay compensation mechanisms.

In **Chapter VII**, I will explain the contributions of this dissertation; discuss the relationship between my work and other related works; discuss issues that have emerged from my work; and present future work. In **Chapter VIII**, finally, I will conclude with a brief summary.

# CHAPTER II

# BACKGROUND

In this chapter, I will review flash-lag effect as a psychophysical evidence for extrapolation and discuss the limitation of the extrapolation model as observed in motion reversal flash-lag effect. Also, as a potential neural basis of extrapolation, facilitating synapses will be introduced.

## II.1 Evidence for extrapolation: Flash-Lag Effect (FLE)

Flash-lag effect (FLE) occurs in visual perception when the state of a changing stimulus such as luminance [16], position of a moving object [12], or orientation of a rotating object [13] is misperceived. For example, orientation FLE shows that the rotating bar in the center is perceived to be tilted at the time of flash of the flanking bars when in fact it is horizontally aligned with the flanking bars. (See the Fig. 5 in Chap. I for a better understanding.) Since its initial discovery [36], flash-lag effect has drawn great interest because such a peculiar visual phenomenon can help reveal the neural mechanisms underlying visual perception, especially relating to time.

As introduced in Chap. I, a prominent hypothesis for FLE is motion extrapolation [13, 18, 19]: To overcome neural delay and to have accurate perception, the nervous system may carry out extrapolation. Thus, FLE may be the result of a delay compensation mechanism.

Besides motion extrapolation, several other hypotheses for FLE have been explored. Differential latency model [3, 37] proposes that flash-lag effect occurs simply because the visual system responds with shorter latency to moving stimuli than to

flashed, stationary stimuli. However, recent experimental results from auditory and cross-modal flash-lag effect indicated that differential latency model may be inaccurate: The effect of auditory FLE was found to be much stronger than visual FLE, whereas neural latency in the auditory system are known to be much shorter than those in the visual system [15, 17]. This is counter to the prediction of the differential latency model.

On the other hand, attention hypothesis [38] assumes that flash acts as a "pull" cue to grab the observer's attention away from the continuously changing stimulus. However, flash-initiated-cycle experiment demonstrated that if the stimuli were turned on simultaneously (i.e., attention is not only pulled toward the flash but also toward the object with the onset of motion), observers still perceived that the continuously moving disk leads the flashed disk [16].

Temporal averaging [39] and postdiction model [40] proposed that the visual system collects position information over time and estimates the position based on the integrated signals. Under this model, the difference between the estimated mean position of the moving object and the flashed one is supposed to produce the flash-lag effect. However, precisely how the temporal averaging is set up and which neural mechanisms are responsible have not yet been clearly specified, leading to considerable debate [41].

Among these models, the extrapolation model has more desirable properties [20, 22, 21, 23]. (See Sec. I.2 for specific details.) The model suggests that the perceptual effect demonstrated in various sensorimotor modalities indicate that the human nervous system performs extrapolation at several different levels. With this, a living organism can align its internal perceptual state with the environmental state with high temporal accuracy. Fig. 6 and 7 illustrate motion flash-lag effect in view of the extrapolation hypothesis. In Fig. 6, the state $S(t)$ of a moving object (blue rectangle)

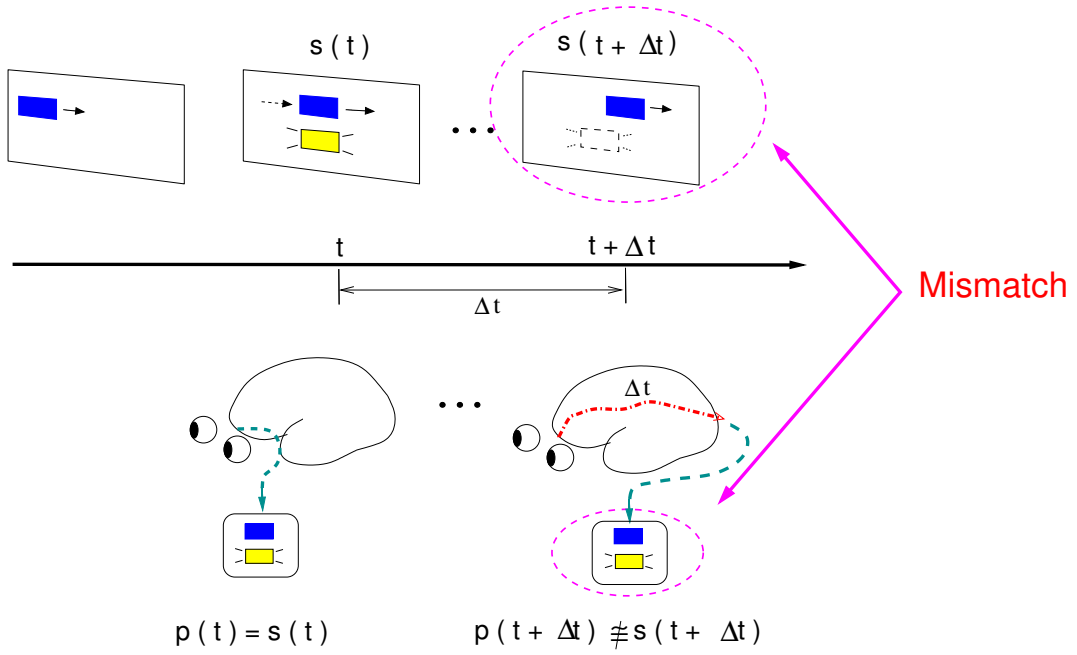


Fig. 6. **No Flash-lag effect without delay compensation.** In view of motion extrapolation, flash-lag effect does not occur if delay is not compensated for. The state $S(t)$ of a moving object (blue rectangle) which is physically aligned with a flashed object (yellow rectangle) in the environment is received at the sensors in a natural agent at time $t$. The state information $S(t)$ takes time $(= \Delta t)$ to travel from the sensors to the central nervous system of the agent. If the delay is not taken into consideration, the perceived location of the moving object based on state $S(t)$ will be mismatched with that of the external state at the time of perception. Because the perceived location of the moving stimulus and the flashed stimulus is aligned, there is no Flash-lag effect.

which is physically aligned with a flashed object (yellow rectangle) in the environment is received at a peripheral sensor (such as in the retina) at time $t$. The state information $S(t)$ takes time $(= \Delta t)$ to travel from the sensor to the central nervous system in the organism. If the delay is not taken into consideration, the perceived location of the moving object based on state $S(t)$ will be outdated by time $t + \Delta t$ (Fig. 6). In that case, a mismatch occurs between perceived state and real environmental state at the time of perception. There will be no flash-lag effect because the location in-

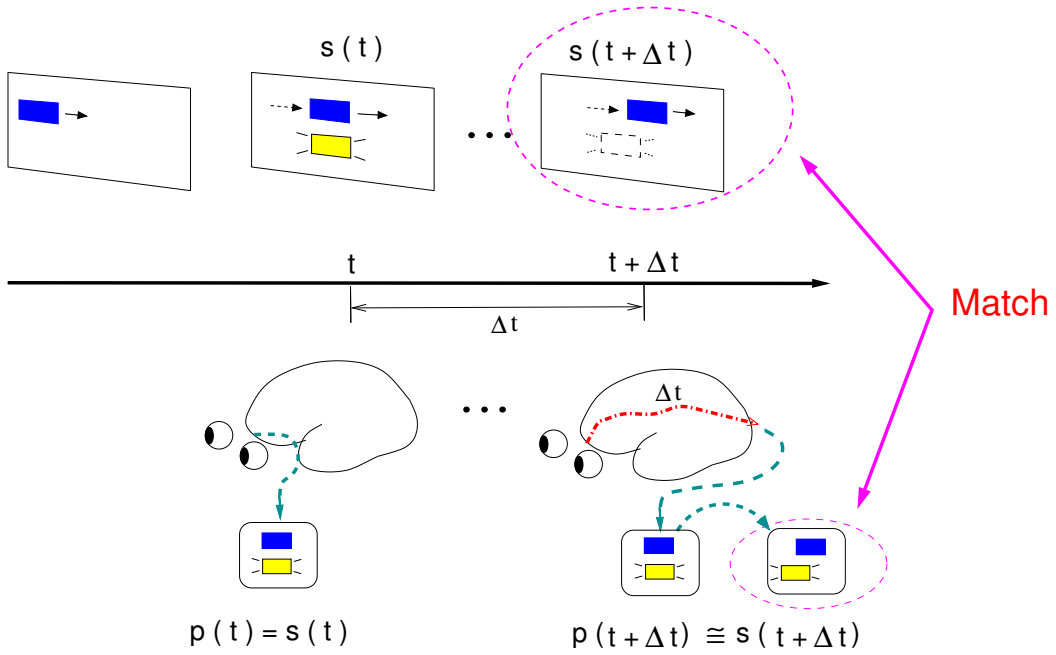


Fig. 7. **Flash-lag effect with delay compensation.** In view of motion extrapolation, flash-lag effect occurs if delay is compensated. That is, if the perception for the moving object is corrected based on a predicted (or extrapolated) state of the object at $t + \Delta t$, then the perceived location becomes close to the actual environmental state at $t + \Delta t$ (i.e., achieving match with the environmental state). The flashed object is perceived at a fixed location because the abrupt flashing stimulus has no previous history to extrapolated from. This discrepancy caused flash-lag effect.

formation of the moving stimulus and that of the flashed stimulus are the same. On the other hand, as shown in Fig. 7, if the received object location is corrected based on a predicted (or extrapolated) state of the moving object for $t + \Delta t$, i.e., $S(t + \Delta t)$, then the extrapolated object location will be closer to the actual environmental state (i.e., a match occurs between the perceived location and the environmental location of the moving object) at the time of perception (Fig. 7). The flashed object, on the contrary, is perceived without extrapolation because the abrupt flashing has no previous history to be extrapolated from. Thus, visual displacement occurs between the

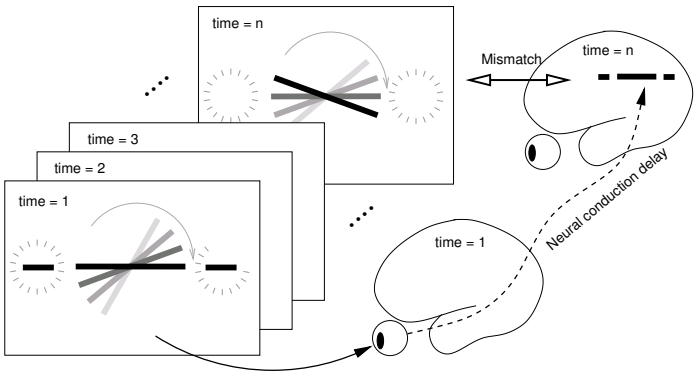


Fig. 8. **Neural delay causing mismatch in internal and external state.** The rotating bar (black bar in the middle) is horizontal when the flanking bars are flashed (time = 1). The same input is received at the retina (bottom right). The input takes time $n - 1$ to reach higher visual areas (top right). If the delay is not taken into consideration, the perceived orientation of the rotating bar will be misaligned with the environmental state at time = $n$, since the bar continues to rotate during the $n - 1$ time period.

moving bar and the flashed bar due to such a discrepancy in extrapolation.

Orientation FLE can be explained in the same manner. As shown in Fig. 8, the locations of flanking bars (located at the two ends of the bar in the middle) and a rotating bar in the middle are captured at the retina (time = 1). With neural conduction delay of $n - 1$, the neural information reaches the visual cortex. In the meanwhile, the rotating bar in the environment further rotates to a different orientation. Without extrapolation, the rotating bar is perceived to be aligned with the flanking bars (i.e., no flash-lag effect). If extrapolation is carried out, the neural information is corrected (i.e., tilted to the rotating direction) to be in synchrony with the present environmental state (i.e., flash-lag effect occurs).

## II.2 Limitation of the extrapolation model

The motion extrapolation model, however, has some limitations. For example, humans do not perceive displacement between a flashed object and a moving object when the moving object stops or reverses its direction of motion at the time of the flash [3]. In motion reversal tests, as briefly sketched in Fig. 9, the direction of motion of a vertically translating bar is reversed at a random time and location. In the meanwhile, a flash could appear at various time points before or after motion reversal. The puzzling phenomena happening around the motion reversal are illustrated in Fig. 10. It shows a mismatch between the prediction of motion extrapolation model (Fig. 10*b*) and the actual perception reported from human subjects (Fig. 10*c*).

Fig. 11*a* shows the locations of the moving bar and the flashed bar ($y$-axis) over time ($x$-axis), where flashes appear at a fixed interval, with a flash at the motion reversal point. Physically, the actual trajectories of the moving bar (solid line) and the flashed bar (marked as rectangle) are delivered from the distal (i.e., the retina) to the proximal (i.e., the central nervous system) with time delay $\Delta t$ as shown in Fig. 11*a*.

According to the extrapolation model (Fig. 11*b*), the received location of the moving bar is corrected based on a predicted (or extrapolated) state. Then, the extrapolated object location will be closer to the actual environmental state at the time of perception. Under this model, the predicted location of the moving bar will generate an overshoot around the reversal point. However, the perceived trajectory found in human experimental data shows the absence of overshoot at the reversal point (Fig. 11*c*). Moreover, as the position of the moving bar approaches the motion reversal point, the gap between the perceived location of the two objects smoothly decreases, and after the motion reversal point, it increases again. How can such an

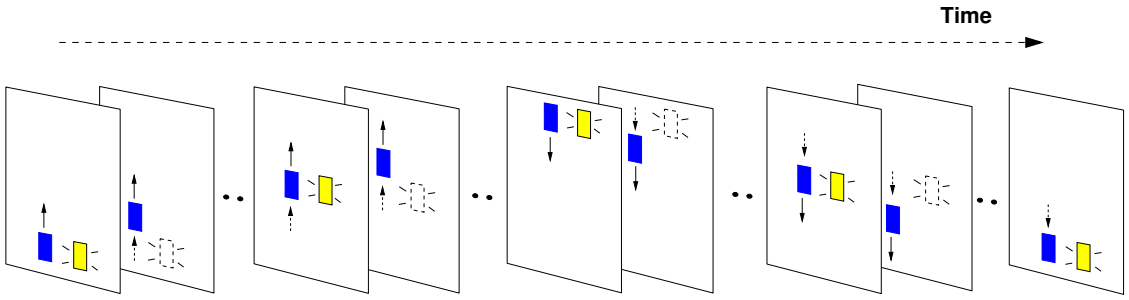


Fig. 9. **Illustration of the motion reversal flash-lag effect.** In motion reversal experiments by [3], the direction of motion of a vertically translating bar is reversed at a random time and location. A flash could appear at various time points before or after motion reversal. In here, flashes appear at a even interval including the motion reversal point.

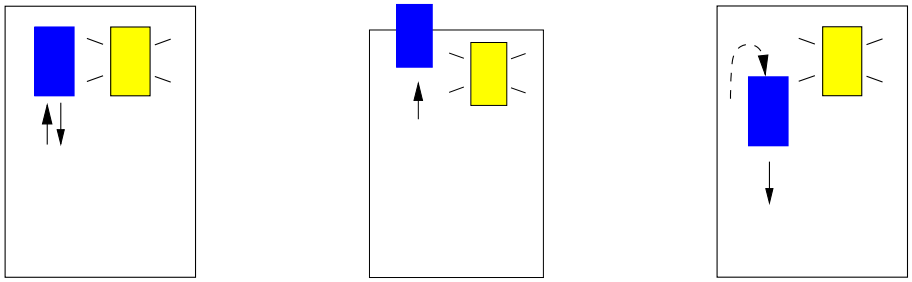

(*a*) Physical (*b*) Extrapolated (*c*) Perceived

Fig. 10. **Lack of FLE at the motion reversal point.** The lack of FLE at the motion reversal point is illustrated. (*a*) The flashed bar is presented at the time of motion reversal. Physically, the two bars are aligned. (*b*) Through extrapolation, the perceived location of the moving bar should lead the flashed bar (i.e. overshoot) based on the previous moving trajectory. (*c*) In humans, the overshoot is not perceived at the reversal point. The moving bar appears ahead of the flash in the reverse direction.

absence of FLE at the reversal point be explained under the extrapolation model?

Postdiction, an alternative hypothesis, suggests that information received in the future is incorporated into the estimation of a past perceptual event [40, 5]. Postdiction helps explain anomalies near motion reversal or motion termination point (more detail will be given in Sec. III.2). However, with this scheme, the nervous system

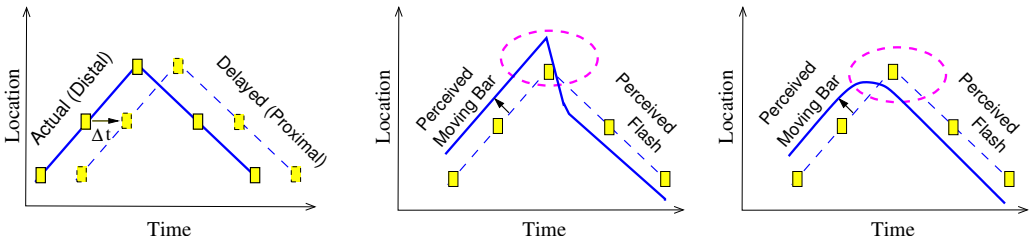


(*a*) Physical (*b*) Extrapolated (*c*) Perceived

Fig. 11. **Limitation of motion extrapolation model.** Extrapolation model has some difficulty in explaining motion reversal FLE. (*a*) The actual location of the flashed bar (rectangles) and the trajectory of moving bar (solid line) take time ($= \Delta t$) to travel from the retina (i.e. distal) to the central nervous system (i.e. proximal). (*b*) Through extrapolation, the perceived location of the moving bar leads, while that of the flashed object lags behind as delayed. Under this model, humans should perceive overshoot of the moving bar at the motion reversal point (marked with dashed oval). (*c*) However, in reality, humans do not perceive overshoot at the reversal point. As the position of the moving bar approaches the motion reversal point, the gap between the perceived location of the two objects decreases, and after motion reversal, it increases again.

would face perceptual processing delay (around 80 ms; see [40]) in addition to neural transmission delay (hundreds of milliseconds), which can become a serious problem for real-time response.

Despite the limitations of motion extrapolation model in explaining the lack of FLE at the motion reversal point, it has desirable properties [20, 22, 21, 23], and the limitation can be overcome computationally and neurophysiologically [24] (details of computational and biological methods will be described in Sec. III.3 and Sec. IV.3, respectively).

## II.3 Facilitating synapses as a neural basis of extrapolation

The relevant question at this point is then, "What is the neural mechanism that implements such an extrapolation process?" This is an important question that has not been fully investigated. I suggest that facilitatory neural dynamics in facilitating synapses can serve as a neural mechanism for motion extrapolation. Recent neurophysiological experiments have uncovered neural mechanisms that can potentially contribute to delay compensation. Researchers have shown that different dynamics exist at the synapse level, as found in two classes of synapses: depressing, and facilitating synapses. In these synapses, the activation level (the membrane potential) of the postsynaptic neuron is not only based on the immediate input at that instant but also on the rate of change in the activation level in the near past.

These synapses, called dynamic synapses, generate short-term plasticity which shows activity-dependent decrease (depression) or increase (facilitation) in synaptic transmission. Also, these dynamic activities occur within several hundred milliseconds from the onset of the activity (for reviews see [42, 31, 43]). As shown in Fig. 12, postsynaptic responses are determined by the interaction between dynamic synaptic parameters such as synaptic efficacy $U$, and available resource $R$. Synaptic efficacy is the fraction of neural transmitter released when presynaptic action potentials arrive at the axon terminal. Available resource is the fraction of recovered vesicles containing neurotransmitters. Other variables include time constant of recovery from depression $\tau_{\mathrm{rec}}$ and that from facilitation $\tau_{\mathrm{f}}$. These synaptic parameter values are adapted based on the presynaptic pattern of spikes.

Depressing synapses cause decrease of available resource in the presynapse so that a short interspike interval is most likely to be followed by a small postsynaptic response (Fig. 13, bottom trace), and they play a role in low-pass filtering [4]. Fa-

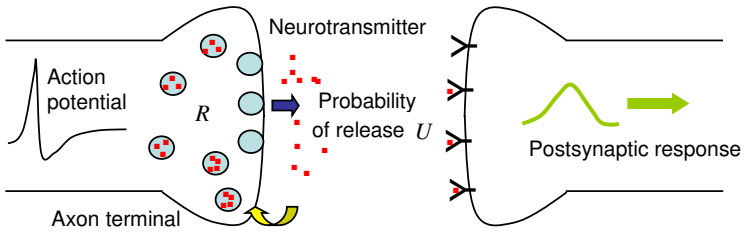


Fig. 12. **Synaptic transmission.** Dynamic synaptic transmission is dependent on the available resource $R$ (i.e. fraction of recovered vesicles containing neurotransmitters), the synaptic efficacy $U$ (the probability of release of neurotransmitter), and time constant for recovery from depression $\tau_{\text{rec}}$ or from facilitation $\tau_{\text{f}}$.

cilitating synapses express a different dynamic in which postsynaptic response grows through increasing synaptic efficacy with successive presynaptic spikes. To make facilitating synapses to turn on, at least four spikes in rapid succession (firing rate of over 50 Hz) are needed [31]. That is, facilitating synapse needs boosting time to reach the peak point where the spike is generated (see Fig. 13, middle trace). Therefore, facilitation will be triggered when a high-frequency series of burst of 100 ms duration arrives, and after several spikes at this frequency, a larger accumulated excitatory postsynaptic potential (EPSP) is generated by the facilitating synapse. With this, postsynaptic neuron will respond in higher firing rate than that of the original input spike train. Such a behavior suggests an extrapolatory role of facilitating synapses.

As discussed above, dynamic synapses have been studied in the context of memory such as sensitization (increase in the response to an innocuous stimulus) and habituation (the opposite of sensitization) [27, 28] or in relation to temporal coding [44, 4, 43, 29, 45]. However, to my knowledge, these mechanisms have not yet been investigated in relation to delay compensation. In this dissertation, I suggest that facilitating synapses may also play an important role in compensating for neural delays, and as a result it may cause extrapolation in perception, and subsequently

leading to visual flash-lag effect.

## II.4 Summary

In this chapter, I reviewed psychophysical evidence for the extrapolation model and a potential neural basis of extrapolation: (1) flash-lag effect might arise from an extrapolatory process to compensate for neural delay, and (2) facilitating synapses can implement extrapolation at a single-neuron level through its facilitating capability, given a sequence of input spikes. I also discussed the limitations of the extrapolation model in explaining some visual phenomena. In the next chapter, a model motivated by the works described above will be presented and described in detail.

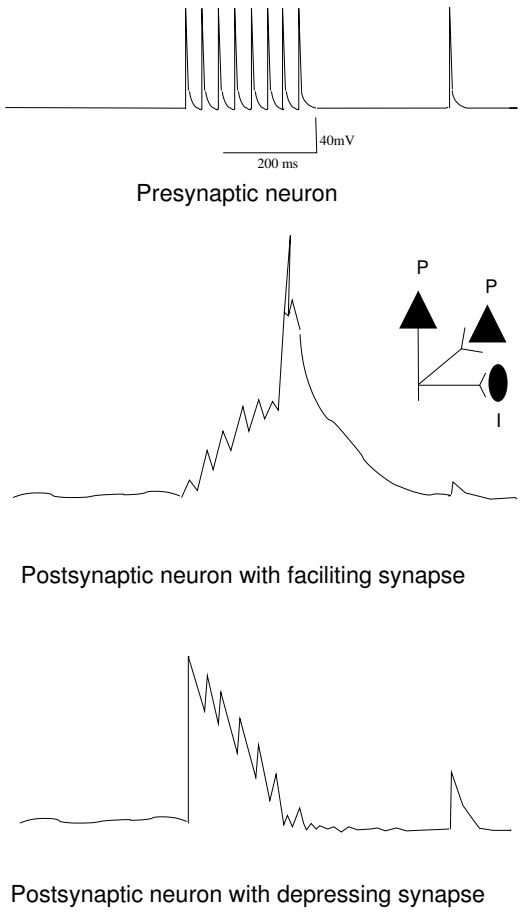


Fig. 13. **Dynamic synapses.** The behavior of dynamic synapses are shown. From the same axon innervating two different postsynaptic neurons, different postsynaptic responses were observed. From top to bottom, the traces show the input spike train, the facilitating response, and the depressing response. With the same input spikes (top), the postsynaptic neuron connected by facilitating synapse gradually increases its membrane potential and generates a spike when the membrane potential reaches a threshold (middle trace). On the contrary, through depressing synapses, the postsynaptic neuron shows a high response to the first input spike but rapidly decreases its membrane potential as subsequent spikes arrive. With this, the postsynaptic neuron failed to generate any spike (bottom). (Adapted from [4].)

# CHAPTER III

# FACILITATORY ACTIVATION MODEL

In this chapter, first, I will derive a *Facilitatory Activation Model* (FAM) which can implement an extrapolatory mechanism at a single-neuron level (Sec. III.1). Second, an alternative hypothesis for FLE (i.e., the postdiction model [40]) and its application to the motion reversal FLE [5] will be briefly reviewed (Sec. III.2). Third, *Facilitated Smoothing* model (i.e., extended FAM) will be derived, and it will be tested in the motion reversal domain. Compared to the results of postdiction, facilitated smoothing model can successfully explain the lack of effect at the motion reversal point as well as extrapolation during continuous motion in motion reversal FLE. These results suggest that our visual perception system may use an extrapolatory neural mechanism to compensate for neural delay, and also smoothing (i.e., implemented by backward masking; see Sec. IV.2 for details) to increase perceptual accuracy.

## III.1 Model description

How can the motion extrapolation model be implemented in the nervous system? My hypothesis is that for fast extrapolation, single neurons should be able to extrapolate. As discussed in Sec. II.3, biological neurons show different dynamics found in depressing and facilitating synapses. In these synapses the activation level (the membrane potential) of the postsynaptic neuron is not only based on the immediate input at a particular instant but is also dependent on the rate of change in the activation level in the near past. Such a mode of activation is quite different from conventional artificial neural networks (ANNs) where the activation level of the neuron is solely determined

by the current input and the connection weight values.

For example, in conventional ANNs, activation value $X_i(t)$ of a neuron $i$ at time $t$ is defined as follows:

$$X_i(t) = g\left(\sum_{j \in N_i} w_{ij} X_j(t)\right), \tag{3.1}$$

where $g(\cdot)$ is a nonlinear activation function (such as a sigmoid function), $N_i$ the set of neurons sending activation to neuron $i$ (the connectivity graph should be free of cycles), and $w_{ij}$ the connection weight from neuron $j$ to neuron $i$. As we can see from the equation, the past activation values of $X_i$ are not considered, thus the activation value cannot be updated based on the rate of change in $X_i$. An exception to this is recurrent neural networks where past activation in the network can also have an effect on the current activity [25, 26]. However, in our experimental results, it turns out that such recurrent dynamics alone is not sufficient to effectively counter the effects of delay. (More will be discussed in Chap. VI).

There are at least two ways in which we can introduce temporal dynamics at a single-neuron level: The activity $X_i(t)$ can be either decayed or facilitated based on its past activation. Let us denote this modified activity as $A_i(t)$ to distinguish it from $X_i(t)$. With this, we can now define the decaying and facilitating dynamics in a continuous-valued neuron (i.e., a firing-rate neuron).

The activity of a neuron with facilitating synapses can be defined as follows (for the convenience of notation, we will drop the index $i$):

$$A(t) = X(t) + r_{\mathrm{f}}(X(t) - A(t-1)), \tag{3.2}$$

where $A(t)$ is the facilitated activation level at time $t$, $X(t)$ the instantaneous activation solely based on the instantaneous input at time $t$, and $r_{\mathrm{f}}$ the *facilitation rate*

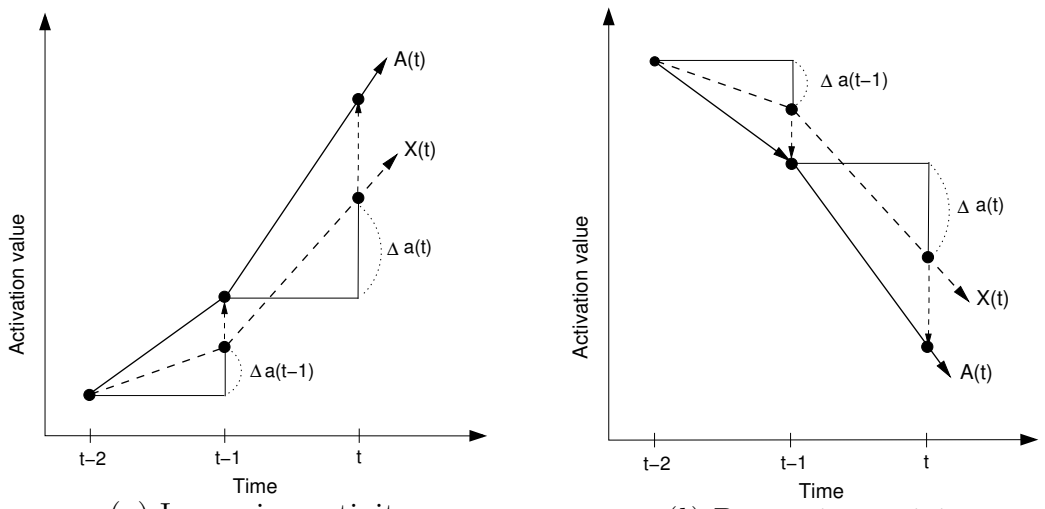


($a$) Increasing activity ($b$) Decreasing activity

Fig. 14. **Facilitating neural activity.** The effects of facilitating activity of neurons based on their past activation history are shown. The term $X(t)$ (dashed line) represents the activation value based on only the current input, while $A(t)$ (solid line) denotes that based on the past activity level as well as the current input. ($a$) A neuron with increasing activation value augments its immediate activation level using its past activation level. When the facilitation rate is close to 1, the final activation level $A(t)$ is increased as much as $\Delta a(t) = X(t) - A(t-1)$. Thus, the activity is facilitated in proportion to its rate of change (Eq. 3.3). ($b$) A neuron with decreasing firing rate reduces its immediate activation level $X(t)$ based on its previous activation level $A(t-1)$ to reach its final activation level $A(t)$.

$(0 \leq r_{\mathrm{f}} \leq 1)$. The basic idea is that the instantaneous activation $X(t)$ should be augmented with the rate of change $X(t) - A(t-1)$ modulated by the facilitation rate $r_{\mathrm{f}}$. For later use, we will call this rate of change $\Delta a(t)$:

$$\Delta a(t) = X(t) - A(t-1). \tag{3.3}$$

Note that Eq. 3.2 is similar to extrapolation using forward Euler's method where the continuous derivative $A'(\cdot)$ is replaced with its discrete approximation $\Delta a(\cdot)$ [46] (p.

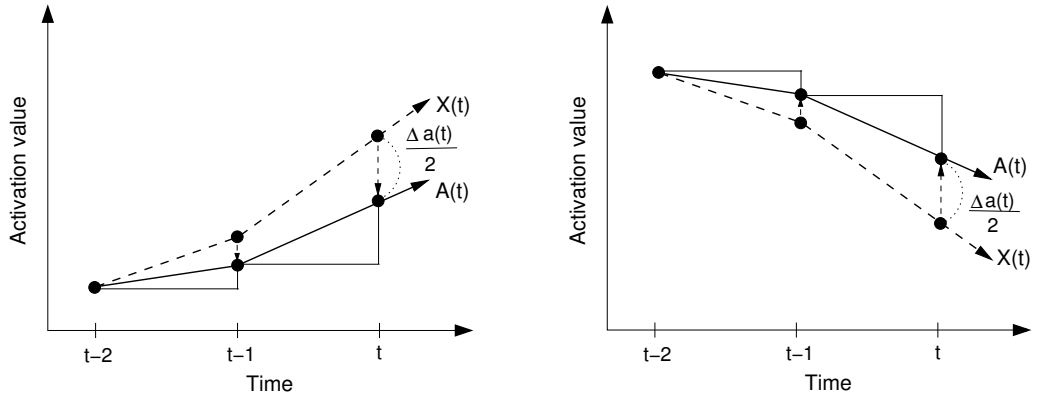


($a$) Increasing activity ($b$) Decreasing activity

Fig. 15. **Decaying neural activity.** The effects of decaying activity of neurons based on their past activation history are shown. ($a$) A neuron with decaying activity decreases its immediate activation level $X(t)$ based on its previous activation level $A(t-1)$ to reach its final activation level $A(t)$. When the decay rate is 0.5, the amount of decrease is $\frac{\Delta a(t)}{2}$ where $\Delta a(t) = X(t) - A(t-1)$. Thus, the activity is dampened in proportion to its rate of change (Eq. 3.2). ($b$) A neuron with decreasing firing rate decreases its immediate activation level $X(t)$ based on its previous activation level $A(t-1)$ to reach its final activation level $A(t)$. With decaying dynamics, a neuron decreases its activation value less, compared to the amount of immediate decrease.

710). Fig. 14 shows how facilitatory activity is derived from the current and past neural activity. Basically, the activation level $A(t)$ at time $t$ (where $t$ coincides with the environmental time) is estimated using the input $X(t - \Delta t)$ that arrived with a delay of $\Delta t$. If the facilitation rate $r_{\mathrm{f}}$ is close to 0, $A(t)$ reduces to $X(t)$, thus it represents old information compared to the current environmental state. If $r_{\mathrm{f}}$ is close to 1, maximum extrapolation is achieved.

A neuron's activity with decaying synapses can be calculated as follows:

$$A(t) = r_{\mathrm{d}} A(t-1) + (1 - r_{\mathrm{d}}) X(t), \tag{3.4}$$

where $A(t)$ is the decayed activation level at time $t$, $X(t)$ the instantaneous activation solely based on the current input at time $t$, and $r_{\mathrm{d}}$ the decay rate ($0 \leq r_{\mathrm{d}} \leq 1$). Thus, if $r_{\mathrm{d}}$ is close to 0, the equation will reduce to $X(t)$, becoming identical to Eq. 3.1 as in conventional neural networks. However, if $r_{\mathrm{d}}$ approaches 1, the activation at time $t$ will be close to $A(t-1)$. Notice that the decay rate $r_{\mathrm{d}}$, as defined above, represents how much the decay dynamics is utilized, and not how fast previous activity decays over time. Fig. 15 shows an example of decaying activation value when $r_{\mathrm{d}} = 0.5$. Note that the equation is essentially the same as Eq. 3.2, since $A(t) = r_{\mathrm{d}}A(t-1)+(1-r_{\mathrm{d}})X(t) = X(t) + r'(X(t) - A(t-1))$, where $r' = -r_{\mathrm{d}}$. So, both equations, Eq.3.2 and Eq.3.4, can be written as:

$$A(t) = X(t) + r\Delta a(t), \tag{3.5}$$

where $-1 \leq r \leq 1$. The parameter $r$, which we will call the *dynamic activation rate*, introduces a facilitating dynamic to a neuron when the $r$ value is positive and a decaying dynamic when $r$ is negative. Thus, the neural activation values in the facilitating or the decaying neurons falls within the range of $X(t) - \Delta a(t) \leq A(t) \leq X(t) + \Delta a(t)$.

The basic idea behind the facilitating and decaying activity dynamics described above is very simple, but it turns out that such a small change can bring about powerful temporal characteristics to the neural network. Especially, facilitating activity dynamics significantly improves the ability of the network in compensating for delay.

## III.2 Related work: optimal smoothing

To show how the facilitatory activation model (FAM) can successfully explain FLE in terms of delay compensation, I applied FAM in the motion reversal domain. Before

evaluating my results, in this section, I will show an alternative approach and its results in the motion reversal domain.

Rao et al. formalized postdiction using *optimal smoothing* [5], a commonly used method in engineering applications [47]. They tested the model in motion reversal FLE and showed that optimal smoothing can successfully account for the curve around the reversal point which is also observed in human experiments.

Using Kalman filtering [48], the best estimate of the location $\hat{X}(t)$ of a moving object at time $t$ is derived from its predicted location $\bar{X}(t)$ with error correction $G(t)(X(t) - \bar{X}(t))$ after observing the current value $X(t)$ [5]:

$$\hat{X}(t) = \bar{X}(t) + G(t)(X(t) - \bar{X}(t)), \tag{3.6}$$

$$\bar{X}(t) = \hat{X}(t-1) + c(t-1)\hat{Y}(t-1), \tag{3.7}$$

where $G(t)$ is a gain term, $c(t-1)$ denotes motion direction at time $t-1$ (1 for forward and $-1$ for reverse trajectory), and $\hat{Y}(t-1) = \bar{Y}(0) = a$, which indicates the velocity of the object ($a = 1$). To estimate the final perceived location, the best estimate $\hat{X}$ is recursively smoothed using the estimation from future time steps:

$$X_{\mathrm{sm}}(t) = \hat{X}(t) + h(t)(X_{\mathrm{sm}}(t+1) - \bar{X}(t+1)), \tag{3.8}$$

where $h(t)$ is a gain term and $X_{\mathrm{sm}}(t)$ the final perceived location of the moving object at time $t$.

Fig. 16 shows results from motion reversal experiments modeled by Eq. 3.6 through Eq. 3.8 (with $G(t) = 0.7$, $h(t) = 0.5$). The $x$ axis represents time (100 millisecond for unit) and the $y$ axis the location of the object (10 cm for unit). The

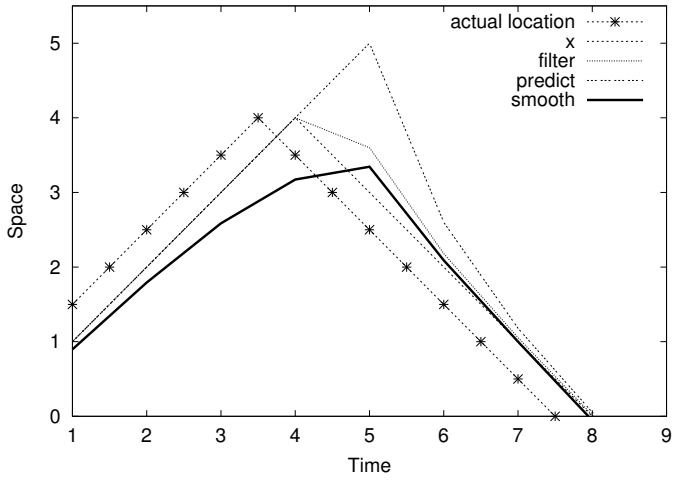


Fig. 16. **Perceived trajectory through optimal smoothing model.** The trajectory of a moving bar generated by each step of optimal smoothing is shown. The dotted line with '$*$' denotes the actual location of moving bar ('$*$' the flashed bar presented to be aligned with the moving bar), and the plain dotted line labeled "$x$" is for the neural activity arrived in the central nervous system with delay. By using Eq. 3.7, the predicted trajectory is generated (overshoot around the reversal point is observed). Filtering (Eq. 3.6) generates curve around the reversal point (dotted line labeled "filter"). (Note that the location of moving bar is still aligned with flashed bar.) After smoothing by using Eq. 3.8, the final perceived location is generated (dark solid line). It successfully reproduces the curve around the reversal point (i.e., moving bar is below the flashed bar), but cannot generate standard flash-lag effect for continuous trajectory (it rather undershoots the input data) [5].

velocity of the moving bar was 1 m/sec and the neural delay 50 ms. The actual trajectory of the two objects (dotted line for the moving bar and $*$ for the flashed bar) resulted in delayed neural activity $X$. Based on the input $X$, the optimal smoothing method generates a predicted, filtered, and smoothed estimation for the perceived object location. Notice that even though the smoothed trajectory (solid dark line) faithfully reproduced the observed curve around the reversal point, the estimated location undershoots the actual locations (the solid curve is shifted to the right) unlike

in the standard flash-lag effect for continuous motion without reversal. Certain problems arise here since the final perceived location is determined by recursive smoothing (which is possible only *after* observing all the input data), and the temporal window needs visual integration mark (i.e., flash) to be set on, which contradicts with the finding that localization error exists when there is no accompanying flash [20, 21]. In sum, the smoothing model may be difficult to apply in the nervous system, which has to work in almost real time.

### III.3 Facilitation with smoothing: Experiments and results

In order to test whether the facilitation model can explain FLE in terms of delay compensation, I applied the facilitation model to the motion reversal experiment under the same conditions as in Sec. III.2. Fig. 17 shows the results where $X(t)$ corresponds to the delayed neural activity arrived in the visual cortex and $A(t)$ the facilitated perception for the location of the moving bar ($r = 0.5$). If there is no facilitating neural activity, the perceived location will be significantly behind the real positions (refer to Fig. 6 for a better understanding of this point). With facilitatory neural activity, however, the delayed neural signal is facilitated so that the perceived location (dark solid line) become closer to the actual location (dashed line with $*$) of the moving bar in the environment at that same instant. Notice that the visual FLE occurs due to the spatial gap between the facilitated activity for the moving bar (dark solid line) and the non-facilitated activity for the flashed bar (dashed line). However, as mentioned above as a shortcoming of the extrapolation model, the facilitated perception generates an overshoot around the reversal point (around time 4 in Fig. 17), which is not observed in human experiments [3].

What happens at the instant of motion termination or reversal? A potential answer is that the misperception (i.e., overshoot at reversal) is corrected by backward masking with an immediate change termination signal [49]. The motion termination signal which arrives at the time of extrapolation can cancel out the extrapolatory neural activity so that there is no overshooting perceived at the terminating (or reversal) point. This is consistent with the postdiction model to some extent such that information occurring after time $t$ can affect the judgment about the perceived location at time $t$ [40, 5]. However, differentiating from optimal smoothing, the model below uses extrapolated activity $A(t)$ instead of the filtered estimate $\hat{X}(t)$ for smoothing, and considers only one time step into the future to modify the estimate. (I assumed that the time step is 100 ms as shown in Fig. 16.) Thus, the perceived location can be redefined as follows:

$$A_{\mathrm{sm}}(t) = A(t) + h(t)(X(t+1) - A(t)), \tag{3.9}$$

where $A_{\mathrm{sm}}$ (facilitated-smoothing value) represents the perceived location of the moving object. Compared to Eq. 3.8, Eq. 3.9 is much simpler and is also suitable for real-time perception.

Fig. 18 shows the result using Eq. 3.9 (with $h(t)$ set to 0.4). Compared to Fig. 17, facilitated smoothing ($A_{\mathrm{sm}}$; dark solid line) successfully produces no-overshoot at the time of reversal, and at the same time closely approximates the overshoot events for continuous visual motion. This computational result strongly suggests that our nervous system may use extrapolatory neural mechanisms for delay compensation as well as a small delay in perception to avoid this perception.

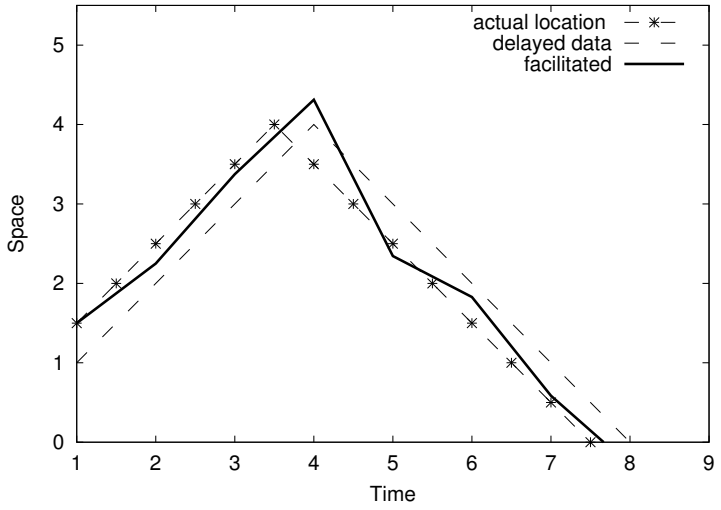


Fig. 17. **Perceived trajectory in the facilitation model.** The dashed line with '$*$' represents the actual location of the moving bar ('$*$' is the flashed bar presented to be aligned with the moving bar), the plain dashed line the delayed neural activity, and the solid dark line the perceived locations. The facilitation model generates trajectory close to the actual location. The perceived location of the moving bar (solid dark line) is ahead of the flashed bar (dashed line) in continuous moving condition, expressing flash-lag effect. However, it generates overshoot around the reversal point (around time 4), which has been pointed out as the limitation of extrapolation model by Whitney et al. [3].

### III.4 Summary

From a computational perspective, I proposed the *facilitatory activation model* which can express extrapolatory neural activity. To test the capability of FAM as a delay compensation method and, at the same time, to show that the limitation of extrapolation model can be overcome, I applied the model to motion reversal FLE and compared the results with that of the postdiction model. FAM with smoothing showed similar characteristics as those observed in human experimental data [3]. In sum, facilitatory neural activity may play an important role in compensating for neural delay, which helps an organism to perceive the environment in real time. In the

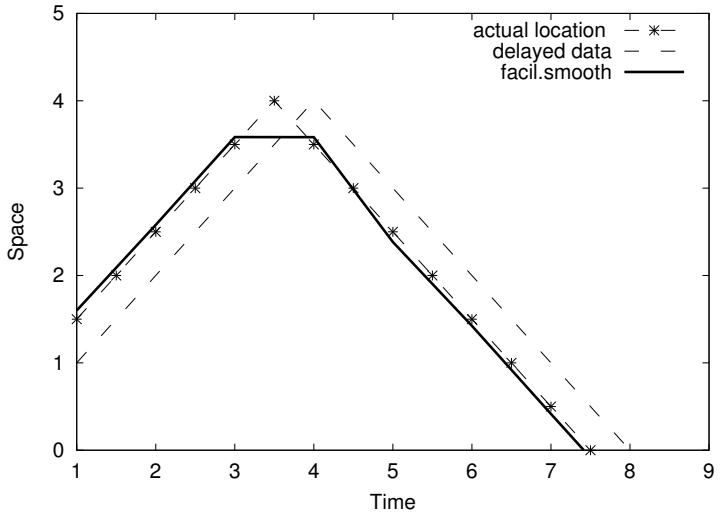


Fig. 18. **Perceived trajectory in the facilitated-smoothing model.** See Fig. 17 for plotting conventions. Facilitated-smoothing generates the most perceptually accurate trajectory in spite of neural delay. It successfully generates both no overshoot at the time of reversal and extrapolation during continuous visual motion.

next chapter, I will derive a spike-based facilitation model which can firmly ground FAM on a biologically plausible neuron model.

# CHAPTER IV

# SPIKE-BASED FACILITATION MODEL

In facilitatory activation model (FAM), the neural activity was represented as a single real number. However, biological neurons communicate via spikes, so the biological plausibility of the facilitation model may come under question. How could the facilitatory dynamics and smoothing effect discussed in Chap. III be implemented in a biologically plausible manners?

In this chapter, I will describe a spike-based model based on known neurophysiological mechanisms. The previous models of facilitating synapses by Markram et. al [4, 29, 50] will be extended to derive spike-based model of facilitation. Also, inhibitory synaptic transmission will be suggested as a neural mechanism for smoothing (i.e., suppressing the overshoot, cf. Sec. III.3). The model will be tested with luminance FLE which is simple enough to be modeled at a single-neuron level.

## IV.1 Model description

One potential cellular process for the spike-based FAM is the synaptic dynamics of facilitating synapses found in biological neurons, as briefly mentioned in Sec. II.3. These synapses generate short-term plasticity which shows activity-dependent decrease (depression) or increase (facilitation) in synaptic transmission occurring within several hundred milliseconds from the onset of activity (for reviews see [42, 31]). Especially, facilitating synapses cause augmentation of postsynaptic response by increasing synaptic efficacy with successive presynaptic spikes.

According to the dynamic synapse model by Markram and colleagues [4, 29, 50]

synaptic efficacy $U$ of facilitating synapses evolves over time as follows:

$$\frac{dU}{dt} = -\frac{U}{\tau_f} + C(1-U)\delta(t-t_s), \tag{4.1}$$

where $\tau_f$ is the time constant for the decay of $U$; $C$ a constant determining the increase in $U$ when a successive action potential (AP) arrives at time $t_s$ at the synaptic terminal; and $\delta(\cdot)$ the Dirac delta function. This equation is already suitable enough to replicate the facilitating dynamics in Eq. 3.2 when the activation level is increasing (as in Fig. 14*a*). However, it is not capable of handling cases where the activation level is decreasing (as in Fig. 14*b*). Ideally, extrapolation should work for both increasing and decreasing directions.

To address this issue, the equation can be modified by redefining $C$ as a dynamic variable which is varied in proportion to the change of input firing rate:

$$C = \mathrm{Sgn}\left(I(n-1) - I(n)\right)\left(\frac{I(n-1)}{I(n)}\right)r, \tag{4.2}$$

where $\mathrm{Sgn}(\cdot)$ is the sign function, and $I(n)$ is the interspike interval between the $n$-th spike and the $(n-1)$-th spike which reflects whether a spike train consists of high-frequency APs or low-frequency APs. The first term in Eq. 4.2 determines the sign of $C$: "+" for increase or "−" for decrease in firing rate. The second term represents the ratio of the change in firing frequency, and the third term $r$ is a gain parameter. As the input firing rate increases, $C$ becomes positive and increases proportional to the rate of change in frequency. On the contrary, as the firing rate decreases, $I(n)$ becomes larger which results in a negative $C$ and thus leads to the decrease in the synaptic efficacy $U$.

With this, we can now fully describe an updated membrane potential model (cf. [4, 29, 51]). The time course of postsynaptic current $P(t)$ at time $t$ triggered by incoming spikes is defined as follows:

$$P(t) = Ee^{-\frac{t}{\tau_{\mathrm{p}}}}, \tag{4.3}$$

$$E = wAU, \tag{4.4}$$

where $E$ is the excitatory postsynaptic potential (EPSP) amplitude; $\tau_{\mathrm{p}}$ the time constant of decay in $P(t)$; $w$ the weight or scaling factor of $A$ (note $w$ is constant in a single neuron model); $A$ a constant for maximum postsynaptic response amplitude; and $U$ the synaptic efficacy as defined above.

Finally, according to a standard leaky integrate-and-fire neuron model [52], the membrane potential $V_m(t)$ at time $t$ can be calculated as follows:

$$V_m(t) = V_m(t-1)e^{-\frac{t}{\tau_m}} + P(t)(1 - e^{-\frac{t}{\tau_m}}). \tag{4.5}$$

The membrane potential is determined by the membrane current $P(t)$ at that moment and the previous membrane potential $V_m(t-1)$, both of which are regulated by a membrane time constant $\tau_m$. The last part of the spiking neuron model is the spike generation mechanism. Once $V_m$ exceeds the spike threshold $\theta$, a spike is generated, and return to $V_{\mathrm{rest}}$ ($\sim -70$ mV) after an absolute refractory period of $\tau_{\mathrm{refrac}}$ during which spikes cannot be generated. After the refractory period, membrane potential $V_m(t)$ immediately increases by facilitated postsynaptic current $P(t)$ and generates subsequent spikes in the postsynaptic neuron. With the model above, I simulated a single neuron under increasing or decreasing input firing rate to test the

extrapolative functionality in facilitating synapses (Sec. IV.3).

## IV.2 Backward masking

Another question to be resolved is what neural mechanisms can cancel out potential overshooting occurring at a motion-reversal point as shown in Fig. 18. Nijhawan [49] suggested that backward masking can be used to reduce the misperception (i.e., overshoot) at the motion reversal point.

Backward masking refers to reduction of target visibility when another stimulus (i.e., mask) immediately follows the target. Macknit and Livingstone showed that visual stimulus that strikes the retina after an image (up to 100 ms) can cancel out conscious perception of the image during subsequent processing [53]. Thus, stimulus offset signal is important as well as onset signal, by which the ongoing visual processing can be inhibited. Recently, experiments with macaque monkeys showed that there is a group of neurons responding to event-specific stimulus such as pursuit termination or target offset [54]. Thus, event-specific information such as motion offset signal seems to be processed separately from those of ongoing visual stimulus.

One potential biological model which can explain backward masking is the boundary contour system model [55, 56]. In that model, persistent visual perception can be reduced by a reset signal that can suppress an ongoing activity with feedforward inhibition [57, 58]. (For a review of alternative hypotheses for backward masking, see [59].) Based on these, I suggest that stimulus offset (or motion offset) signal may be conveyed by inhibitory synaptic transmission, which suppresses the facilitated postsynaptic membrane potential. With this, overshoot at motion termination can be canceled out, implementing a smoothing effect in the facilitation model. In

the following section (Sec. IV.3), spike-based FAM and inhibitory synaptic masking will be tested within the luminance flash-lag effect domain.

## IV.3 Experiments and results with luminance FLE

In luminance FLE, a stationary disk continuously becoming brighter in luminance appears brighter than a neighboring flashed object of equal luminance (and analogously, darker for a disk becoming darker) [16] (Fig. 19). It has been shown that neurons in the primary visual cortex respond in a manner correlated with perceived brightness rather than responding strictly to the light level in the receptive field [60, 61]. This finding shows that what we perceive is not the same as the physical stimulus. Such perceptual phenomena in luminance FLE, expressing extrapolation (brighter than bright and darker than dark), can be modeled at a single-neuron level using facilitating synapses as described in Sec. IV.1.

Sensory signals such as photons hitting the retina are converted into spikes (or action potentials) through sensory transduction. These spikes cause a chain reaction through the sensory pathway to reach the primary sensory area (the primary visual cortex, in case of vision). Let us focus on the last part of the journey of these spikes, where the thalamocortical input spike train releases neurotransmitters from the presynaptic neurons to a postsynaptic neuron through facilitating synapses. Further simplifying this, let us assume that there is only one synapse. With this setup, we can model the extrapolatory phenomenon described above, by varying the spike firing rate in the presynaptic neuron (i.e., the brighter the more action potentials; the darker the less action potentials).

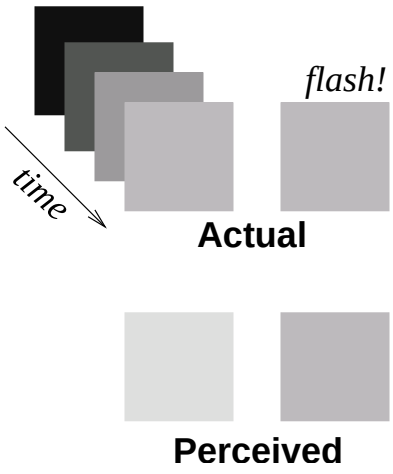


Fig. 19. **Flash-lag effect in luminance change.** Flash-lag effect is also observed in a stationary time-varying stimulus. A stationary visual patch becomes brighter over time (top left) and, at a random time, a patch with equal luminance (top right) is flashed next to the changing patch. Physically, the two objects have the same brightness. However, the time-varying patch appears brighter than the flashed patch (bottom). When the object becomes darker, it is perceived darker than the flashed one.

## 1 Continuous change in luminance

I tested two types of input: (1) increasing firing rate (visual stimulus becoming brighter) and (2) decreasing firing rate (visual stimulus becoming darker). The parameters used for the simulation below were as follows: initial value for synaptic efficacy $U = 0.3$; $U$-recovery time constant $\tau_f = 220$ ms; postsynaptic potential time constant $\tau_p = 30$ ms; membrane current time constant $\tau_m = 250$ ms; spike threshold $\theta = 175$ mV; $V_{\text{rest}} = 0$ mV; duration of absolute refractory period $\tau_{\text{refrac}} = 5$ ms; maximum postsynaptic response amplitude $A = 300$; and $C$-gain $r = 0.35$.

The results are shown in Fig. 20 and Fig. 21. The facilitating synapse model generated extrapolatory neural activity for both increasing and decreasing firing rate conditions. Dynamic change in the synaptic efficacy $U$ caused the postsynaptic neuron to generate more spikes than the input when the input firing rate was increasing

(Fig. 20). On the other hand, the postsynaptic neuron generated less spikes than what it received when the input firing rate was decreasing (Fig. 21).

This kind of behavior is quite reasonable if we consider conduction delay. Suppose the spikes in the presynaptic neuron (the second row in Fig. 20) originated earlier (about 100 ms) in peripheral sensors (the top row). Here is an example sequence of events. (1) Peripheral spiking at 400 ms would be replicated at 500 ms in the presynaptic neuron in the second row, due to the delay. (2) The postsynaptic neuron (bottom row) receiving input from the presynaptic neuron (second row) at 500 ms fires based on information from 400 ms in the periphery. (3) However, the postsynaptic neuron's firing rate at 500 ms (bottom row) is the same as that of the presynaptic neuron's firing rate at 600 ms (second row). This means that the postsynaptic neuron, at time 500 ms, is exactly firing at the same frequency as the peripheral neuron at time 500 ms (refer to (1) above), precisely reflecting the present environmental state. Note that the presynaptic (second row) and the postsynaptic (bottom row) neuron in Fig. 20 are both located in the central nervous system as shown in Fig. 7. The changes of firing rates from three neurons (peripheral, presynaptic, and postsynaptic neuron) are shown in Fig. 22.

In case of decreasing firing rate (Fig. 21), all the experimental conditions and notations are the same as the increasing case except that the input spikes frequency is decreasing. According to Eq. 4.1 and Eq. 4.2, the constant $C$ for determining the increase in synaptic efficacy becomes negative which leads to a gradual decrease in membrane potential of the postsynaptic neuron. The third row in Fig. 21 shows the decreasing membrane potential, and the bottom row the output spikes generating less number of spikes than that of the input spikes. As shown in the increasing case, the postsynaptic neuron's firing rates are closely matched with those of the peripheral neuron in spite of neural delay. Fig. 22*b* shows that, around 400 ms to 600 ms, the

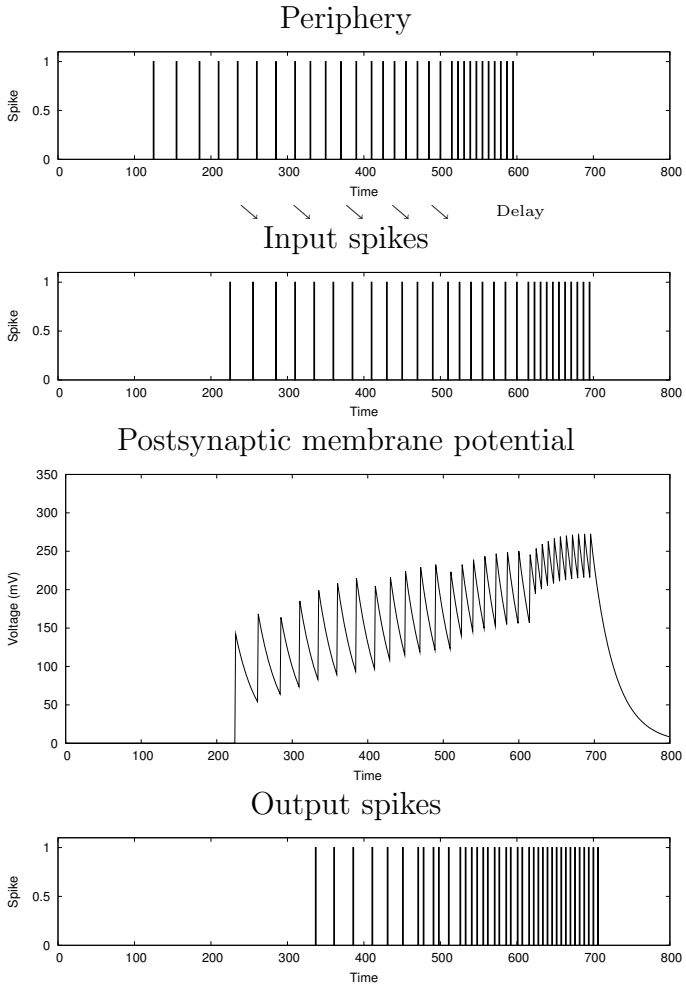


Fig. 20. **Extrapolation with facilitating synapses under increasing firing rate.** Activation in neurons with facilitating synapses are shown, where a sequence of input spikes are under increasing firing rate. The top row shows the input spike sequence generated at a peripheral neuron, the second row the input spikes arrived at a presynaptic neuron with neural delay (around 100 ms), the third row the membrane potential of the output neuron, and the bottom row the output spike sequence. The output firing frequency from 400 ms to 600 ms (bottom row) are closely matched with those of the presynaptic neuron's firing rate, from 500 ms to 700 ms (second row), and those of the peripheral neuron's firing rate, from 400 ms to 600 ms (top). (See Fig. 22*a* for the exact number of spikes.) This shows that, in spite of the delay ($\Delta t = 100$ ms), the output firing rate exactly reflects the input firing rate in the periphery at that instant and help the internal state to be in synchrony with outer state.

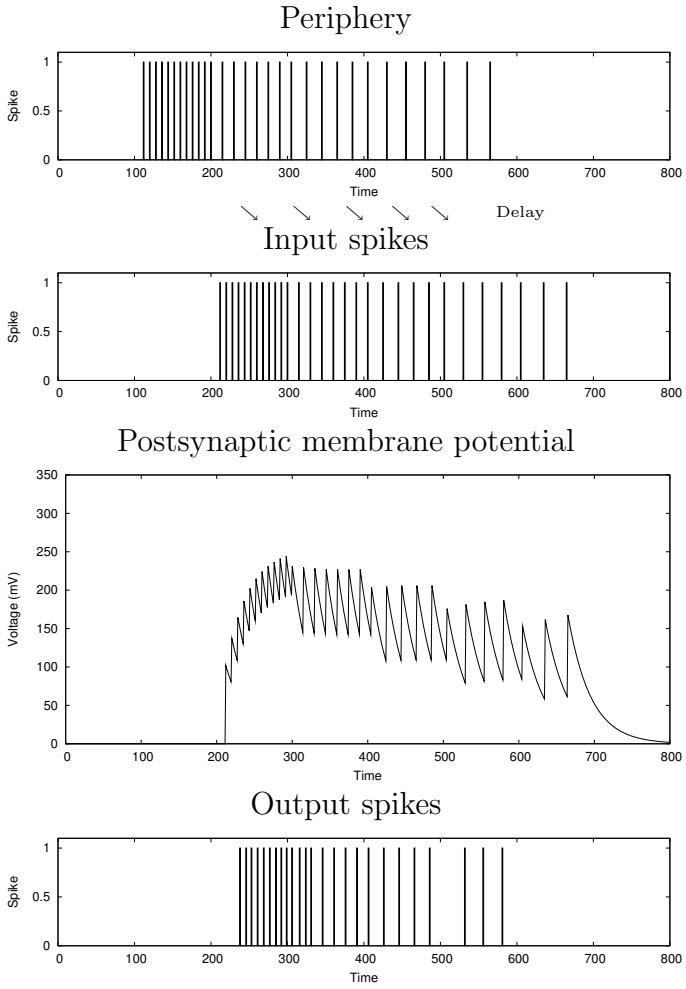


Fig. 21. **Extrapolation with facilitating synapses under decreasing firing rate.** All the experimental conditions and notations are the same as the increasing case shown in Fig. 20. Decreasing firing frequency in the input causes facilitating synapses to decrease its synaptic efficacy and make the postsynaptic neuron generate less spikes than input spikes. The output firing frequencies from 400 ms to 600 ms (bottom row) are closely matched with those of the presynaptic neuron's firing rate, from 500 ms to 700 ms, and those of the peripheral neurons' firing rate from 400 ms to 600 ms. Thus, in spite of the delay ($\Delta t$ = 100 ms), the output neuron exactly reflects the neural state at the periphery as in the increasing firing rate case (Fig. 20).

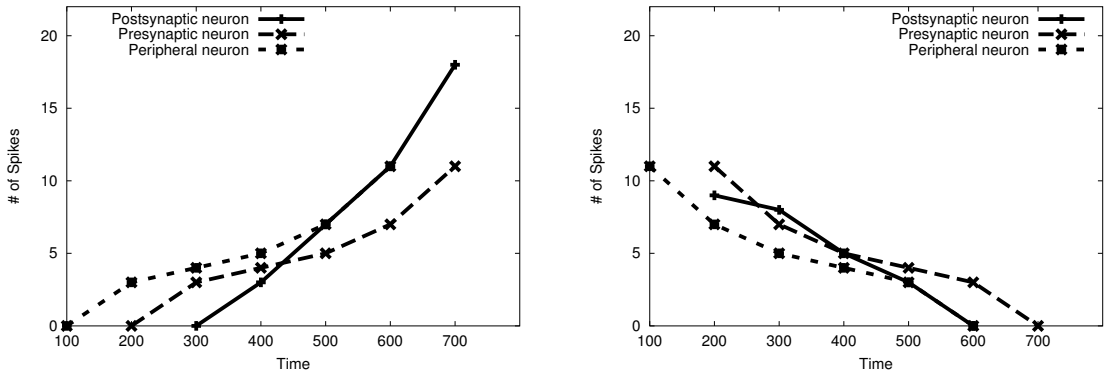


(*a*) Increasing firing rate (*b*) Decreasing firing rate

Fig. 22. **Firing rate in the continuous change in luminance.** The change of firing rate over time is shown for (*a*) increasing luminance and (*b*) decreasing luminance case. The $x$ axis represents time (e.g., 200 represents the time frame between 100 ms and 200 ms) and $y$ axis the number of spikes generated during that time frame. The peripheral (dotted line with '$*$'), the presynaptic (dashed line with 'x'), and the postsynaptic (solid line with '$+$') neurons' firing rates are shown. (*a*) In the increasing luminance experiment, the postsynaptic neuron needed some boosting time for the facilitatory activity (about 100 ms) to be invoked, and it started to generate more spikes than the presynaptic neuron after 400 ms. This means that the postsynaptic neuron is exactly firing at the same frequency as the peripheral neuron from time 400 to 600 ms. However, overshooting is observed at the terminating point (700 ms) due to the facilitated neural activity. (*b*) In the decreasing case, the postsynaptic neuron generates less spikes than the presynaptic neuron showing the same firing rate as the peripheral neuron after 400 ms.

number of spikes in the postsynaptic neuron is close to that of the peripheral neuron.

In contrast to the previous models by Markram et. al [4, 29, 50], the modified equation (Eq. 4.1 and Eq. 4.2) was able to generate extrapolated neural activity under both increasing and decreasing firing rate. These experiments suggest that facilitating synapses can implement a general extrapolatory neural activity, thus providing a neurophysiological basis for the facilitatory activation model described in Sec. III.1.

In sum, the time-varying static stimuli (brighter or darker in luminance) were

extrapolated to be perceived close to the present intensity of light, while the firing rate of the abrupt stimulus (i.e., flashed patch) was the same as the presynaptic neuron. Such different firing rates between two stimuli might cause FLE in visual luminance change. With such a mechanism, the organisms can keep the inner state close to that of the physical environment in real time.

## 2 Termination of change in luminance

How can the smoothing effect discussed in Sec. III.3 be implemented in a biologically plausible manners? In other words, what neural mechanism can account for the smoothing effect described in Eq. 3.9? Backward masking can be a possible method [49], however, a precise neural basis for that is unknown. In this section, I will show that inhibitory synaptic transmission combined with facilitating synapses can implement backward masking. To test this idea, I used the luminance FLE domain as above.

Fig. 23 shows the neural activity where luminance offset signal follows the input spike train (top row) in case of increasing firing rate. The second row shows the event-specific spikes generated by the termination in the change in luminance. This neural information is supposed to be delivered by an inhibitory synapses immediately after stimulus termination. Influenced by inhibitory postsynaptic potential (IPSP), the increased postsynaptic membrane current is pulled down (the third row), which makes the postsynaptic neuron to fire with similar frequency as the presynaptic neuron (i.e., no overshooting). As shown in Fig. 24, the extrapolated neural activity in the postsynaptic neuron was reduced, generating less spikes than that of the continuously changing case. (Notice that compared to Fig. 22*a*, the number of spikes of the postsynaptic neuron around 700 ms was reduced.) Through inhibitory synaptic

transmission, the extrapolatory neural activity was suppressed, showing that the lack of effect can also be explained by backward masking.

## IV.4 Summary

In this chapter, I proposed a spike-based facilitation model by extending the facilitating synapse model of Markram and colleagues [4]. The model allowed FAM, introduced in Chap. III, to be firmly grounded on neurophysiology. Experiments with visual luminance FLE turned out that facilitating postsynaptic activity can generate extrapolated neural activity under both increasing and decreasing firing rate cases. Also, I showed that the lack of FLE (i.e., no overshoot at stimulus termination) can be explained by a backward masking mechanism, which is implemented by inhibitory synaptic transmission. In the next chapter, I will extend this single-neuron level FAM into a multi-neuron level model to explain other FLEs such as orientation FLE.

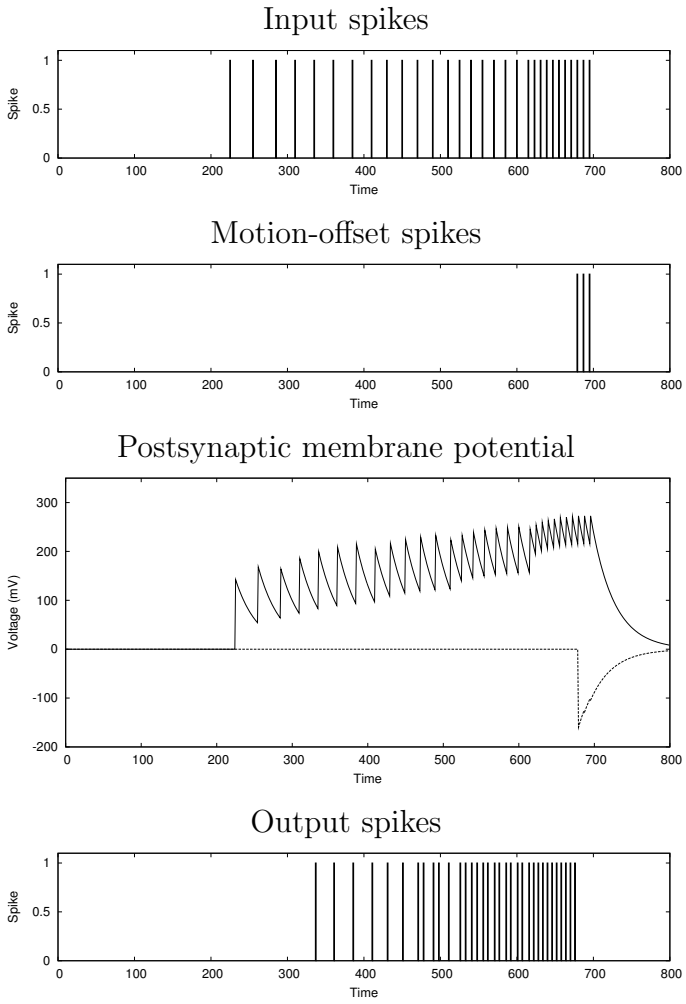


Fig. 23. **Facilitating synapse with luminance-off signal.** The absence of overshooting in interrupted changing condition can be explained by inhibitory synaptic transmission. The top row shows the input spikes arriving at a presynaptic neuron, the second row the luminance-off signal delivered by an inhibitory synapse at the time of stimulus termination, the third row the membrane potential of a postsynaptic neuron having excitatory and inhibitory dynamics, and the bottom row the output spike sequence. The inhibitory postsynaptic potential (IPSP) decreased the facilitated postsynaptic potentials (third row), which results in a decrease in the number of spikes generated in the postsynaptic neuron. Thus the number of spikes generated by the postsynaptic neuron was reduced compared to the case without the inhibitory signal (cf. Fig. 20).

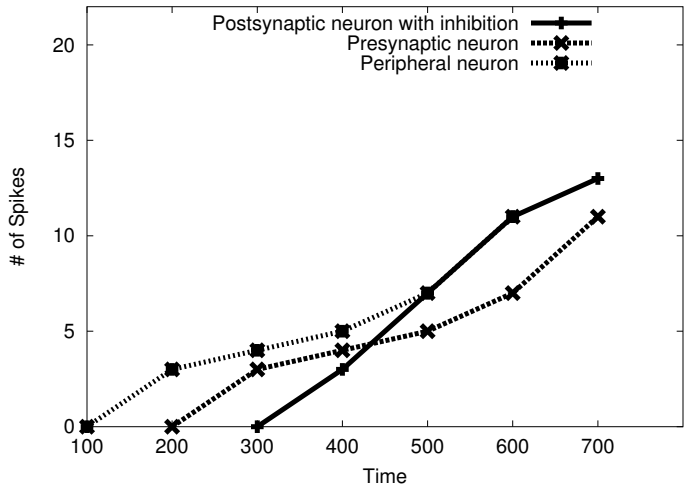


Fig. 24. **Firing rates in the termination of change.** The firing rates over time are shown for the termination of increasing luminance. The three neurons generate the same number of spikes as shown in the increasing luminance case (Fig. 22*a*) until the terminating point. Due to the inhibitory signal, the augmented membrane potential of the postsynaptic neuron was pulled down, generating less number of spikes at 700 ms than the case without the inhibitory signal.

# CHAPTER V

## CROSS-NEURONAL FACILITATION MODEL

In Chap. IV, I showed that facilitating synapses, a form of dynamic synapse, can function as an extrapolator to undo the effect of neural delay, thus serving as a neural basis of the luminance flash-lag effect. However, the same approach cannot be applied to other forms of FLE such as orientation FLE (see Fig. 5), since unlike luminance, the full range of orientation cannot be represented by a single neuron. Changing firing rate may be able to represent dark to bright, but orientation-tuned cells in the visual cortex are narrowly tuned, thus one neuron can only represent a narrow range of orientation (see [7] for a review). To address this issue, I extended the spike-based facilitation model to include synaptic input from neighboring neurons as well as direct input spikes from presynaptic neuron (i.e., input signal corresponding to a specific orientation). With this, facilitation in a single neuron can go across multiple neurons.

It turns out that mechanisms such as spike-timing-dependent plasticity (STDP) [33, 34] is necessary to set up the connection strengths, so that cross-neuron facilitation can carry out extrapolation in the direction of change. In this chapter, I will first provide details of the model, explain how cross-neuronal facilitating dynamics can be implemented by combining with STDP, and test the model with orientation FLE.

### V.1 Model Description

To make the facilitatory neural activity to propagate across multiple neurons, a neural network was set up, consisting of bilaterally connected neurons. Also, in order to test

the network with orientation FLE, I confined the model to have twelve orientation-sensitive neurons at a 15° increment. (With this, the neurons can represent the full range of orientation.) Fig. 25 shows the arrangement of the target neuron, and their lateral excitatory connectivity. In this structure, the neurons have connections only between immediate neighbors (i.e., bilateral connection), where each connection has a facilitatory synapse. Visual stimulus of a rotating bar will cause the neurons on the network (Fig. 25) to receive input spikes in a sequence (clockwise or counterclockwise). (For simplicity, the input connections to presynaptic neurons are not shown in Fig. 25.)

Cross-neuronal facilitating dynamic follows the single facilitation dynamics as described in Sec. IV.1. The only difference is that $w$ is a variable not a constant. Let us review the equations defined in Sec. IV.1. The time course of postsynaptic current $P(t)$ at time $t$ was defined as: $P(t) = Ee^{-\frac{t}{\tau_p}}$, and $E = wAU$, where $E$ is the excitatory postsynaptic potential (EPSP) amplitude; $\tau_p$ the time constant of decay in $P(t)$; and $w$ weight or scaling factor of $A$. Through the sequence of spikes from presynaptic neuron to target neuron, facilitating dynamics are activated. In contrast to the single-neuron model described in Sec. IV.1, the connection weight $w$ in $E = wAU$ is not a constant, but a variable in the multi-neuron model. A potential synaptic mechanism to update $w$ is spike-timing-dependent plasticity (STDP). The following section will describe STDP in detail.

## V.2 Spike-Timing-Dependent Plasticity

The lateral connections in this model (Fig. 25) are initially directionally symmetric, meaning that there is no preferential activation in the clockwise or the counter-

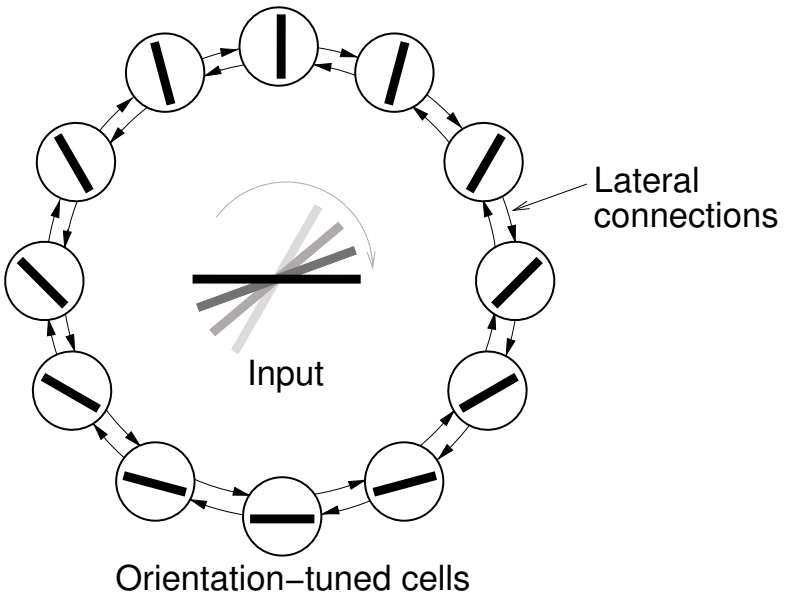


Fig. 25. **Bilaterally connected orientation-tuned cells.** Twelve orientation-tuned neurons are shown, with excitatory lateral connections between immediate neighbors. The connectivity shown here is a simplification of similar arrangements near orientation pinwheels in the primary visual cortex [6, 7].

clockwise direction. However, for extrapolation to happen in a particular direction, there needs to be directionality. A learning process that can give rise to such a directionality is found in Spike-Timing-Dependent Plasticity (STDP). STDP changes the synaptic weight between two neurons when they fire together within a small time interval [33, 34]. Fig. 26 shows the basic principle underlying STDP. When the presynaptic neuron fires first (firing time $t_{\text{pre}}$), and then the postsynaptic neuron spikes (firing time $t_{\text{post}}$), then the difference $\Delta t = t_{\text{post}} - t_{\text{pre}} > 0$, since $t_{\text{post}} > t_{\text{pre}}$. On the other hand, if the postsynaptic neuron fires first, $\Delta t < 0$. The synapse will be strengthened if $\Delta t > 0$, and weakened if $\Delta t < 0$.

To include STDP in the model, I used the following synaptic modification func-

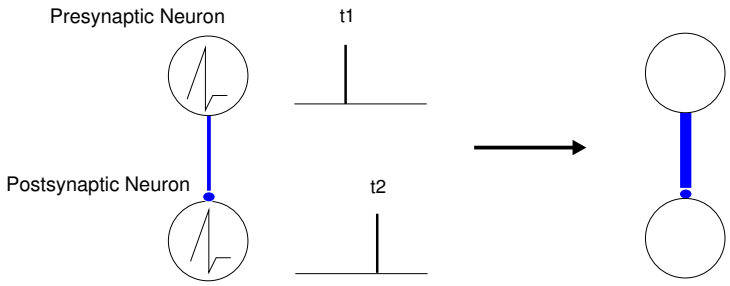


$(a)$ $\Delta t = t_2 - t_1 > 0$

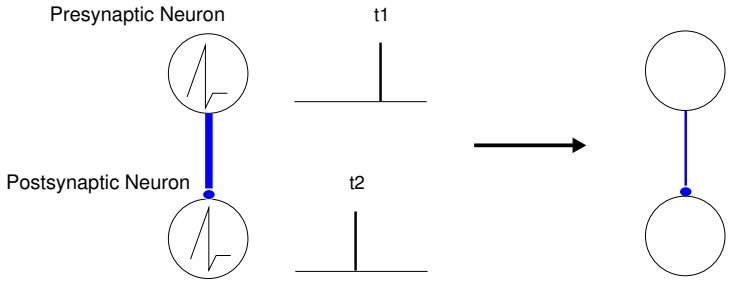


$(b)$ $\Delta t = t_2 - t_1 < 0$

Fig. 26. **Synaptic weight update through spike-timing-dependent plasticity.** $(a)$ Synaptic weight increases when a presynaptic spike at time $t_1$ occurs before a postsynaptic spike at time $t_2$ (the thickness of connection represents the strength of the connection). $(b)$ Synaptic weight decreases in the opposite case. Stimulated by rotating bar, the orientation-sensitive neurons in Fig. 25 will fire in sequence within a small time interval, which allows for STDP to strengthen the weight in that rotating direction.

tion [34] (see Fig. 27):

$$F(\Delta t) = \begin{cases} A_+ e^{-\frac{\Delta t}{\tau_+}} & \text{if } \Delta t > 0 \\ -A_- e^{\frac{\Delta t}{\tau_-}} & \text{if } \Delta t < 0 \end{cases}, \tag{5.1}$$

where $A_+$ and $A_-$ are constants determining the maximum range of modification, and $\tau_+$ and $\tau_-$ the time constants of exponential decay. For the simulations, the following parameter values were used: $A_+ = 5.0$, $A_- = 3.7$, $\tau_+ = 80$, and $\tau_- = 105$.

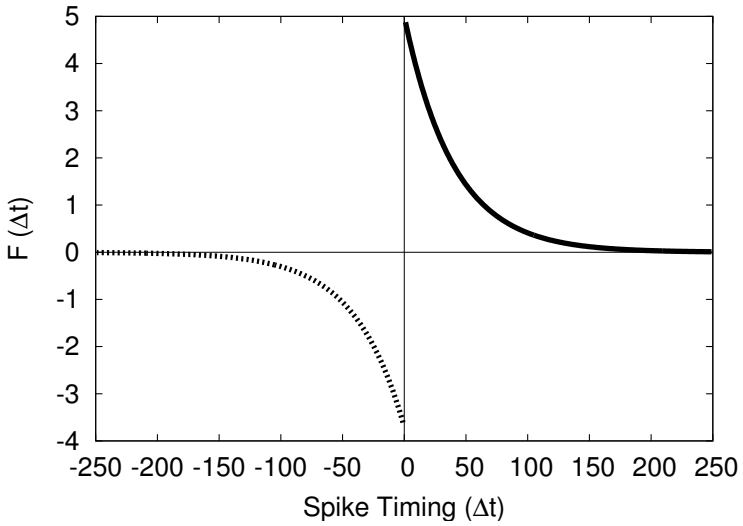


Fig. 27. **Synaptic modification through STDP.** The illustration shows the dynamic increase or decrease in the amount of synaptic modification $F$ based on spike timing $\Delta t$ (= postsynaptic spike time − presynaptic spike time) as shown in Eq. 5.1.

The actual weight adaptation for the connection from neuron $j$ to neuron $i$, with firing time $t_j$ and $t_i$, respectively, was carried out as follows:

$$w_{i,j} \leftarrow w_{i,j} + \alpha F(\Delta t), \tag{5.2}$$

where $\alpha$ is the learning rate (= 0.02) and $\Delta t = t_i - t_j$. In case $w_{i,j}$ reached zero, it was not decreased any further.

Fig. 29 in the next section (Sec. V.3) shows the evolution of the connection weights in the direction and in the opposite direction of input rotation. When a particular target (postsynaptic) neuron has orientation preference that is in the rotating direction relative to the source (presynaptic) neuron, the source neuron fires first and then the target neuron, so STDP strengthens the connection. STDP weakens the connection in the opposite case (i.e., the postsynaptic neuron fires first). A critical

factor in this experiment is that the input rotation should not be too fast nor too slow, so that neighboring neurons can fire *within* the adaptation window (the width of positive or negative range in Fig. 27, which is found to be around ±80 ms in the experimental literature [62]). Note that the parameters $\tau_+$ and $\tau_-$ in Eq. 5.1 control the width of positive and negative adaptation windows. Interestingly, the above timing roughly corresponds with the timescale of orientation FLE. For example, as the orientation of the stimulus sweeps by at 100 ms per neuron (i.e., 25 RPM), the neurons generate several spikes while the input is at their preferred orientation. With this, the bilaterally connected presynaptic and postsynaptic neurons fire together within a short time interval (about 100 ms) and $\Delta t$ will fall within the STDP range. Thus, the synaptic weights between the neurons can be changed.

## V.3 Experiments and results with orientation FLE

To test, in a multi-neuron environment, the contribution of facilitating dynamics and STDP in delay compensation, orientation FLE was modeled. In view of orientation FLE, each neuron fires according to a distribution centered around its preferred orientation, maximally firing when the preferred orientation is present in the input, and gradually less as the input veers away (Fig. 28, "No FLE"). Note that during orientation FLE, the distribution shifts toward the direction of rotation (Fig. 28, "FLE").

I conducted three separate experiments: orientation perception with (1) STDP only, (2) facilitating synapses only, and (3) both STDP and facilitating synapses. In all experiments, the input was rotated in the clockwise direction, at a speed of 25 RPM, and the input firing rate was set to 10 spikes/100 ms.

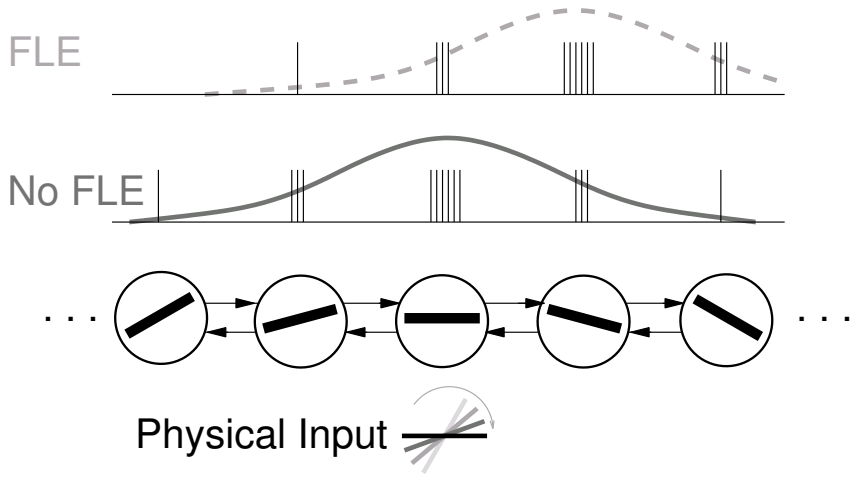


Fig. 28. **Response of orientation cells with and without FLE.** The spike responses (vertical bars) and firing-rate distributions (curves) are shown, with (top; dashed) and without (bottom; solid) Flash-Lag Effect. The $x$-axis represents the spatial span across the connected orientation-tuned cells (Fig. 25). Without FLE (solid), the firing-rate distribution is centered around the middle (cf. Fig. 5*a*). With FLE (dashed), the distribution is shifted toward the direction of input rotation (cf. Fig. 5*b*).

## 1 STDP only

First, I tested the model with STDP only, without facilitating synapses. The input bar was rotated at the speed of 25 RPM, while the connection weights were allowed to adapt according to Eq. 5.2. For those connections pointing toward the direction of input rotation, the weight increased (solid curve) since presynaptic spike preceded postsynaptic spike within the small time interval (Fig. 27). On the other hand, for the connections pointing in the opposite direction, the weight decreased (dotted curve). Fig. 29 shows these results.

To calculate the firing rate at any given moment, I used a fixed sliding window of width 100 ms. I measured the firing rate when the input was oriented to optimally stimulate neuron 2. Fig. 30 shows the results. Initially, when the weights have not

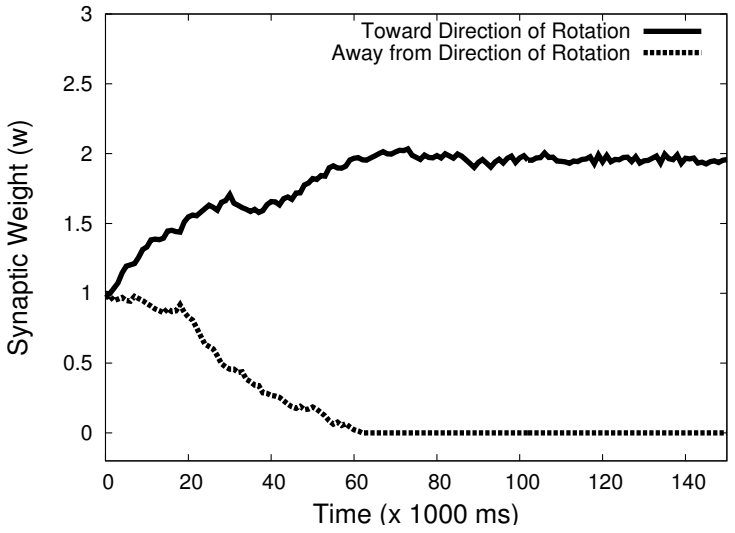


Fig. 29. **Adaptation of synaptic weight using STDP.** The synaptic weights $w$ in the conenctions from neuron 2 to two immediate neighbors are shown. The weight to the neuron in the direction of input rotation increases (solid curve), while that in the opposite direction decreases (dotted curve).

adapted much, the firing-rate distribution is peaked at neuron 2 and is symmetric. After the weights have reached a stable state, the distribution becomes asymmetric, with a shift toward the right, the direction of input rotation. However, the location of the peak did not change (neuron 2). The results can be interpreted as no orientation FLE occurring with STDP only.

## 2 Facilitating synapses only

In this experiment, I used only facilitating synapses, without STDP. All weights were initialized to 1.0, and remained fixed throughout the experiment. Since the weights did not have any directionality, I expected that orientation FLE would not occur, which turned out to be the case. (Facilitation cannot selectively propagate to a specific direction, if the connection weights in all directions are the same.) The

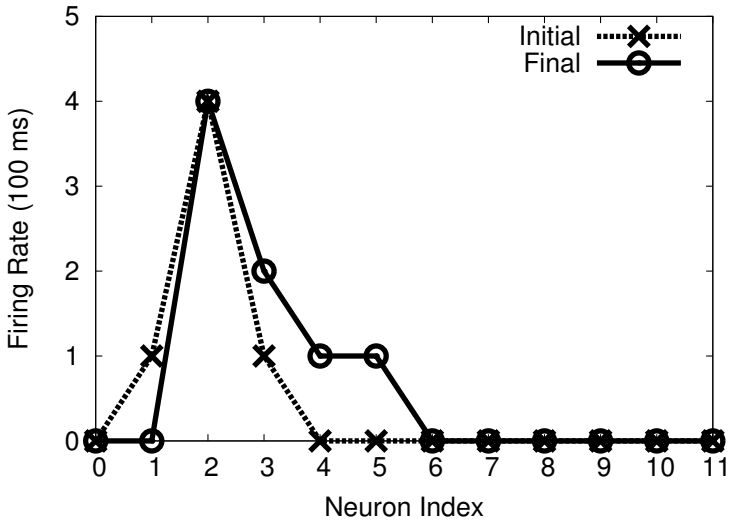


Fig. 30. **Firing rate distribution of STDP-only experiment.** The dotted line with 'x' represents the initial firing rates of neurons. The solid line with 'o' represents the changed firing rate after the synaptic weights reached a stable state through STDP. This is a snapshot of firing rates (i.e. number of spikes for 100 ms) when the actual input orientation was neuron 2's preferred stimulus. With STDP, the firing rates of the neurons changed due to the synaptic weight modification (skewed toward direction of rotation). However, the maximally firing neuron (neuron 2) did not change (i.e., no FLE).

only changing quantity in this experiment was the synaptic efficacy in the facilitating synapses, following Eq. 4.1. Fig. 31 shows the evolution of the synaptic efficacy $U$ over time, for a single neuron. The $U$ value increases while the input bar is optimally stimulating the neuron, and decays as soon as the input bar rotates out of the optimal range.

As expected, the firing rate distribution did not change from its symmetric, peaked distribution centered around the optimally tuned neuron, for the given input orientation (Fig. 32). The results suggest that, again, orientation FLE did not occur, and shows that facilitating synapses alone are not enough to account for cross-neuron facilitation (or extrapolation across neurons).

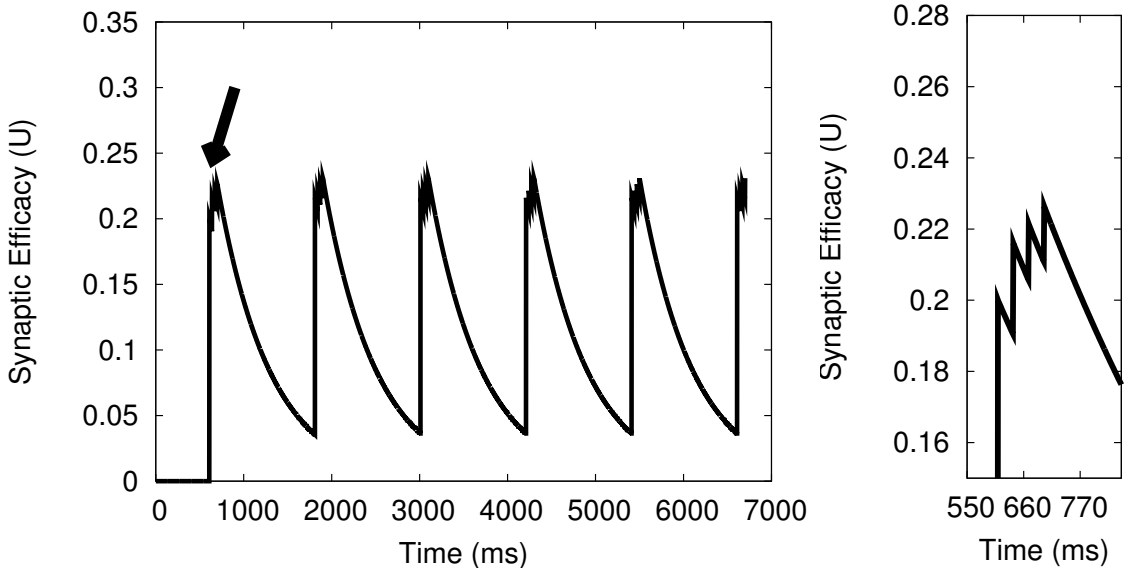


Fig. 31. **Adaptation of synaptic efficacy through facilitating synapses.** The synaptic efficacy in a single neuron is shown. During the period of stimulation (when the rotating input is stimulating the neuron) synaptic efficacy increases. Shown to the right is a close-up of the part on the left marked with an arrow.

## 3 STDP with Facilitating Synapses

The final experiment combined STDP and facilitating synapses. The experimental condition was the same as in the two experiments above for the STDP and the facilitating synapse parameters. In this experiment two factors contributed to synaptic transmission between two neurons: the very short-term increase in synaptic efficacy due to facilitating dynamics, and the relatively longer-term increase in synaptic strength due to STDP. Fig. 33 shows the combined effect of these two factors over time. The gradually increasing relatively long-term trend in STDP weight is accented with rapidly changing facilitating dynamics.

STDP gives the model directionality, and facilitating dynamics provides extra influence in the direction of input rotation, thus, allowing the model to shift its firing rate distribution significantly. Fig. 34 (thick arrow) shows that the peak in the firing

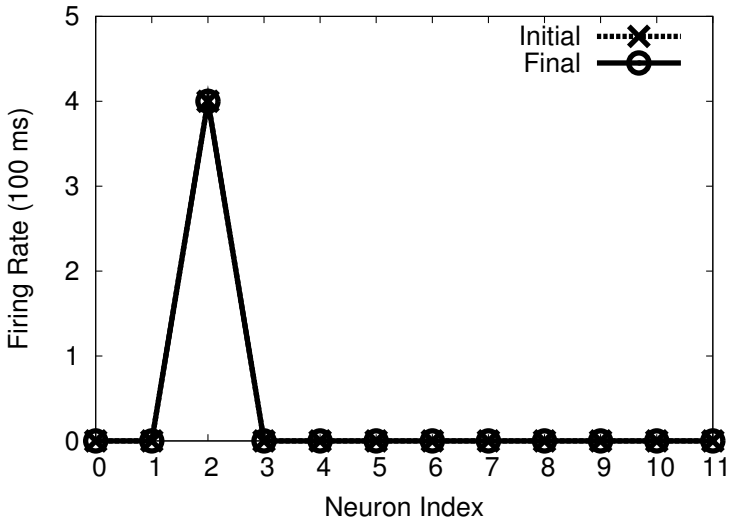


Fig. 32. **Firing rate distribution of facilitating-synapse-only experiment.** The distributions of firing rates of the initial state (dotted line with 'x') and the final state (solid line with 'o') are shown. Because the synaptic efficacy $U$ is rapidly changed (increase and decrease) by a small amount (see Fig. 31, right), facilitating synapse alone did not affect the firing rate of the neighboring neurons. Thus, the maximally firing neuron (neuron 2) did not change (i.e., no FLE).

rate distribution shifts toward the direction of input rotation (that is, to the right) by two steps (neuron 4), when the actual input at that moment is optimally stimulating neuron 2. Thus, we can conclude that orientation FLE occurred in this case.

An important result to be noted is that when the input firing rate was low (e.g. 5 spikes/100 ms), the shift of the firing rate distribution was not observed (i.e., no FLE; the data are not shown here). The reason is that to make facilitating dynamics to be activated, the neuron should receive high frequency input spikes [31]. This result can be a potential answer to a puzzling phenomenon, the Flash-Lead effect: When the luminance of the rotating bar is sufficiently low (relative to the flashed objects), the rotating bar appears behind the flashed object (opposite of FLE; [63]). Although these results, i.e., no shift of firing rate distribution (not shown), could not explain

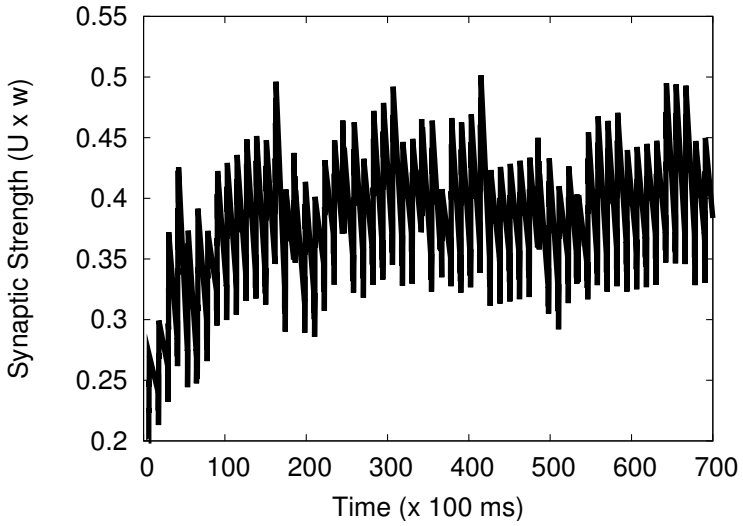


Fig. 33. **Adaptation of synaptic strength ($U \cdot w$ in Eq. 4.4) through STDP plus facilitating synapses (along the direction of rotation).** Synaptic strength ($U \cdot w$) dynamically increases because of the gradually increasing synaptic weight $w$ and the fast changing synaptic efficacy $U$.

the Flash-Lead effect exactly (i.e., shift of firing rate distribution toward the opposite direction), it was shown that the sensitivity of facilitating activity to spike frequency may play a role in modulating the degree of misalignment.

## 4 Summary of results

The computational results showed that STDP or facilitating synapses alone cannot serve as a robust mechanism for delay compensation, when multiple neurons are necessary for the representation of the full feature dimension. An example of this can be seen in orientation FLE in a multi-neuron setting. Only when both are combined, delay compensation can work properly, thus giving rise to orientation FLE.

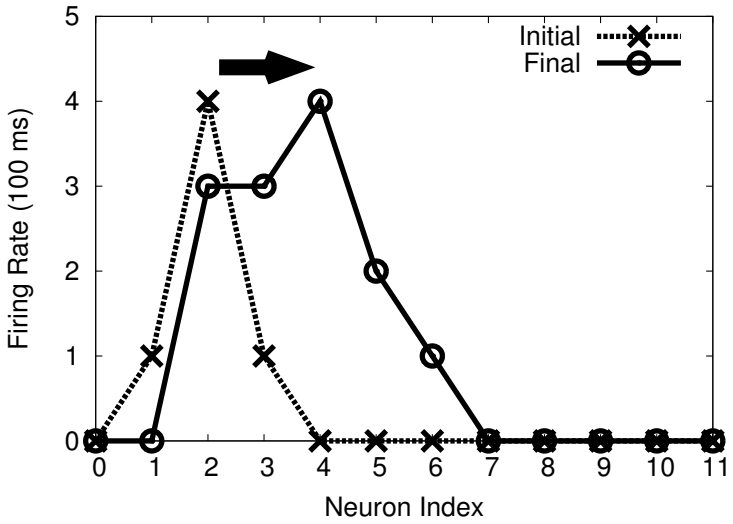


Fig. 34. **Firing rate distribution of STDP plus facilitating-synapse experiment.** The distribution of firing rates significantly shifted toward the rotating direction (as marked with an arrow). The position of maximally firing neuron changed from neuron 2 to neuron 4 (dotted line with 'x' for initial state; solid line with 'o' for final state). After training with STDP plus facilitating synapse, with the input at neuron 2's preferred orientation, neuron 4 showed maximum firing rate instead of neuron 2. This result indicates that the perception of the rotating bar shifted, just like in orientation FLE.

## V.4 Summary

In this chapter, I extended the spike-based facilitating model (single-neuron level model) to a cross-neuronal facilitation model (multi-neuron level model). It was shown that spike-timing-dependent plasticity is necessary to set up the directionality in a multi-neuron network so that cross-neuron facilitation can carry out extrapolation in the direction of change. I tested the cross-neuronal facilitation model with orientation FLE using a bilaterally connected neural network. The results showed that facilitation synapses combined with STDP can serve as a neural basis for delay compensation and give rise to orientation FLE.

# CHAPTER VI

## APPLICATION TO REAL TIME CONTROL

In previous chapters (Chap. IV and V), I have shown that facilitatory (extrapolatory) dynamics found in facilitating synapses can be used to compensate for neural delay at a single-neuron level as well as at a multi-neuron level. An interesting question arising here is, whether the FAM (a model based on facilitating synapses) can also help to overcome the problem of delay in engineering applications.

As a delay compensation scheme, recurrence in connected networks can be used. Recurrent neural networks can retain information about the history of previous activations [25, 26], and with this, they can possibly develop the ability to overcome input delay. However, such historical data alone may not be sufficient to effectively compensate for neural delay since the evolving dynamics of the network may not be fast enough. For fast extrapolation, the mechanism has to be implemented at a single-neuron level. To test this idea, I applied the firing-rate FAM model to a 2D pole-balancing problem modified to include sensory delays. Moreover, to test whether facilitatory activity can help when delay increases and when external uncertainty exists, I conducted gradually increasing delay tests and input blank-out experiment.

In this chapter, I will introduce *facilitating activity network* (FAN), a recurrent neural network including facilitatory neural dynamics at a single-neuron level; describe the experiments with the pole-balancing problem to test FAN under various input delay conditions; and analyze the network's behavior, performance, and the evolved networks' parameters in detail.

## VI.1 Pole-balancing problem with delayed input

The main domain I tested the idea of facilitatory neural dynamics was the pole-balancing (or inverted pendulum) problem. The problem has been established as a standard benchmark for adaptive control systems [64, 65]. Also, the pole-balancing problem is a nonlinear problem; and yet easy to visualize and analyze. In the standard task, a cart is allowed to move along a straight line while trying to keep balanced the pole attached to it.

A more difficult task than the above is the 2D version, where the cart is allowed to move on a 2D plane (Fig. 35). The goal of the controller here is to produce a sequence of force to be applied to the cart to keep the pole balanced (within 15$^{o}$ from the up-right position) and to maintain the cart position within the 2D boundary for a certain amount of time. The state of the cart-environment system at a given instant can be fully described by the cart's location $(c_x, c_y)$, their derivatives over time $(\dot{c_x}, \dot{c_y})$, the configuration of the pole relative to the $z$ and the $x$ axes $(\theta_z, \theta_x)$, and their derivatives over time $(\dot{\theta_z}, \dot{\theta_x})$. The standard problem without delay can be solved by feedforward neural networks when such a full state information is available. However, if the derivatives (velocity) are not available (i.e., only $c_x, c_y, \theta_z$, and $\theta_x$ are given), a recurrent neural network is needed. The recurrent dynamics of the network can serve as a form of memory from which the velocity information can be recovered [66].

The equations of motion for a pole balanced on a cart are defined as follows (see Tab. 1 for the definition of the parameters and their values) [8]:

$$\ddot{c_x} = \frac{F - \mu_c \operatorname{Sgn}(\dot{c_x}) + \tilde{F}}{M + \tilde{m}}, \tag{6.1}$$

$$\ddot{\theta_z} = -\frac{3}{4l}(\ddot{c_x} \cos\theta_z + g \sin\theta_z + \frac{\mu_p \dot{\theta_z}}{ml}), \tag{6.2}$$

where $\tilde{F}$ is the effective force from the pole on the cart, which is defined as:

$$\tilde{F} = ml\dot{\theta}_z \sin\theta_z + \frac{3}{4}m\cos\theta_z(\frac{\mu_p\dot{\theta}_z}{ml} + g\sin\theta_z), \tag{6.3}$$

and $\tilde{m}$ the effective mass of the pole,

$$\tilde{m} = m(1 - \frac{3}{4}\cos^2\theta_z). \tag{6.4}$$

The derivatives $\ddot{c_y}$ and $\ddot{\theta_x}$ are calculated using the same equations as above. In the simulations below, as noted above, only the four observable inputs ($c_x$, $c_y$, $\theta_z$, and $\theta_x$) are available to the controller. The parameters in the above equations were set as shown in Tab. 1.

## VI.2 Neuroevolution controller

In this section, I will provide an overview of the Enforced Subpopulation (ESP) algorithm [67, 66, 8, 68] which was used as a baseline implementation for pole-balancing. I will also describe the network structure of the pole-balancing controller using ESP and the experimental setup for the 2D pole-balancing task.

### 1 Enforced Subpopulation (ESP)

There are two main branches of reinforcement learning that effectively solve the pole-balancing problem: methods that (1) search the space of value functions that assess the utility of behaviors (e.g., temporal difference approach [69, 70, 71, 72]) and those

Table 1. Parameters used for the simulation of the pole-balancing problem

| Symbol | Description | Value |
|---|---|---|
| $x$ | position of the cart on the track | [-1.5,1.5] m |
| $\theta_z$ | angle of the pole from the vertical reference | [-15,15] deg |
| $\theta_x$ | angle of the pole from the horizontal reference | [-15,15] deg |
| $F_x$ | force applied to the cart in the $x$-axis | [-10,10] N |
| $F_y$ | force applied to the cart in the $y$-axis | [-10,10] N |
| $l$ | half length of the pole | 5 cm |
| $M$ | mass of the cart | 1 kg |
| $m$ | mass of the pole | 0.02 kg |
| $\mu_c$ | coefficient of friction of the cart on the track | 0.0005 |
| $\mu_p$ | coefficient of friction of the pole's hinge | 0.000002 |
| $g$ | gravitational constant | -9.8 m/s$^2$ |

that (2) directly search the space of behaviors (e.g., neuroevolution approach; see [73] for a review of neuroevolution methods). Without explicitly assessing their utility, neuroevolution directly maps observations to actions and gradually adapts individuals' (neurons) genotypes, resulting in fast learning in complex non-linear problems [74, 65, 66].

One effective reinforcement learning method using neuroevolution is the Enforced Subpopulation algorithm (ESP [68, 8]) by Gomez and Miikkulainen. ESP is a fully connected recurrent network, in which the connection weights between neurons are determined through evolutionary learning. In contrast to other neuroevolution networks, each hidden neuron has its own population (i.e., subpopulation) and are drawn from its population to construct a network. A neuron can only be recombined with

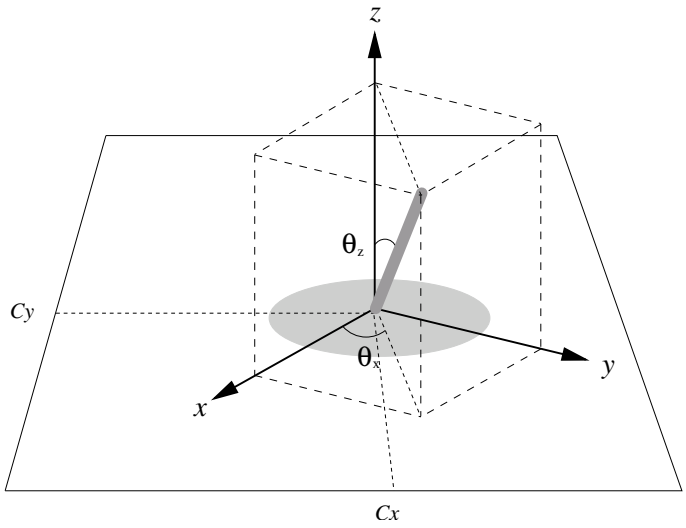


Fig. 35. **2D pole-balancing problem.** A pole (dark gray bar) on a cart (light gray oval) is shown. In a 2D cart-pole balancing problem, the cart has to be moved on a 2D plane to prevent the pole from falling, while staying within a fixed bounding box. The value $\theta_z$ is the angle between the pole and the local $z$ axis, and $\theta_x$ the angle it makes with the local $x$ axis. The two values uniquely define the configuration of the pole relative to the local coordinate system of the cart. The values ($c_x$, $c_y$) represent the location of the cart within the square boundary.

members of its own subpopulation and thus evolve independently of other subpopulations. With this method, subpopulations can rapidly learn compatible subtasks [68, 67].

Evolution in ESP proceeds as follows [8] (Fig. 37).

1. Initialization: The number of hidden units $n$ (= 5) is specified and $n$ subpopulations of size $p$ (= 40) chromosomes are created. Each chromosome encodes the input, output, and possibly recurrent connection weights of a neuron with a random string of real numbers.

2. Evaluation: A set of $n$ neurons is selected at random, to form the hidden layer of the network of a specified type. The network is tested in a pole-balancing trial

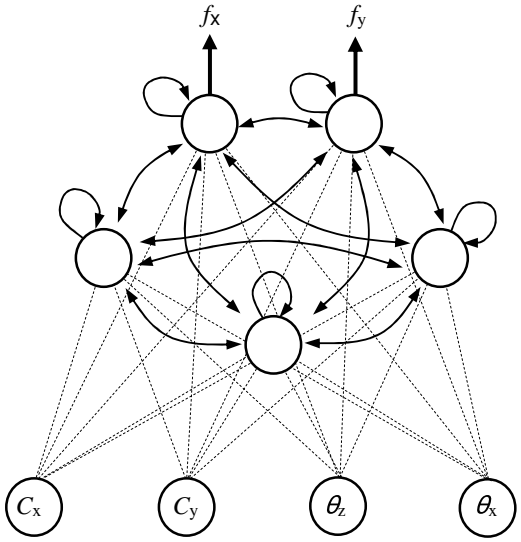


Fig. 36. **Recurrent neural network for pole balancing.** The network receives the current state of cart-pole system through its input layer: the location of the cart $(c_x, c_y)$, the angle of pole relative to the $z$-axis $\theta_z$, and to the $x$-axis $\theta_x$. The five hidden-layer neurons are fully recurrently connected (thick solid arrows), and they receive input from all four sources (thin dashed lines). The activation value in each neuron is either facilitated (FAN), decayed (DAN), or unmodified (control). Activations in the two output neurons $f_x$ and $f_y$ indicate the force to be applied to the cart in the $x$- and the $y$-axis direction, respectively.

and evaluated on the given task. After fitness evaluation (fitness is defined as the number of steps the pole is balanced), the score is added to the cumulative fitness of each neuron that participated in the network. This process is repeated until each neuron has participated in 10 trials on average.

3. Recombination: The neurons showing high fitness are mated using crossover, and then mutated (mutation rate = 0.7, i.e., 70% of neurons in the subpopulation are mutated) to produce new offsprings.

4. The Evaluation and Recombination cycle is repeated until a network successfully

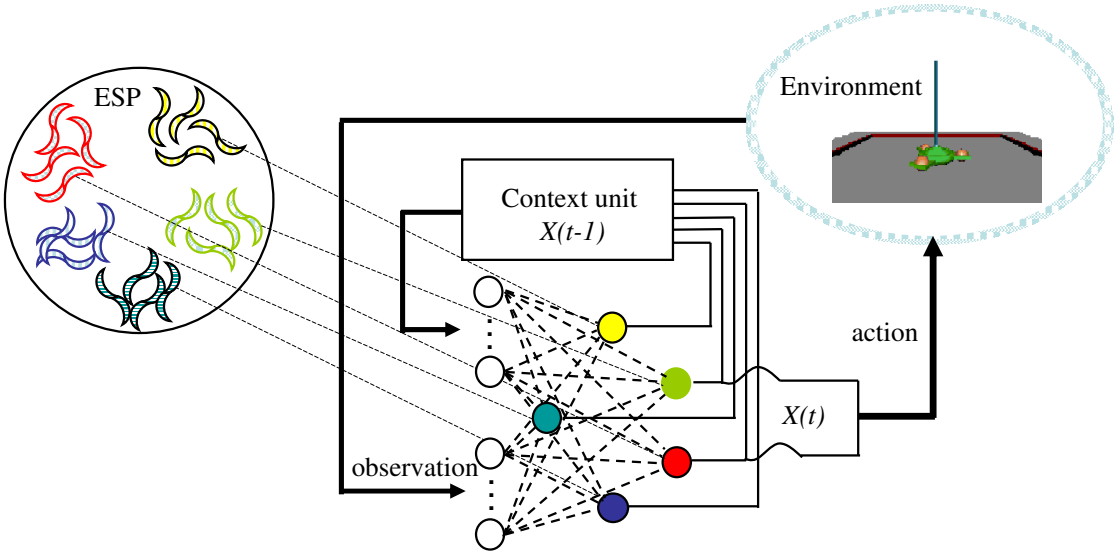


Fig. 37. **Neuroevolution of recurrent neural network controller.** A fully recurrent neural network controller was trained through the Enforced Subpopulation algorithm [8]. For each trial, 5 neurons were drawn from five subpopulations to randomly construct a controller network. The activation values generated from the neurons are retained in the context units, and at the next time step, they are fed into the network along with the current input data from the environment. In each generation, 400 randomly combined networks were evaluated. Based on fitness evaluation (the number of steps the pole was balanced), the neurons were sorted. The neurons showing high fitness were mated using crossover, and then mutated to produce new offsprings. The controller was considered successful if it succeeded in balancing the pole for 10,000 steps (i.e. 100 seconds) within 70 generations. (Adapted from [8].)

completes a task or reaches the final generation.

## 2 Pole-balancing controller using ESP

To test the idea (i.e., for fast extrapolation, extrapolation has to be implemented at a single-neuron level), I used ESP as the basis of my simulations. With ESP, the

neurons in each subpopulation can evolve independently, and rapidly specialize into good network sub-functions.

As shown in Fig. 37, the neurons were drawn from five populations, each consisting of forty neurons, to randomly construct a controller network. In each generation, 400 randomly combined networks were evaluated (each individual in a subpopulation participated in the task 10 times), and the number of generations was limited to 70 for each trial. The controller was considered successful if it succeeded in balancing the pole for 10,000 steps (i.e., 100 seconds) within 70 generations.

By using ESP as a basic framework, we can effectively observe how a single neuron, located in a particular position in the network, develops extrapolatory capability. It turns out that two output neurons which generate force to be applied to the cart (i.e., $f_{\mathrm{x}}$ and $f_{\mathrm{y}}$ in Fig. 36) greatly evolve their facilitation rates while the other neurons do not.

## 3 Experimental setup

For realistic physical modeling with friction, the pole balancing behavior was modeled with fourth-order Runge-Kutta integration (see Eq. 6.1 to Eq. 6.4 for full details) [8]. To control the pole cart, I used a recurrent neural network with five neurons (Fig. 36). The neurons were fully recurrently connected, and all neurons received input from four sources: $c_x$, $c_y$, $\theta_z$, and $\theta_x$, as introduced in Sec. VI.1 (Fig 35). The final activation values were generated by using the sigmoid function.

Two output neurons generated the force in the $x$ and the $y$ direction. The optimal values for the configurable parameters in each neuron were found through ESP. Each neuron was assigned a chromosome containing the connection weights (for DAN, control, and FAN) and optionally the decaying activation rate $r_d$ for DAN and

the facilitation rate $r_f$ for FAN (see Fig. 38). The physical parameters for the cart-pole system were given as in Tab. 1. Notice that due to the difficulty of the delay problem, a short pole length (0.1 m) was used.

The activation value of each neuron constituting FAN is defined as follows (see Sec. III.1 for details):

$$A(t) = X(t) + r_{\mathrm{f}}(X(t) - A(t-1)), \tag{6.5}$$

where $A(t)$ is the facilitated activation level at time $t$, $X(t)$ the instantaneous activation solely based on the instantaneous input at time $t$, and $r_{\mathrm{f}}$ the *facilitation rate* ($0 \leq r_{\mathrm{f}} \leq 1$).

The activation value for DAN is defined as follows (see Sec. III.1):

$$A(t) = r_{\mathrm{d}}A(t-1) + (1 - r_{\mathrm{d}})X(t), \tag{6.6}$$

where $A(t)$ is the decayed activation level at time $t$, $X(t)$ the instantaneous activation solely based on the current input at time $t$, and $r_{\mathrm{d}}$ the decay rate ($0 \leq r_{\mathrm{d}} \leq 1$). With these simple equations, I implemented networks with facilitating activity and decaying activity. Finding appropriate values for the parameters was done through neuroevolution (ESP).

I compared the performance of three different network types (250 experiments each): (1) Facilitating Activity Network (FAN), where facilitation rate $r_{\mathrm{f}}$ was included as an evolvable parameter along with the standard connection weights; (2) Control, which was the baseline ESP implementation where only the weights were evolvable; and (3) Decaying Activity Network (DAN), where decay rate $r_{\mathrm{d}}$ was evolvable in the same manner as in FAN. To compare fairly the performance of the three networks, I set

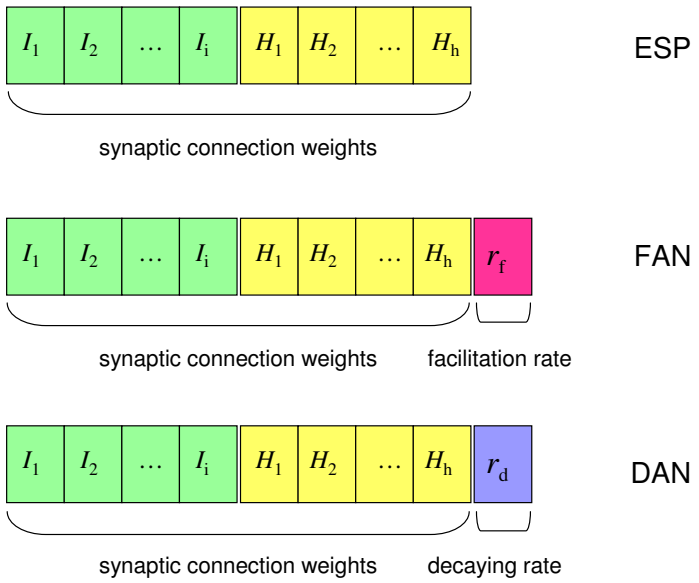


Fig. 38. **Genotypes of facilitating activity network (FAN) and decaying activity network (DAN).** In the original ESP, synaptic connections and their weights are encoded in the chromosome ($I_i$ represents the weight value of the connection from the input neuron $i$ and $H_h$ the hidden neuron $h$). ESP was modified to use facilitating or decaying dynamics. To add facilitating dynamics, facilitation rate parameter $r_{\mathrm{f}}$ was encoded in the chromosome of each neuron (FAN; middle). Thus, facilitation rate could evolve as well as the connection weight. For decaying dynamics, $r_{\mathrm{d}}$ was encoded in the chromosome (DAN; bottom).

parameters other than those in the chromosome to be equal (e.g., number of neurons, mutation rate, etc.; see above). All weight values and the facilitation/decay rate parameter values were uniformly randomly initialized between 0.0 and 1.0. Initially, the cart was located in the center of the 2D boundary ($c_x = c_y = 0.0$) and the pole was initialized with a tilt of 0.01 radians ($\theta_z = \theta_x = 0.01$).

## VI.3 Experiments and Results

I tested the three networks (FAN, Control, and DAN), under different internal delay conditions as well as under the baseline case without delay. The results from each experiment are reported in this section. I will also analyze the neuronal activation and the internal state of each network; the networks' behavior; and the performance under various input delays.

### 1 Neural activation and internal state trajectory

First, I compared the neural activity in the three networks to generally characterize the effects of adding facilitation/decay in the neural dynamics in the controller network. In these experiments, all four inputs were given with a 1-step (10 ms) delay beginning from 50 and lasting at 150 evaluation steps within each individual trial. (The results were similar for other delay conditions.)

I traced the activation values generated by an output neuron (top left unit in Fig. 36) from the three different networks. Fig. 39 shows the results. The activities of the other output neuron (top right neuron in Fig. 36) showed a similar pattern as in Fig. 39 and 40 (data are not shown here). In each plot, the first 1,000 steps of the activation values are shown. Because of the early introduction of input delay (50 to 150 steps), DAN and control network showed large fluctuation in their neural activation level. FAN, on the hand, initially showed a large fluctuation (Fig. 39*c*), but quickly settled to a very stable low-amplitude oscillation, and maintained the stability (Fig. 40*c*).

Fig. 40 shows the last 1,000 steps of activation values (from the same networks as in Fig. 39). Although the results from all three networks are from successful trials,

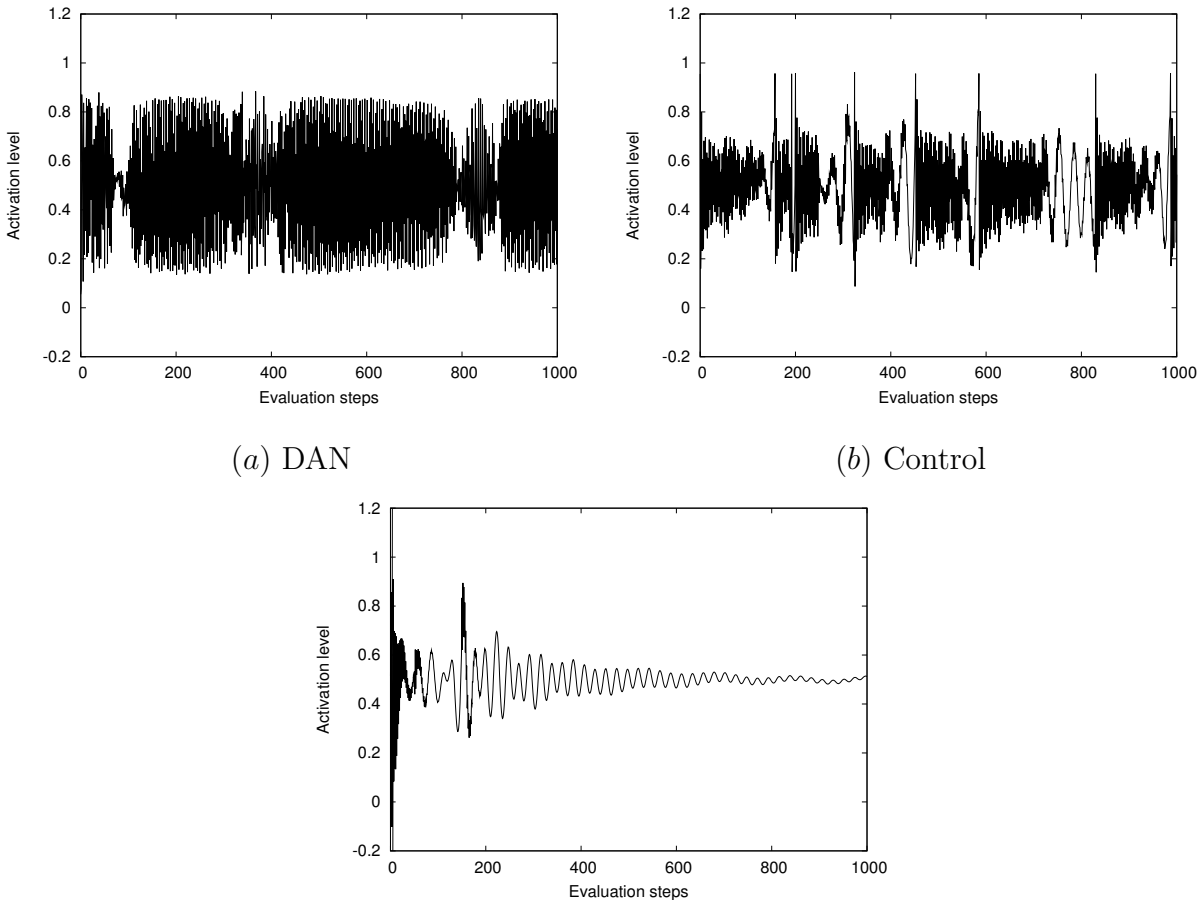


(*a*) DAN (*b*) Control

(*c*) FAN

Fig. 39. **Activation level of output neurons: first 1,000 steps.** The first 1,000 steps of activation levels from successful cart controller networks with different activation dynamics are shown. The $x$ axis is the evaluation step and the $y$ axis the activation level of one output neuron ($f_x$ in Fig. 36). The neurons received all four inputs with a 1-step delay (10 ms) during 50 to 150 evaluation steps ($x$-axis). (*a*) Decaying Activity Network (DAN), even though successful in balancing the pole, shows a large, noisy fluctuation from the beginning. (*b*) The unmodified network (i.e., the control) is slightly less noisy than DAN. (*c*) Facilitating Activity Network (FAN) shows a large fluctuation in the beginning and at the introduction of delay ($t = 50$), but quickly settles into a very low-amplitude, low-frequency oscillation.

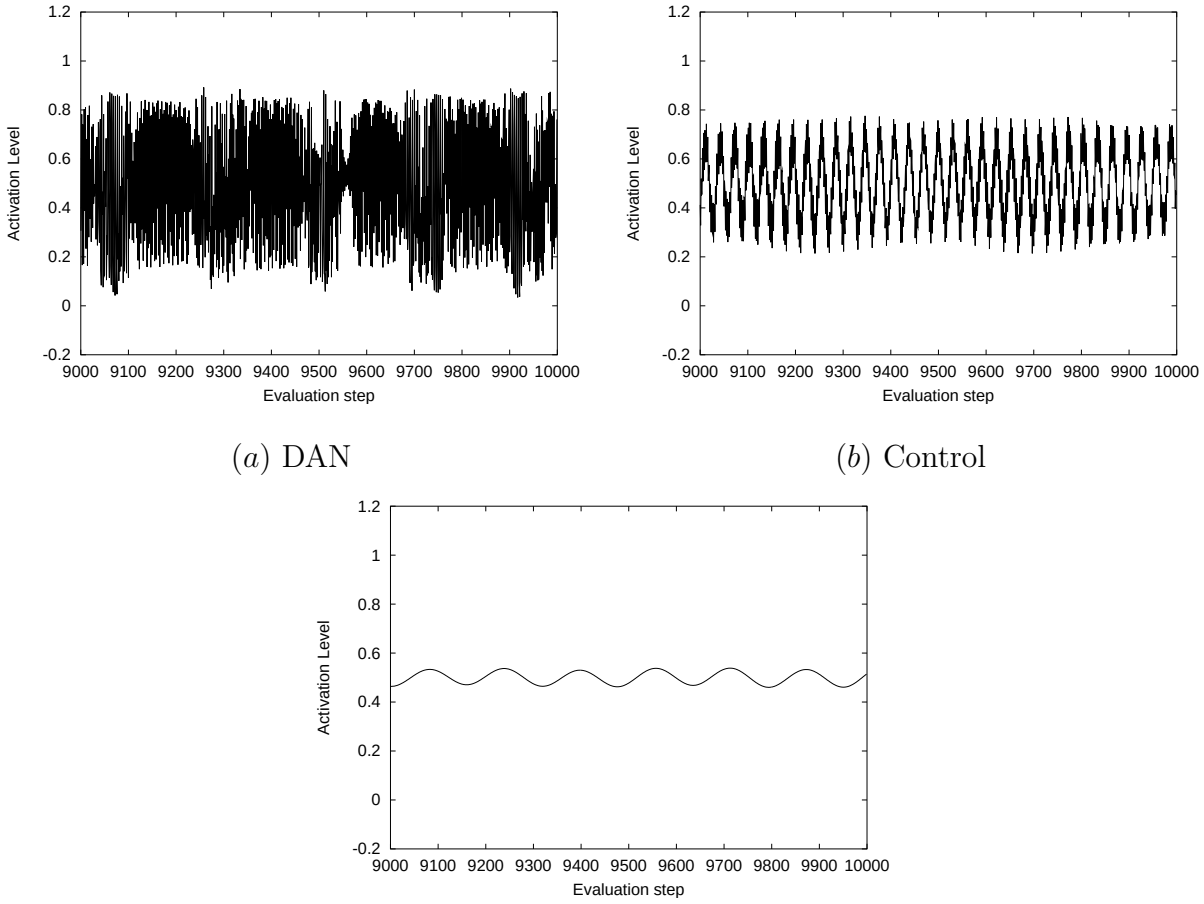


($a$) DAN

($b$) Control

($c$) FAN

Fig. 40. **Activation level of output neurons: last 1,000 steps.** The last 1,000 steps of activation levels from successful cart controller networks with different activation dynamics are shown. The plotting conventions are the same as in Fig. 39. ($a$) DAN shows a large, noisy fluctuation to the end of task. ($b$) Control network becomes less noisy than the initial 1,000 steps (as shown in Fig. 39$b$), but it still shows a high-amplitude oscillation compared to FAN. ($c$) FAN settled into a very stable state showing a low-amplitude and low-frequency oscillation.

the activity traces are markedly different across different controller networks. DAN produced an on-going, noisy, and high-amplitude oscillation in its neural activity (Fig. 39$a$ and Fig. 40$a$). Compared to DAN, the control showed less noise but the

oscillation had a relatively high amplitude (Fig. 39*b* and Fig. 40*b*). FAN, on the other hand, initially showed a large fluctuation (Fig. 39*c*), but quickly settled to a very stable low-amplitude oscillation, and maintained the stability (Fig. 40*c*). These results suggest that even though extrapolation is generally known to be unstable, if used in a short term, and sparingly, it can help faster convergence to a stable state in tasks with delay.

Also, to trace how the internal states of the three networks are different from each other, I used principal components analysis on the activation values of the five hidden neurons. The three networks showed markedly different internal states (Fig. 41). The PCA projections from the last 1,000 steps are shown in Fig. 42. The difference in internal states persisted to the end of the trials. FAN kept relatively continuous and stable states whereas DAN and the control network endured discrete and scattered internal states under input delay conditions.

## 2 Behavioral trajectory

The next step is to compare the overall behavior of the cart under the three different controller networks. The delay condition was the same as above. I traced the cart trajectories to gain insight into how the differing neural dynamics translate into the behavior of the cart. Cart trajectories are shown in Fig. 43 for the first 1,000 steps and Fig. 44 for the last 1,000 steps. Note that the relative scale of the $x$- and the $y$-axis is the same in all three plots $(a)$ to $(c)$ while they are different in the three plots $(d)$ to $(f)$. That is, $(a)$ to $(c)$ show the same data as $(d)$ to $(f)$, at a different scale. Not much difference in behavior is found between the first and the last 1,000 steps. The cart trajectory in DAN was erratic and involved large motions, reflecting the noisy high-amplitude oscillation seen in its activation (Fig. 43*a*, *d* and 44*a*, *d*). The

control on the other hand had a wiggly trajectory (Fig. 43*b*, *e* and 44*b*, *e*). However, FAN had a trajectory with a very small footprint that was also very smooth (Fig. 43*c*, *f* and 44*c*, *f*), suggesting that the facilitating dynamics in single neurons contributed to a more accurate control of the cart. Other successful trials showed similar relative difference in behavior (data not shown).

### 3 Performance under different input delay conditions

In order to test the ability of the three networks in delay compensation, I conducted experiments under four different delay conditions: (1) without delay, (2) with a uniform amount of delay for all input sources ($c_x$, $c_y$, $\theta_z$, and $\theta_x$) for a fixed, limited period of time during each run, (3) delay in $\theta_z$, and (4) delay in $\theta_x$ throughout the entire duration of each run. Fig. 45 summarizes the results under these different experimental conditions.

In experiment 1, the base case, I tested the standard task without any delay. Under this condition, FAN had an average success rate of 0.76 (average of success rates from 5 sets, each set consisting of 50 trials), the best performance compared to the two other controllers ($t$-test, $p < 0.001$, $n = 5$ sets). The control did fairly well (success rate 0.62), while DAN showed the lowest success rate (0.17). It is interesting to note that even without delay, FAN showed the best performance. These results establish a benchmark against which the more difficult tasks below can be assessed.

In experiment 2, all sensor inputs were delivered with one step delay (10 ms) in the middle of the evaluation, beginning from 50 iterations and lasting until 150. Note that this is a difficult task because all the inputs are delayed. If the delays were introduced from the beginning or if they lasted longer than 100 iterations, performance in all controllers significantly degraded.

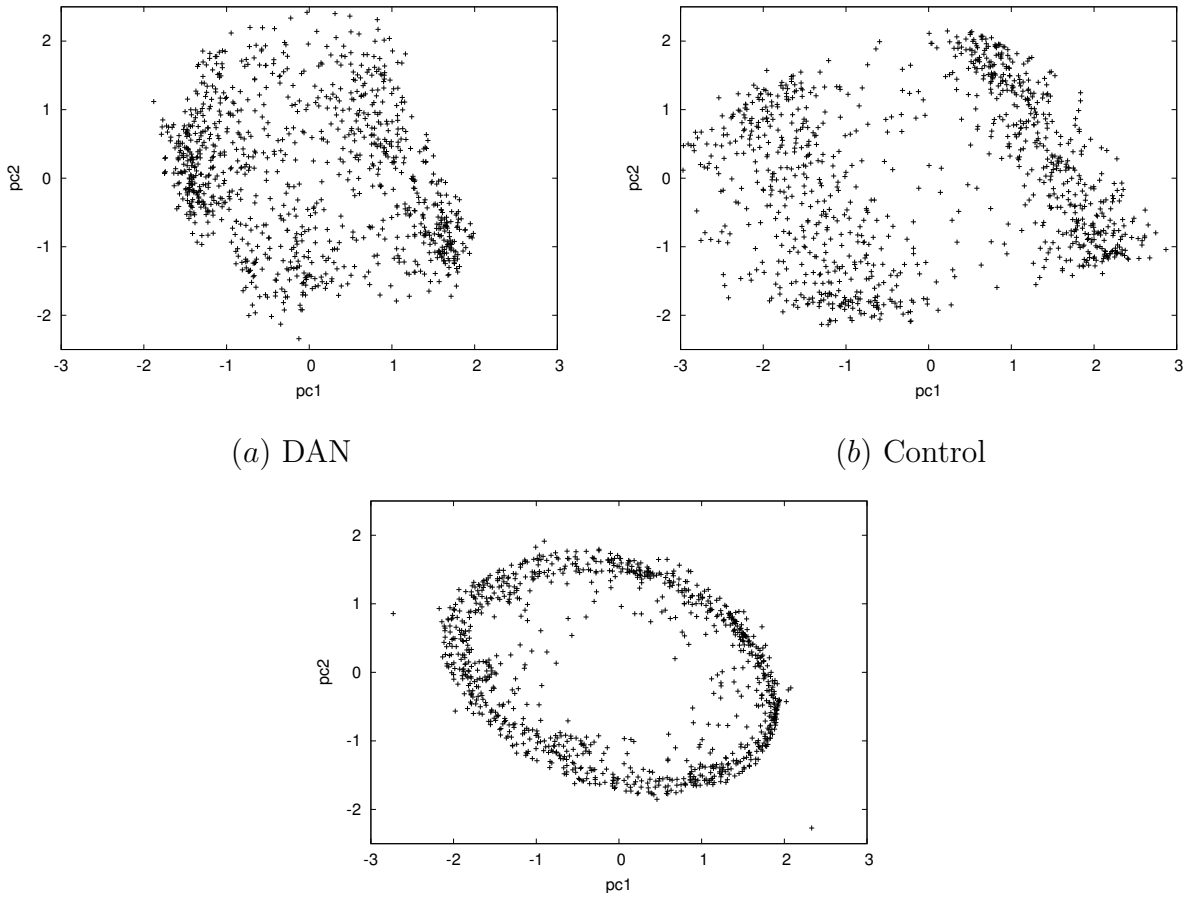


($a$) DAN ($b$) Control

($c$) FAN

Fig. 41. **Internal state of hidden neurons: first 1,000 steps.** First 1,000 steps of projections of the hidden neuron (five neuron) states to their first and second principal component axes (PC1 and PC2) are shown. The networks had delay in all inputs from 50 to 150 steps for each trial. The three networks shows different internal states from the first 1,000 steps of the trial to the end of trial (Fig. 42 shows the internal states from the final 1,000 steps). ($a$) DAN shows randomly scattered internal states from the beginning of the trial. ($b$) Control network shows divided and scattered states. ($c$) FAN shows more organized internal states compared to control and DAN starting from the early steps.

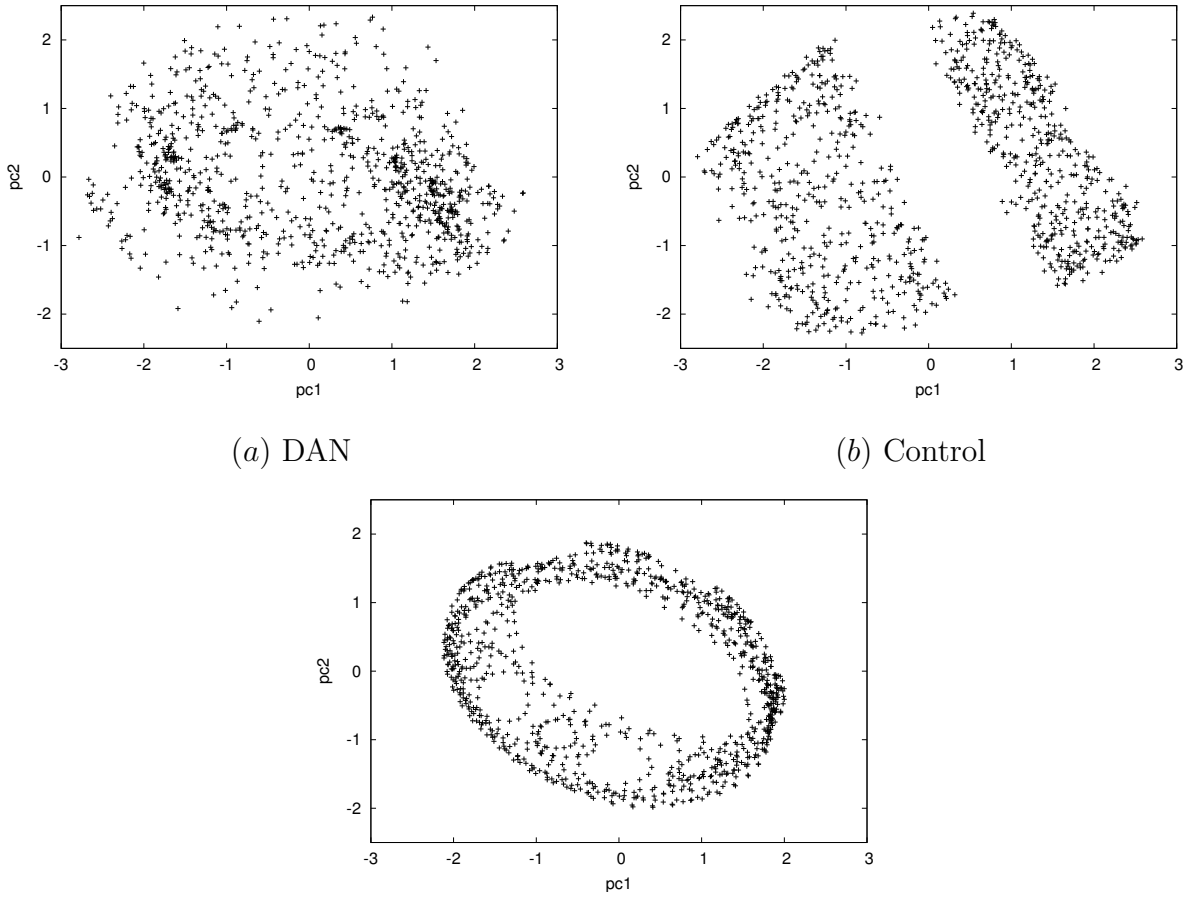


($a$) DAN ($b$) Control

($c$) FAN

Fig. 42. **Internal state of hidden neurons: last 1,000 steps.** Last 1,000 steps of PCA projections of the hidden neuron states are shown. The experimental conditions and plotting conventions are the same as in Fig. 41. ($a$) DAN maintained randomly scattered internal states throughout the trial. ($b$) Control network showed more organized internal state than DAN, but had divided and discrete states compared to FAN. ($c$) FAN kept relatively continuous and organized internal state trajectory.

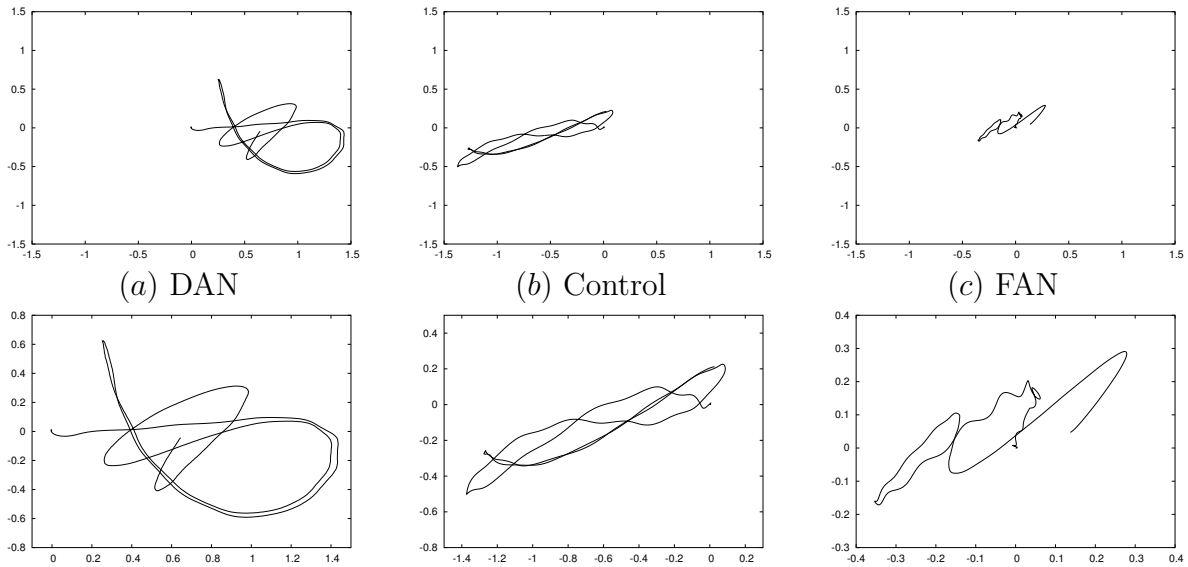

($a$) DAN ($b$) Control ($c$) FAN

($d$) DAN ($e$) Control ($f$) FAN

Fig. 43. **Cart trajectories under input delay condition: first 1,000 steps.** The trajectory of carts using different controllers are shown when there was delay in the input (the first 1,000 steps are shown). The $x$ and the $y$ axes represent the ($x$, $y$) location of the cart. The networks received all four inputs with a 1-step delay (10 ms) during 50 to 150 evaluation steps. Note that the relative scale of the $x$- and the $y$-axis is same in the three plots ($a$) to ($c$) while they are different in the three plots ($d$) to ($f$). ($a$), ($d$) The trajectory of Decaying Activity Network (DAN) is large and erratic. ($b$), ($e$) The control is stabler than DAN but exhibits a wiggly trajectory. ($c$), ($f$) The Facilitating Activity Network (FAN) shows a smooth trajectory with a very small footprint.

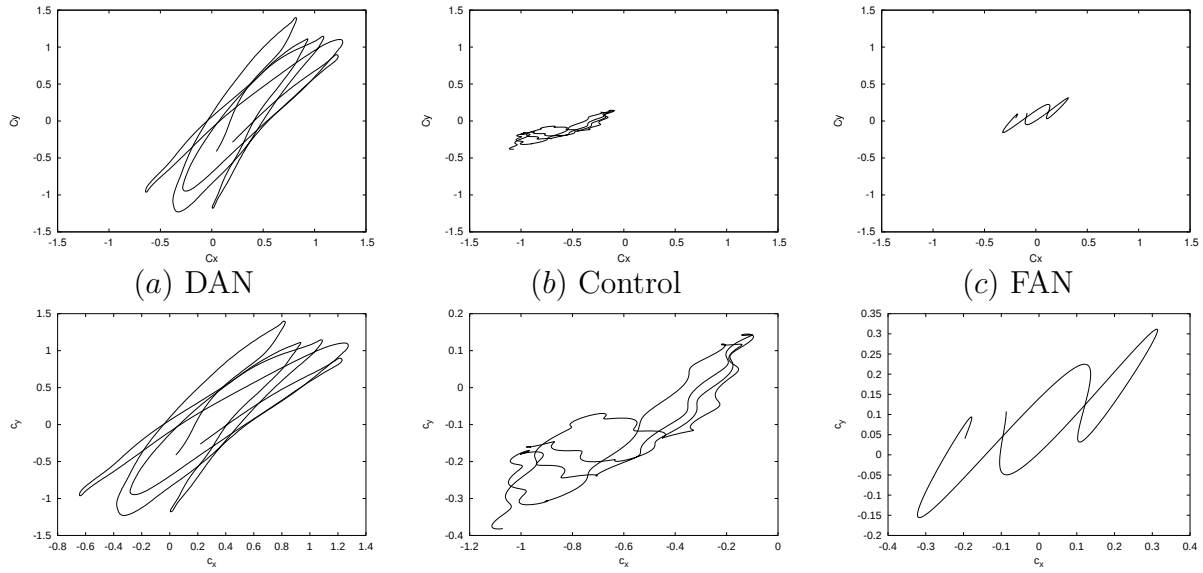


($a$) DAN ($b$) Control ($c$) FAN

($d$) DAN ($e$) Control ($f$) FAN

Fig. 44. **Cart trajectories under input delay condition: last 1,000 steps.** The trajectory of carts using different controllers are shown when there was delay in the input (the last 1,000 steps are shown). See Fig. 43 for the plotting conventions and experimental conditions. The behaviors of the three carts are similar to those from the first 1,000 steps as shown in Fig. 43. ($a$), ($d$) DAN shows large and erratic trajectory as in the first 1,000 steps. ($b$), ($e$) The control shows stable and much smaller footprint than DAN but exhibits a wiggly trajectory compared to FAN. ($c$), ($f$) FAN shows a smooth trajectory with a very small footprint.

For this delay condition, again FAN did the best ($t$-test, $p < 0.005, n = 5$): success rate of 0.52 for FAN, 0.33 for control, and 0.03 for DAN. An important observation at this point is that FAN was more robust than the two other controllers. In case of FAN, the success rate decreased by 32% from that in experiment 1, the base case. However, the control degraded by 48%, and DAN by 82%. These results indicate that the facilitatory dynamics in FAN is effective in compensating for delay.

In experiments 3 and 4, one step delay in either $\theta_z$ or $\theta_x$ was introduced throughout the entire duration of each trial (Fig. 45, 3rd and 4th experiments from the left).

Note that in these experiments, the delay in these two inputs persisted over the entire trial, unlike in experiment 2. Since all inputs except for $\theta_z$ or $\theta_x$ were received on time, the controllers were able to maintain some balance (for FAN and the control). However, DAN totally failed in both experiments (thus the results are not reported in Fig 45). As for the successful controllers, FAN significantly outperformed the control under both conditions ($t$-test, $p < 0.002, n = 5$): The success rates in experiment 3 were 0.09 for FAN and 0.02 for the control; and for experiment 4, 0.27 for FAN and 0.08 for the control network. An interesting trend in these results is that the delay in $\theta_z$ had a more severe effect on the performance than that in the other input. This was somewhat expected, because $\theta_z$ is the angle from the vertical axis, and that angle was used to determine whether the pole fell or not (the pole is considered down if $\theta_z > 15^o$).

Another interesting question is how fast these networks learn to balance the pole. For this I compared the number of generations each of the three controllers took to successfully balance the pole for the first time. For each controller, 250 evolutionary trials (5 sets of 50 trials each) were run where each trial was limited to 70 generations beyond which the controller was treated as failed. The results are summarized in Fig. 46 for experiments 1 to 4. FAN required the least number of generations before successfully balancing the pole in all cases (t-test, $p < 0.0002$, $n = 5$) except for experiment 3 (delay in $\theta_z$) where no difference was found between FAN and the control ($p = 0.84$, $n = 5$). As before, DAN could not learn in the time limit of 70 generations for experiments 3 and 4, thus the results are not reported here.

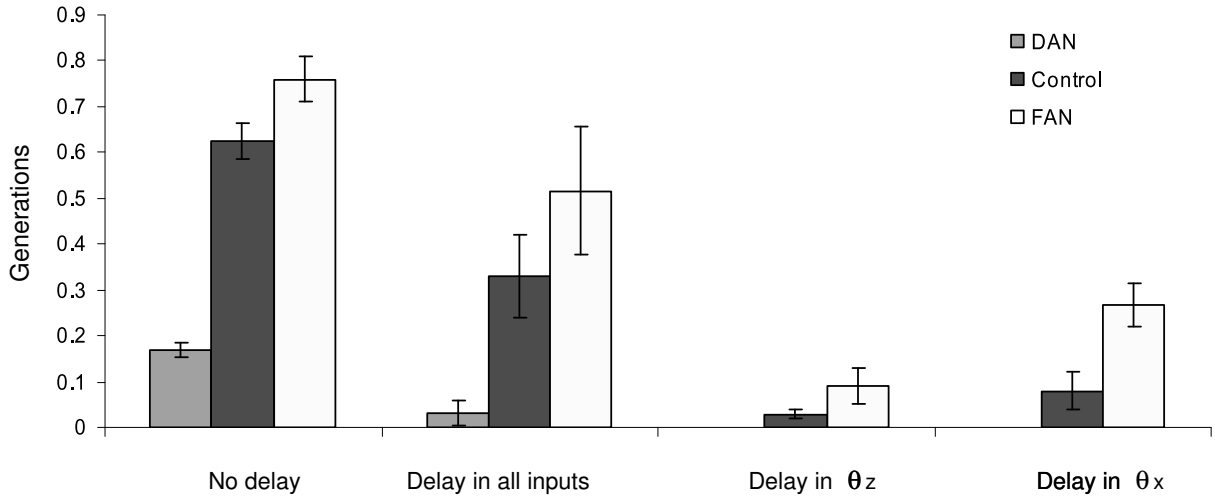


Fig. 45. **Success rate under different delay conditions.** The success rates for balancing the pole using different controllers are shown for four different delay conditions. From left to right, (1) default condition without delay, (2) delay in all inputs $c_x$, $c_y$, $\theta_z$, and $\theta_x$ from step 50 to 150, (3) delay in $\theta_z$ only during the entire period, and (4) delay in $\theta_x$ only during the entire period are shown. Dark gray bars represent the success rate of the control network, gray bars that of the decaying activity network (DAN), and light gray bars that of the facilitating activity network (FAN). For conditions (3) and (4), DAN failed in all experiments, thus the data are not shown here. Error bars indicate $\pm 1$ standard deviation. In all cases, FAN outperformed the rest (t-test, $p < 0.005$, $n = 5$).

## 4 Performance under increasing delay

As a biological organism grows, its size increases and thus the neural processing delay increases as well. How can the nervous system cope with the increase in neural delay? Although certain tasks such as synchronization over a delay line can be achieved via Hebbian learning [35], little is known about how information content can be delivered over a delay line in a timely manner.

To test whether FAN can maintain performance under increasing delay, I in-

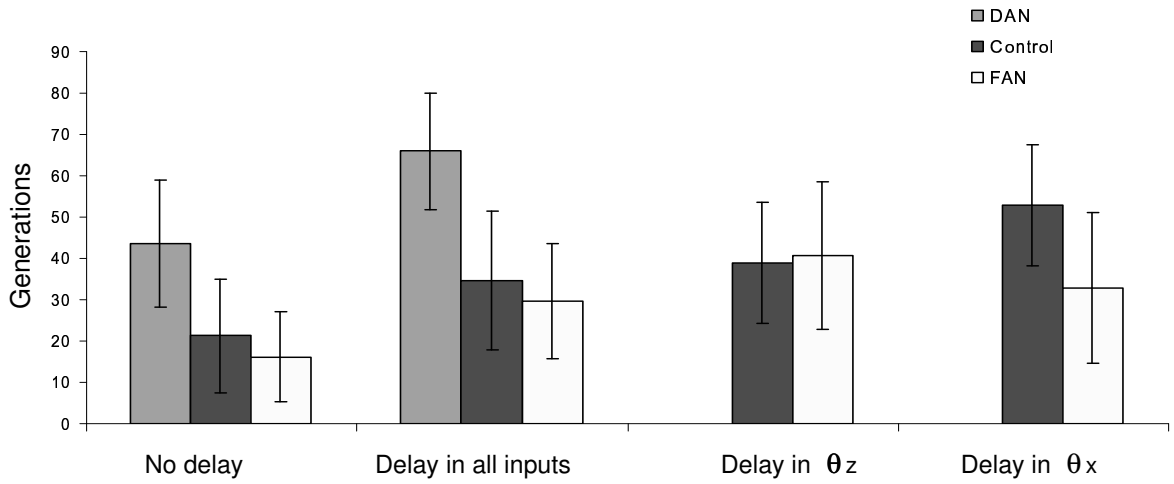


Fig. 46. **Comparison of learning time under different delay conditions.** The learning time (in the number of generations) is shown for different controllers under different delay conditions (see Fig. 45 for plotting conventions). In all cases, the Facilitating Activity Network (FAN) took less time to learn than both the Decaying Activity Network (DAN) and the control network (t-test, $p < 0.0002$, $n = 5$), except for the $\theta_z$-delay case ($p = 0.84$). Again, DAN never reached the goal under the last two delay conditions, thus the data are not shown.

creased the delay from 10 ms (1 step) to 30 ms (3 steps) across evolutionary trials. In this experiment, $\theta_z$ was delivered with delay, beginning from 50 steps and lasting until 150 steps within each trial. The performance results were compared to those of the control and of DAN. The results are reported in Fig. 47. All three networks showed a decrease in their success rate as the delay length increase. In this example, DAN could not sustain even 1-step input delay (see Fig. 45, 3rd experiment). However, FAN showed a slower degradation in performance compared to the control network, demonstrating that FAN is more sustainable to the increasing delay. These results suggest that facilitating dynamic can help overcome increasing delay during growth.

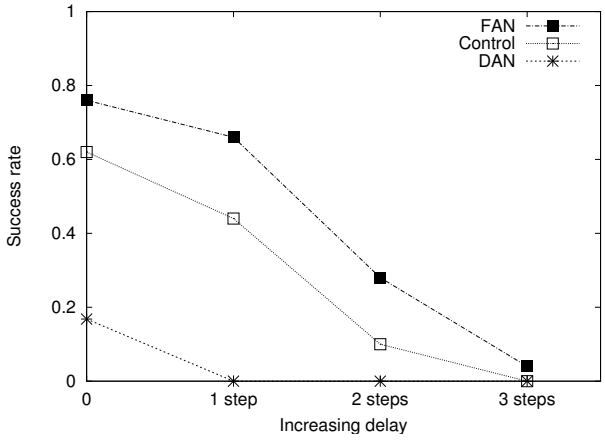


Fig. 47. **Effect of increasing delay.** The effects of increasing the input delay duration are shown for the three different controllers: the Decaying Activity Network (DAN), the control network, and the Facilitating Activity Network (FAN). The success rates ($y$ axis) are shown for a range of delay in $\theta_z$, from one to three steps ($x$ axis). FAN outperformed the control and DAN under all conditions. Notice that DAN could not solve the problem even under 1-step delay of $\theta_z$.

## 5 Performance under input blank-out

An interesting question arising here is whether facilitatory activity can counteract delay in the *external* environment. Suppose a moving object goes behind another object (i.e., it is occluded). Until that moving object comes out again, the input may be unavailable. In fact, humans are known to be good at dealing with such a "blank out" of input in the external environment. Mehta and Schaal conducted "virtual pole" experiments where human subjects were asked to balance the pole on the computer screen where the input was blanked out for up to 600 ms at a time [9]. (See Fig. 48 for details.) They found that, after some training, humans can overcome input blank-out up to 600 ms. Based on these results, they proposed that internal forward model exists in the central nervous system, which can extrapolate the current input into the future state based on the past input (see Chap. 7 for more discussion).

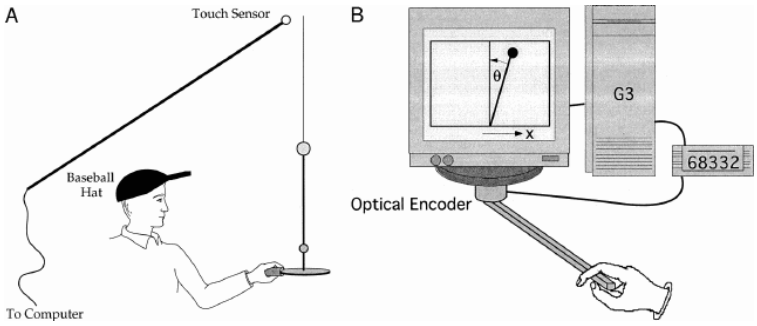


Fig. 48. **Virtual pole balancing task.** To measure the predictive ability in humans under visual occlusion, Mehta and Schaal [9] conducted blank-out test during virtual pole-balancing. In the blank-out test, the pole disappeared from the computer screen at random times for a randomly chosen period between 450 and 550 ms, while the subject was balancing the virtual pole. Subjects were instructed to ignore the blank-out and to continue balancing. It was shown that after some training, subjects could tolerate 500 ms to 600 ms blank-out times. (Adapted from [9].)

It is conceivable that facilitatory dynamics can also help in this kind of situation as well.

To test if this is the case, I conducted two input blank-out experiments. One assumption was that the neurons would maintain steady-state firing during the blank-out for both tests so that the neurons will remain signaling their last-seen state. Thus the input data last seen immediately before the blank-out were fed into the neurons during the blank-out period.

In experiment 1, the input was blanked out for a short period of time analogous to an occlusion event as described above. Blank-out was applied to the network when the controller reached 500 steps of balancing the pole during learning. With this we can test how good the networks are in overcoming the external uncertainty, before convergence.

Fig. 49 shows the result of experiment 1. FAN showed higher performance than

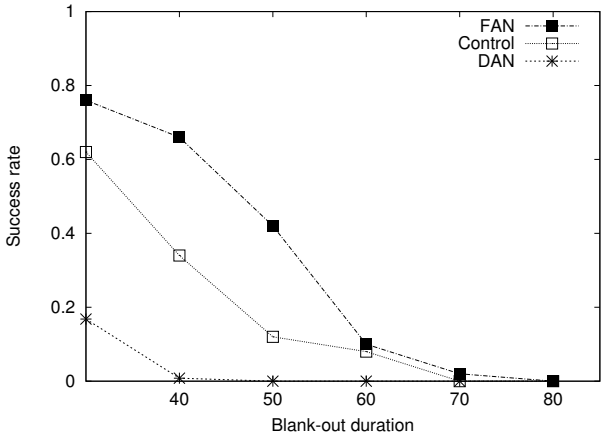


Fig. 49. **Effect of increased blank-out duration.** The effects of increasing the input blank-out duration are shown for the three different controllers. The success rates ($y$ axis) are shown for different blank-out durations, from 40 steps to 80 steps ($x$ axis). In the blank-out experiments, the input to the network was clamped, for a limited duration, to the input value at the beginning of that clamping period, effectively blocking any current information from entering the network. Again, FAN showed a slow decrease in performance compared to the others. Notice that beyond 60 steps of blank-out, performance degraded significantly in all controllers.

the other controllers. Compared to the control network, FAN showed slow decrease of performance by 50 steps and this trend is very similar to the sustainable blank-out period observed in humans [9].

In experiment 2, successful networks from the experiment with "delay in all input" condition (Fig. 45, 2nd experiment) were saved and loaded to be tested under blank-out condition. This test will show how good the successful networks (developed with internal delay) are in dealing with environmental uncertainty with specific neural dynamics built in the neurons.

For the experimental setup, first, the control and FAN networks were trained under delay (1-step delay in $\theta_z$ from 50 to 150 iterations). (Notice that DAN could not develop successful controller under $\theta_z$ delay so we have no result from DAN.) When a

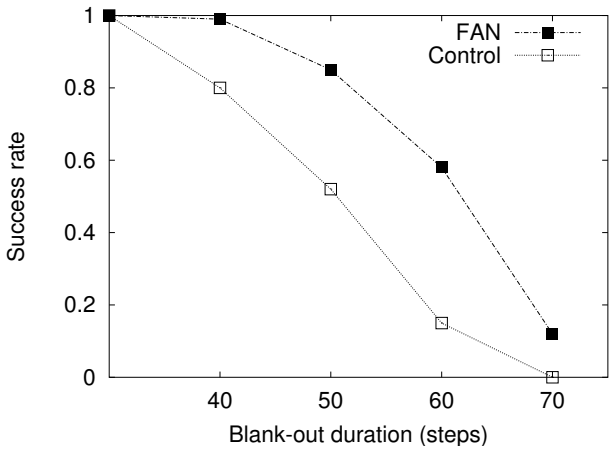


($a$) Success rate

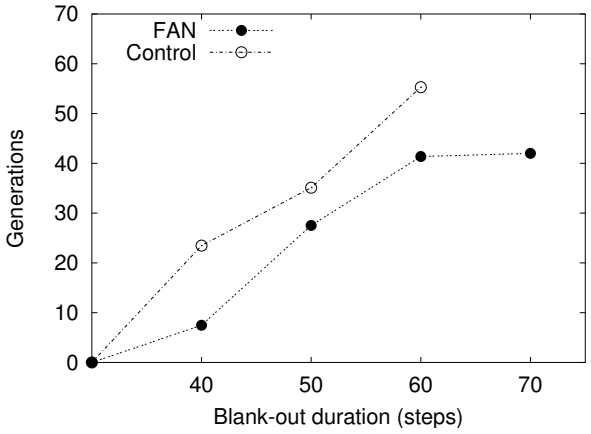


($b$) Learning time

Fig. 50. **Blank-out test: after development.** Successfully trained networks under input delay were tested under input blank-out condition. Note that due to the low success rate of DAN in the input delay test, only the control and FAN were tested. ($a$) FAN trained under delay condition shows high success rate in performing blank-out test and shows slow decrease in performance until 60 steps (600 ms), which is similar to the observation in human experiments by [9]. ($b$) Compared to the control network, FAN learns quickly to find the solution under input blank-out. On the contrary, the control networks showed a speedy decrease in performance ($a$), and could not solve the problem beyond 70 steps (700 ms).

network succeeded in solving the pole-balancing problem, the learned parameters such as connection weights and dynamic activation rates (i.e., $r_f$ and $r_d$) of the neurons were stored. Then, the successful FAN and control networks were loaded and tested under blank-out condition. A total of 50 successful networks from FAN and control were tested.

As shown in Fig. 50($a$), FAN showed higher performance than the control network and slow degradation in performance until 600 ms (60 steps). Also, the learning time was significantly faster than the control network, as shown in Fig. 50($b$). The control network showed a steep decrease in performance and could not solve the problem beyond 70 steps of blank-out duration (i.e., 700 ms, success rate = 0 in Fig. 50($a$)). Experiments with the blank-out test have shown that FAN can also effectively deal with *external* delay by utilizing its extrapolatory neural activity, initially developed to cope with internal delay.

## 6 Contribution of facilitation and decay rate

The performance results reported in the previous sections suggest that the facilitation rate $r_{\mathrm{f}}$ coded in the gene of the FAN controller serves a useful purpose. To verify if indeed the rate parameters are being utilized, we can look at the evolution of these parameters over the generations. Fig. 51 shows an example from a single run that shows evolution of the rate parameters in FAN and DAN. The $x$-axis represents the index of the neurons in a subpopulation sorted by their fitness values, and the $y$-axis the decay or facilitation rate. Initially, the rates are uniformly randomly distributed between 0 and 1 (Fig. 51$a$ and $c$). However, the rates in the final generation look markedly different in FAN vs. DAN. In case of FAN, the top-performing individuals (those on the left) have a high facilitation rate, near 1 (Fig. 51$d$). This means that

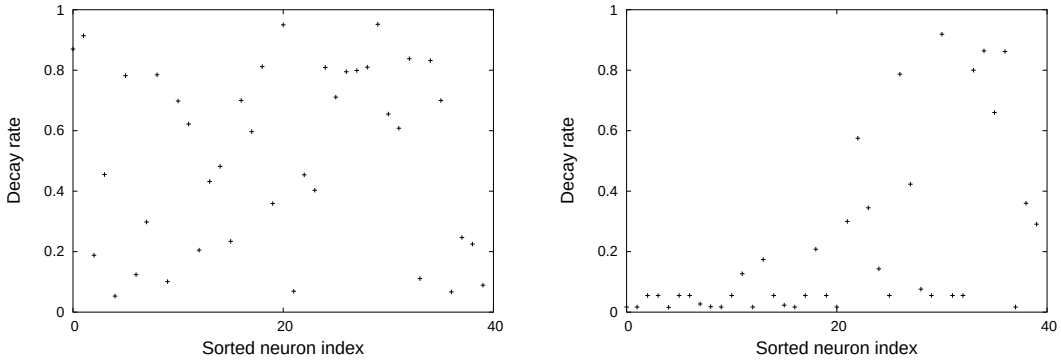


($a$) DAN: Initial state ($b$) DAN: Final state

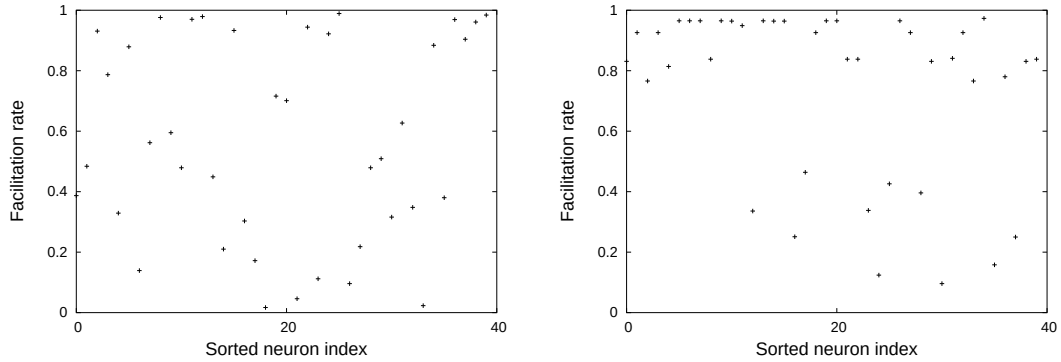


($c$) FAN: Initial state ($d$) FAN: Final state

Fig. 51. **Evolved decay rate and facilitation rate.** The initial and evolved decay and facilitation rates are shown for two sample subpopulations. Each subpopulation, from which one neuron was drawn to participate in a network, consisted of 40 neurons. The $x$ axis represents the sorted neuron index (in decreasing order of fitness) and the $y$ axis the value of the rate parameter (either $r_{\mathrm{f}}$ or $r_{\mathrm{d}}$). ($a$) Initially, the DAN has uniformly randomly distributed rate values across the 40 neurons. ($b$) After successful training (generation 57), the top-performing neurons ($x$ up to about 10) within this individual show near zero decay rate $r_{\mathrm{d}}$, indicating that it is better to have the decay rate low (that is, just use the immediate input). ($c$) FAN also has initially random rate values. ($d$) After successful training (generation 32), the top-performing neurons ($x$ up to about 10) show a very high facilitation rate $r_{\mathrm{f}}$, suggesting that high $r_{\mathrm{f}}$ contributes to higher performance. The reason why not all rates converged to either 0 or 1 may be due to the enforced diversity in the ESP algorithm. In case of the control, the neural activation did not involve any rate parameter, thus nothing can be plotted here.

extrapolation is pushed to the max (Eq. 3.3), suggesting that neuroevolution tried to utilize the facilitating dynamics as much as possible. However, for DAN, the top-performers have very low decay rate, near 0 (Fig. 51*b*), suggesting that previous activity, in a decayed form, is not being utilized at all (Eq. 3.1). In other words, decay dynamics does not contribute at all in task performance, and neuroevolution tried to minimize its effect by decreasing the decay rate to 0.

Fig. 52 shows the change in the rate parameter distributions from the initial generation (initial state: the group of bars on the left in Fig. 52*a* and *b*) to the final generation (final state: the group of bars on the right in Fig. 52*a* and *b*). Fig. 52*a* shows the distribution of evolved decay rate $r_d$ from successful DAN (4 successful trials, subpopulation size $p = 40$: 160 neurons $= 4 \times 40$). We can observe that in the initial state, the $r_d$ values are uniformly randomly distributed across the subpopulation, but after evolution, the successful networks show an increased number of neurons that have low $r_d$. In FAN, on the contrary, the successful networks (18 successful trials: 720 neurons $= 18 \times 40$) show an increased number of neurons that have high $r_f$ in the final state (cf. Fig. 51*c*, *d*). In sum, decaying activity (a form of memory) does not contribute to delay compensation, while a proper amount of extrapolation based on the memory can significantly help overcome the delay.

## 7 Discussion

In sum, facilitatory activation in single neurons significantly improved the ability of cart controllers to compensate for transmission delay within the controller system. Also, such a facilitatory dynamics allowed for faster learning. The failing performance of DAN is in itself an interesting phenomenon. Decay can be seen as a form of memory, where traces of activity from the past linger on in the present activity,

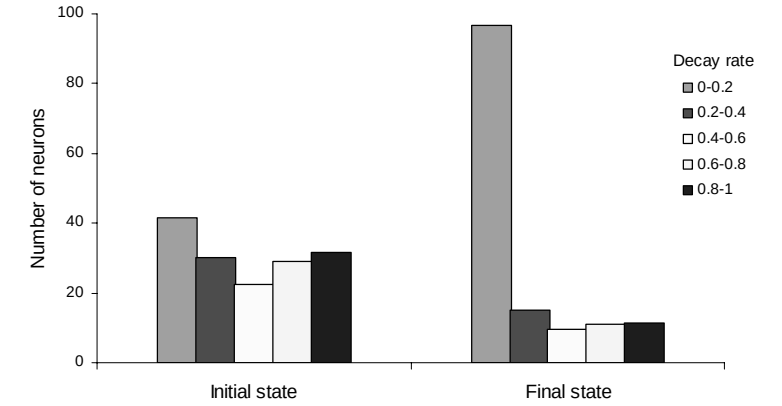


($a$) DAN

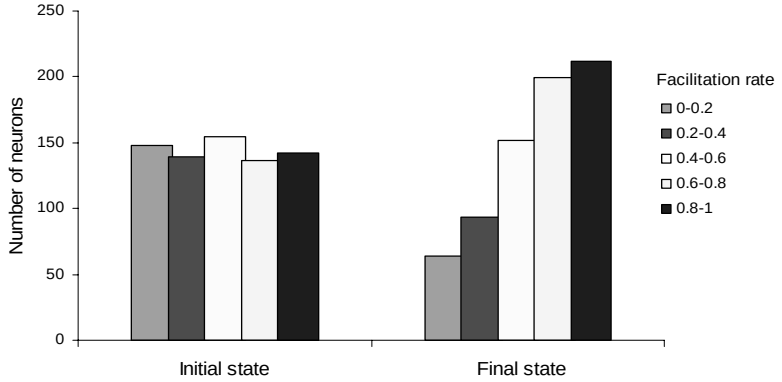


($b$) FAN

Fig. 52. **Distribution of evolved decay rate and facilitation rate from DAN and FAN.** The distribution of initial and evolved decaying rates and facilitation rates are shown. The networks received all four inputs with a 1-step delay (10 ms) during 50 to 150 evaluation steps. The group of bars on the left in $a$ and $b$ represent the distribution of decay (or facilitation) rate of initial generation. Those from the final generation are shown in the group of bars on the right in $a$ and $b$ ($a$) The distribution of evolved decay rate $r_d$ from successful DAN is shown. (4 successful trials out of 50 trials on average.) The subpopulation of an output neuron $f_x$ consists of 40 neurons, so the decaying rates of 160 ($4 \times 40$) neurons are shown. In the initial state, the $r_d$ values are uniformly randomly distributed across the subpopulation, but after evolution, the successful networks show an increased number of neurons that have low $r_d$. ($b$) FAN, on the contrary, shows an increased number of neurons that have high $r_f$ in the final state (18 out of 50 trials on average). The neurons evolved their facilitation rates into high values, suggesting the neurons highly utilized facilitatory neural activity under input delay.

thus we expected it to be beneficial. However, it turns out that such a form of memory does not contribute to delay compensation. On the contrary, it can make things even worse. The results also show that additional computation (as in decaying dynamics) does not always help improve performance. Finally, the adaptability of these dynamics can contribute in dealing with the growth of individual organisms as well as coping with external delay as shown in Fig. 49. The experimental results suggest that extrapolation, anticipation, and prediction, which are characteristics of facilitatory dynamics, may be serving an important role in delay compensation.

## VI.4 Summary

In this chapter, I have shown that the biologically inspired delay compensation model, FAM, can also help to overcome delay problem in real time control. Experiments with a modified 2D pole-balancing problem with sensory delay showed that facilitatory activation greatly helps in coping with delay. The same mechanism was also able to deal with uncertainty in the external environment, as shown in the input blank-out experiment. In summary, it was shown that facilitatory (or extrapolatory) neural activation can effectively deal with delays inside and outside of the system.

# CHAPTER VII

# DISCUSSION

In this chapter, I will describe the contribution of this dissertation, several related works, issues arising from the previous chapters, and future work based on my work presented in this dissertation.

## VII.1 Contributions

The main contributions of this dissertation were that neural delay was recognized as a problem and a biologically plausible neural mechanism was proposed, on which the motion extrapolation model can be grounded. Through the developed model and experiments, I showed a link between (1) psychophysical phenomena in various flash-lag effects (FLE), (2) neurophysiological mechanisms of facilitating synapses and spike-timing-dependent plasticity (STDP), (3) and theoretical issues associated with neural delays and extrapolative compensation.

I proposed a neurophysiologically based facilitatory activation model (FAM) and showed that extrapolatory dynamics can help compensate for neural transmission delay, and various FLEs may arise due to such a mechanism. In FAM, the output of the neurons is represented as a real value that corresponds to the firing rate of each neuron. As shown in the FAM equation (Eq. 3.3), the firing rate is determined not only by the current input but also by the previous history of firing. Thus, instantaneous activation level is extrapolated (either increased or decreased) proportional to the rate of change in activation level. This simple formula reflected the facilitating neural activity inspired by facilitating synaptic dynamics.

I also showed that the lack of FLE at motion reversal (or termination) points can be interpreted as being due to inhibitory backward masking. The motion reversal and the visual luminance experiments showed that facilitatory neural activity helps align the internal state of the nervous system with the present rather than with the past environmental state.

Another important contribution of this paper was to draw attention to the relationship between facilitating synapses (and STDP) and delay compensation. STDP and facilitating synapses are well-known neurophysiological processes, and there are several theories on the possible role of these mechanisms. The view presented in this dissertation provides new insights on an alternative role of facilitating synapses—that of extrapolatory delay compensation. However, it should be noted that the views above may be all complementary: As Hawkins argued, memory may be explicitly linked to predictive functions [75].

## VII.2 Related works and issues

There are several related works and some open issues arising from the previous chapters. I will discuss general issues of neural delay and other possible compensation methods, flash-lag effect in view of postdiction, Kalman filtering and postdiction for estimation of motion trajectory, STDP and its role in direction selectivity, and facilitatory activity as a possible neural basis of internal models.

## 1 Timing and delay in the neural system

Neural transmission delay is wide-spread in biological organisms [76]. Researchers have tried to develop mathematical models and apply them in engineering control and robotic systems (for reviews see [77, 78]). For example, decay and delay have been used as learnable parameters in biologically motivated artificial neural networks, and to represent temporal information in neural networks [79, 80, 81, 82, 83, 84, 85]. However, in these works, the focus was more on utilizing delay for a particular functional purpose such as sound localization [82] or visual analogies [81], rather than recognizing neural transmission *delay as a problem to be solved* in itself.

There are other forms of delay compensation mechanism such as myelination of axons, increase in the thickness of axons and dendrites, and changing the type of ion channels [35, 86]. By myelination the neurons can speed up the rate of information transfer. However, myelination in the brain occurs slowly over biological development, and there is a clear limit in the amount of compensation these processes can bring about. A similar argument is true for change in morphology. Thus, facilitating neural dynamics may still be needed. Furthermore, facilitating neural dynamics is observed during a very short time period (within several hundred millisecond), thus selective, dynamic delay compensation (only for fast-changing stimulus) can be achieved through facilitating neural activities.

## 2 Flash-lag effect and postdiction

My approach to interpreting the flash-lag effect was closer to bottom-up processing framework (i.e., forward processing), in which the underlying neural processes for visual perception is driven by stimulus features. However, it is known that the visual

perception is done not only by bottom-up processing but also by top-down processing [87, 88]. In top-down processing, high level knowledge influences the on-going neural processing and determines the final perception. Eagleman, Rao, and Sejnowski's approach [5, 40], postdiction, can be thought of as top-down processing. Their main idea is that visual perception is not just feedforward: Current visual information can be corrected by future information and the result of integration determine the final perception. It would be interesting to extend low-level neuronal circuits to include high level brain influences. A first step in this direction was to include inhibitory synaptic transmission to correct overshoot of spikes in termination of luminance change (Sec. IV.3).

Flash-Lag Effect is actually a much more complicated perceptual phenomenon and a single hypothesis cannot explain all the rich phenomena found in FLE. Krekelberg and Lappe [41] argued that motion extrapolation is unlikely because it cannot explain the reduced effect where the luminance of moving bar is decreased. They criticized that, according to motion extrapolation, the effect should increase in order to compensate for the increased neural latency (the neural signal for low luminance takes more time to be delivered). However, the effect decreases as the luminance of the moving object decreases, in contradiction to the motion extrapolation theory. These phenomena can be explained by the facilitatory activation model: Low luminance generates low frequency firing, which may not supply sufficient firing frequency to invoke facilitating synaptic process, thus no extrapolative output spikes would be generated in the postsynaptic neuron. As discussed in Sec. V.3, the sensitivity of facilitating activity to spike frequency may play a role in this case.

### 3 STDP and direction selectivity

Existing theories on the role of spike-timing-dependent plasticity (STDP) are varied. For example, STDP is supposed to help reduce spike train variability [89]. It was also argued that STDP may be involved in topology-preserving mapping [90]. Others suggested STDP as a neural mechanism for cortical orientation tuning [91]. One perspective closest to that in this dissertation is that of Rao and Sejnowski [92]: They argued that STDP may implement a predictive function, where the next event in an input sequence is predicted. However, they did not relate this predictive ability to the idea of delay compensation. From my perspective, these predictive mechanisms are actually predicting the present, not the future.

Also, my work further combined facilitating synapses with STDP. In the cross-neuronal facilitation model, STDP turned out to be necessary to set up the directionality. Repeatedly presenting the input (e.g., a rotating bar in orientation FLE) has led neighboring neurons to fire together within a small time interval. With such a repeated firing pattern, STDP systematically updated the synaptic weights. For those connections pointing toward the direction of input rotation, the weight increased and for the opposite direction, the weight decreased.

A biological evidence for direction selectivity can be found in the primary visual cortex [6]. Fig. 53*a* illustrates the columnar organization of orientation selectivity in the monkey's striate cortex. Also, as shown in Fig. 53*b*, there is a pinwheel where the orientation preference changes by 180$^{o}$ along a closed path around the center. (Notice that the bilaterally connected multi-neuron networks developed in Sec. V.1 matches the pinwheel structure.) As shown in Chap. V, STDP can be a potential neural mechanism to set up such a directional selectivity. Through direction selectivity set up by STDP, cross-neuron facilitation can carry out extrapolation in the direction

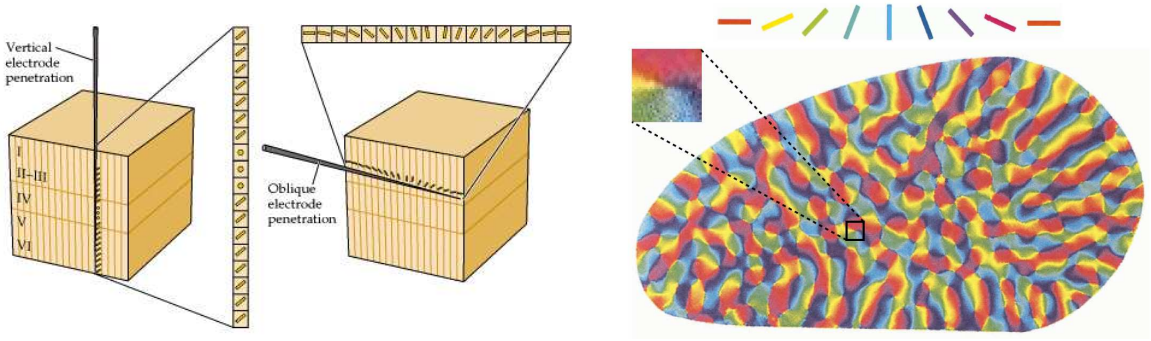


(*a*) Columnized structure in V1 (*a*) Orientation map

Fig. 53. **Orientation Map in V1.** (*a*) Columnar organization of orientation selectivity in the monkey striate cortex is illustrated. With vertical electrode penetration, neurons with the same preferred orientations are encountered. Oblique penetration will show a systematic change in orientation across the cortical surface. (Adapted from [10].) (*b*) Orientation selectivity and their horizontal connections in tree shrew striate cortex is shown. The different colors represent patches that have different orientation preference. The inset shows an orientation pinwheel, where the orientation preference changes by 180° along a closed path around the center. (Adapted from [6].)

of rotation, thus giving rise to orientation FLE. Recent research on STDP's role in shaping neuronal selectivity [93, 91] also support this idea.

## 4 Decay and facilitation in a single neuron

As shown in the pole-balancing experiments, the facilitating activity network (FAN) significantly improved the ability of the cart controller by compensating for transmission delay within the controller system. Also, such a facilitatory dynamics allowed for faster learning. The failing performance of the decaying activity network (DAN) is in itself an interesting phenomenon. Decay can be seen as a form of memory, where traces of activity from the past linger on in the present activity, thus it may be ex-

pected to be beneficial. However, it turns out that such a form of memory does not contribute to delay compensation and actually make things even worse. Thus, extrapolation, anticipation, or prediction, which are characteristics of facilitatory dynamics, may be more important than a generic form of memory in delay compensation.

In principle, extrapolation can be done at a different level such as at a local circuit level or at a large-scale network level. However, my view is that to compensate for delay existing in various levels in the central nervous system and to achieve faster extrapolation, the compensation mechanism needs to be implemented at the single-neuron level [94].

As it was mentioned earlier, the facilitation rate may be an adaptable property of neurons, thus the rate may be adjusted to accommodate different delay durations. Furthermore, and more importantly, I expect that the organism with facilitating neural dynamics can effectively cope with increasing delay in its nervous system due to growth during development by adjusting the facilitation rate. The experiment with increased delay (Sec. VI.3) showed this could be the case. Also, the same mechanism was able to deal with uncertainty in the external environment as shown in the input blank-out experiment (Sec. VI.3), suggesting an important link between delay compensation and prediction/planning.

## 5 Kalman filters and postdiction

To estimate the location of a moving object, ideas based on Kalman filtering has been proposed by Rao et.al [5]. Kalman filters provide a general solution for linear filtering problem by estimating the hidden state $x(i)$ using a sequence of observations $z(1), z(2), ...z(n)$. It is called filtering if $i = n$, prediction if $i > n$, and smoothing if $1 \leq i < n$.

Some researchers assume that internal forward models exist in various levels in the nervous system and produce predictive behaviors which are adjusted by sensory error correction mechanism, similar to that of Kalman filters [95, 9]. These methods may be insufficient when the forward model is unknown. In most of the cases, we do not know the exact forward model which is needed for prediction, i.e., $c(t-1)\hat{y}(t-1)$ in Eq. 3.7 (see Sec. III.2).

In addition, Kalman filter assumes that there is no critical sensory delay which can potentially cause severe instability in the control system. Optimal smoothing used in these approaches (even though accurate in terms of estimation) lag behind in time, thus rendering them unsuitable for real-time processing (as shown in Sec. III.2).

On the contrary, facilitatory activation model (FAM) does not need a forward model and instead only uses the memory of previous facilitated activity $A(t-1)$ and current sensory input $X(t)$, which are regulated by the gain parameter $r$. FAM can provide such a predictive function by extrapolatory neural activity, which is possible through facilitating synapses. The extended *facilitated-smoothing* method (Sec. III.3) uses near future observation $X(t+1)$ to increase perceptual accuracy, thus demonstrating that the FAM is more reasonable for real time processing compared to optimal smoothing. (Note that optimal smoothing needs to observe the complete input data sequence.)

## 6 Smoothing in perception vs. motor response

Kerzel and Gegenfurtner [21] investigated a case where subjects localized the final position of a moving stimulus. Visual perception of the final target position was accurate, but reaching movements were directed toward future positions. Through this experiment they argued that neuronal latencies are not compensated for at early

stages in visual processing. Rather, compensation occurs at a later stage when retinotopic information is transformed into egocentric space used for motor responses. The more important point here is that extrapolation is needed more in motor neurons. This is quite sensible because the motor response should take into account the delay in sensory signal before generating the output action, but that may not be the case in the purely perceptual neurons. The postdictive perception model argues that we can only perceive the past (what happened before) by integrating some period of neural activity which is quite reasonable when only perception is considered. The theory also is consistent with Kerzel and Gegenfurtner's findings. Facilitating neural activity may have initially evolved because of the need to handle motion rather than to provide veridical perception.

## 7 Facilitation and internal forward model

Another question at this point relates to the extrapolatory capacity of facilitating neural dynamics. Extrapolation is usually related to prediction of the future from information from the present. However, in the nervous system, due to the neural transmission delay, extrapolation may have to be used to predict the present based on past information. Prediction or anticipation of future events is an important characteristic needed in mobile, autonomous agents [96, 97]. Also, as Llinás observed in [98] (p. 3), such projection into the future may be a fundamental property of "mindness".

One prominent hypothesis regarding prediction is the internal forward model [78, 99, 9, 14]: Forward models at various levels of processing in the nervous system are supposed to produce predictive behaviors. Internal forward models were suggested from an engineering point of view, where the sensory motor system is re-

garded as a well-structured control system that can generate accurate dynamic behaviors. Although theoretical mechanisms similar to Kalman filter methods were suggested [95, 9, 100], the precise neural basis for the forward models have not been fully investigated.

Recently, several brain imaging studies provided supporting evidence for the existence of internal forward models in the nervous system [101, 102, 103, 104]. However, these results did not suggest what could be the main neuron-level mechanism. Thus, it may be worthwhile investigating how such abilities in autonomous agents may be related to facilitatory dynamics at the cellular level.

General discussion of the role of prediction in brain function can be found in [75] and [98]. However, they did not relate this predictive ability to the idea of delay compensation. The input blank-out experiment conducted in Sec. VI.3 is a first step in this direction, where delay compensation mechanisms evolved to deal with internal delay can be slightly modified to include a predictive ability, to handle environmental delay and uncertainty.

## VII.3 Future work

I expect the work presented here to be extended to computational, psychological, neurophysiological, and clinical research. I plan to continue this line of research in the following directions.

## 1 Neural delay and mental disorders

There is an important implication of this research on detecting and treating neurological disorders such as autism and dyslexia. For example, autistic children have problem detecting coherent motion [105], and have problem in processing moderately rapid motion [106, 107]. People with dyslexia also have difficulty in processing rapidly changing stimulus [108]. These results suggest that people with autism/dyslexia may have problem in motion processing. One reason for the malfunction may be related to delay compensation mechanisms. If this is the case, these deficits can be tested with various forms of FLE: People with autism or dyslexia may not have flash-lag illusions. We can interpret the lack of FLE as the lack of delay compensation in their nervous system.

To test this idea, luminance FLE would be a better paradigm than the other FLEs because it involves a stationary stimulus with a change in its property. Otherwise, alternative explanations can be given. For example, the deficit in perceiving rapidly changing stimulus can be because of the deficit in motion perception itself, not because of problems with delay compensation.

For treatment of these disorders, first, the neurophysiological process that underlies the disorder needs to be identified. My model suggests that the modulation mechanisms for synaptic efficacy in facilitating synapses may be one major substrate of autism/dyslexia. (For a review and a comprehensive neural model of autism, see [109].) The extrapolation mechanism can be disrupted at least in two ways: (1) a normal extrapolation mechanism is not able to catch up with rapid growth, which results in an abnormal increase in axonal conduction delay; and (2) a malfunction in the extrapolation mechanism itself. One anatomical indication that case (1) above may be true is that, in autism, the brain grows rapidly (especially the white matter which

is made up of axons) [110, 111]. In such a case, the delay caused by a sudden growth in spatial dimension may be more than the delay compensation mechanisms can cope with, thus leading to failure. As for case (2), to my knowledge, there has been no systematic experimental investigation under this perspective. Further physiological tests can assess whether case (2) can indeed be the case. Also see Sec. VII.3.4, for possible involvement of $Ca^{2+}$ processes.

## 2 Extension of FAM for other visual illusions

I expect that my approach can be extended to explain other extrapolatory phenomena such as flash-lag effect in color, pattern entropy, or localization. Moreover, I expect that the extended crossneuronal facilitation structure may be able to account for other visual illusions such as the Fröhlich effect [36] and Hess effect [112]. Fröhlich effect refers to a phenomenon where the initial segment of an object's trajectory is perceived to be invisible, when the moving object appears abruptly. This phenomenon can be partly explained by the spike-based FAM experiment in Sec. IV.3. Notice that facilitating synapses generated the first output spike train with a certain amount of delay (see Fig. 20, 21, bottom row). In addition to the neural transmission delay from peripheral neurons to visual cortex neurons, the postsynaptic neuron needed some boosting time to respond to the input spike train. Such an initial build-up time can explain the invisibility.

Hess effect, another interesting visual illusion, occurs when a high-contrast moving object is perceived to lead a low-contrast one where they actually move aligned. If such moving objects are processed in the cross-neuronal facilitation model, facilitation will propagate rapidly for the object with high luminance. Because facilitating activity can be turned on by high frequency of spikes (i.e., 50 Hz) [31], the stimulus

with higher contrast will provoke facilitation faster than the one with low contrast. With fast cross-neuronal facilitation, the moving object with high contrast can be perceived ahead of the object with lower contrast.

## 3 Prediction mechanism for autonomous agents

Making predictions is the essence of intelligence. Prediction is based on stored sequences of internal or environmental states, auto-associative recall, and invariant representations [75]. In nature, the environment presents itself differently every moment and living organisms constantly receive continuously changing input stimuli into their nervous system. To achieve accurate prediction, organisms must combine the invariant structure in the environment with the most recent details. I have begun the first step in this direction with the facilitated-smoothing model as discussed in Sec. III.3, where overshoot at the motion reversal point was corrected by smoothing with observation from one further step in the future. Also, backward masking grounded this model neurophysiologically, as tested with the luminance termination experiment (Sec. IV.2). If this extrapolatory neural dynamics is generalized further, the central nervous system can develop a prediction mechanism.

## 4 Neuroanatomical and neurophysiological verification

Another interesting future direction would be to verify whether neurons with facilitating synapses are more often found in places where delay compensation is needed more, for example, at the end of long, slow axons, or where precise real-time information is needed. Also, it would be worthwhile to verify whether the variable term $C$

defined in Eq. 4.2 is plausible in terms of neurophysiology. (Note that I modeled the synaptic efficacy increase factor $C$ as a variable instead of a constant.) It is known that facilitation is driven by elevated $Ca^{2+}$ levels in presynaptic terminals. Recently, a neurophysiological mechanism (e.g., involving $Ca^{2+}$ chelator BAPTA, which serves as a dynamic calcium buffer) has been found [113], which may be responsible for the variation in $C$.

# CHAPTER VIII

## CONCLUSION

The goal of this thesis was to understand the neural mechanism of delay compensation through biologically plausible computational modeling. Flash-lag effect (FLE) was suggested as a psychophysical evidence of extrapolation in the brain. Through extrapolation, neural delay can be compensated for, thus increasing the accuracy in real time perception.

The next question was regarding the neural basis of extrapolation. I showed that facilitatory (extrapolatory) dynamics found in facilitating synapses can be the neural basis for extrapolation. To test this idea, I developed a computational model called facilitatory activation model (FAM) and experimented with various FLE tasks.

First, using the computational FAM, I showed that facilitation with smoothing can achieve accurate perception for fast moving object in spite of neural delay. In the motion reversal experiment, the facilitated-smoothing model successfully explained the visual illusions in terms of extrapolative perception and smoothing (overshoot during continuous motion and the lack of overshoot at motion reversal).

Second, through spike-based FAM, the computational FAM was firmly grounded on neurophysiology. I developed a spike-based facilitation model by modifying the facilitating synapse model. With this, extrapolative neural activity in both increasing and decreasing direction can be implemented. Experiments with luminance FLE showed that facilitating postsynaptic activity can generate more spikes (or less spikes) than those of the presynaptic neuron under increasing (or decreasing) firing rate conditions. It was also shown that motion offset signal conveyed by inhibitory synaptic transmission can successfully eliminate overshoot at the termination of luminance change. In this way, the backward masking, a potential neural mechanism for smooth-

ing, was implemented in the spike-based facilitation model.

Third, going beyond the single-neuron-level facilitation, I showed that facilitating synapses, if combined with spike-timing-dependent plasticity (STDP), can allow extrapolation to be carried out in a multi-neuron environment. Experiments with bilaterally connected multi-neuron model demonstrated that repeated firing pattern within a small time interval can invoke STDP. Through STDP's directional selectivity, facilitation could go across the neurons in a specific direction, thus giving rise to orientation FLE.

An interesting question was, whether the FAM, a biologically inspired delay compensation model, can also help to overcome the problem of delay in engineering applications. To test this idea, I developed a facilitating activity network (FAN) model, a recurrent neural network including facilitatory neural dynamics at a single-neuron level. FAN was tested with a modified 2D pole-balancing problem under various input delay conditions, and showed that facilitatory activation can significantly improve the ability of controllers to compensate for delay within the controller system. Test with increasing delay and input blank-out experiments also showed that the adaptability of facilitating dynamics can help overcome increasing delay and external uncertainty.

In sum, I showed that facilitating synapses can play an important role in compensating for neural delays. Facilitatory neural activity can effectively compensate for neural delays, and as a result it may cause extrapolation in perception, as expressed in the visual flash-lag effect. Through extrapolating the past to the present, an organism with internal delay can successfully cope with the dynamic environment in real-time, rather than living in the past.

In the future, the suggested models (i.e. FAM, spike-based facilitation model, and cross-neuronal facilitation model) are expected to play a crucial role in understanding neural mechanisms in visual perception, by providing a computational framework

where ideas from psychological, neurophysiological, and clinical research can be integrated. The framework can also lead to application is the early detection and treatment of mental disorders such as autism and dyslexia.

## REFERENCES

[1] S. J. Thorpe and M. Fabre-Thorpe, "Seeking categories in the brain," *Science*, vol. 291, pp. 260–263, 2001.

[2] M. T. Schmolesky, Y. Wang, D. P. Hanes, K. G. Thomas, S. Leutgeb, J. D. Schall, and A. D. Leventhal, "Signal timing across the macaque visual system," *The Journal of Neurophysiology*, vol. 79, pp. 3272–3278, 1998.

[3] D. Whitney and I. Murakami, "Latency difference, not spatial extrapolation," *Nature Neuroscience*, vol. 1, pp. 656–657, 1998.

[4] H. Markram, Y. Wang, and M. Tsodyks, "Differential signaling via the same axon of neocortical pyramidal neurons," in *Proceedings of the National Academy of Sciences, USA*, 1998, vol. 95.

[5] R. P. Rao, D. M. Eagleman, and T. J. Sejnowski, "Optimal smoothing in visual motion perception," *Neural Computation*, vol. 13, pp. 1243–1253, 2001.

[6] W. H. Bosking, Y. Zhang, B. Schofield, and D. Fitzpatrick, "Orientation selectivity and the arrangement of horizontal connections in tree shrew striate cortex," *The Journal of Neuroscience*, vol. 17, pp. 2112–2127, 1997.

[7] Risto Miikkulainen, James A. Bednar, Yoonsuck Choe, and Joseph Sirosh, *Computational Maps in the Visual Cortex*, Springer, Berlin, 2005.

[8] F. Gomez, "Robust non-linear control through neuroevolution," Ph.D. dissertation, Department of Computer Science, The University of Texas at Austin, Austin, TX, 2003, Technical Report AI03-303.

[9] B. Mehta and S. Schaal, "Forward models in visuomotor control," *Journal of Neurophysiology*, vol. 88, pp. 942–953, 2002.

[10] D. Purves, G. J. Augustine, D. Fitzpatrick, L. C. Katz, A-S. Lamantia, and J. O. Mcnamara, *Neuroscience*, Sinauer Associates, Inc., Sunderland, 2nd edition, 1997.

[11] L. G. Nowak and J. Bullier, "The timing of information transfer in the visual system," *Cerebral Cortex*, vol. 12, pp. 205–239, 1997.

[12] D. M. MacKay, "Perceptual stability of a stroboscopically lit visual field coontaining self-luminous objects," *Nature*, vol. 181, pp. 507–508, 1958.

[13] R. Nijhawan, "Motion extrapolation in catching," *Nature*, vol. 370, pp. 256–257, 1994.

[14] R. Nijhawan and K. Kirschfeld, "Analogous mechanisms compensate for neural delays in the sensory and motor pathways: Evidence from motor flash-lag," *Current Biology*, vol. 13, pp. 749–753, 2003.

[15] D. Alais and D. Burr, "The flash-lag effect occurs in audition and cross-modally," *Current Biology*, vol. 13, pp. 59–63, 2003.

[16] B. Sheth, R. Nijhawan, and S. Shimojo, "Changing objects lead breifly flashed ones," *Nature Neuroscience*, vol. 3, pp. 489–495, 2000.

[17] B. Krekelberg, "Sound and vision," *Trends in Cognitive Sciences*, vol. 7, pp. 277–279, 2003.

[18] R. Nijhawan, "Visual decomposition of colour through motion extrapolation," *Nature*, vol. 386, pp. 66–69, 1997.

[19] Wolfram Erlhagen, "The role of action plans and other cognitive factors in motion extrapolation: A modelling study," *Visual Cognition*, vol. 11, pp. 315–340, 2004.

[20] J. Müsseler, S. Storck, and D. Kerzel, "Comparing mislocalizations with moving stimuli: the fröhlich effect, the flash-lag, and representational momentum," *Visual Cognition*, vol. 9, pp. 120–138, 2002.

[21] D. Kerzel and K. R. Gegenfurtner, "Neuronal processing delays are compensated in the sensorimotor branch of the visual system," *Current Biology*, vol. 13, pp. 1975–1978, 2003.

[22] Y-X. Fu, Y. Shen, and Y. Dan, "Motion-induced perceptual extrapolation of blurred visual targets," *The Journal of Neuroscience*, vol. 21, 2001.

[23] R. Nijhawan, K. Watanabe, B. Khurana, and S. Shimojo, "Compensation of neural delays in visual-motor behaviour: No evidence for shorter afferent delays for visual motion," *Visual Cognition*, vol. 11, pp. 275–289, 2004.

[24] H. Lim and Y. Choe, "Facilitatory neural activity compensating for neural delays as a potential cause of the flash-lag effect," in *Proceedings of the International Joint Conference on Neural Networks (IJCNN)*. 2005, pp. 268–273, IEEE.

[25] J. L. Elman, "Distributed representations, simple recurrent networks, and grammatical structure," *Machine Learning*, vol. 7, pp. 195–225, 1991.

[26] J. L. Elman, "Finding structure in time," *Cognitive Science*, vol. 14, pp. 179–211, 1990.

[27] R. S. Zucker, "Short-term synaptic plasticity," *Annual Review of Neuroscience*, vol. 12, pp. 13–31, 1989.

[28] S. A. Fisher, T. M. Fisher, and T. J. Carew, "Multiple overlapping processes underlying short-term synaptic enhancement," *Trends in Neurosciences*, vol. 20, pp. 170–177, 1997.

[29] G. Fuhrmann, I. Segev, H. Markram, and M. Tsodyks, "Coding of temporal information by activity-dependent synapses," *Journal of Neurophysiology*, vol. 87, pp. 140–148, 2002.

[30] D. V. Buonomano, "Decoding temporal information: A model based on short-term synaptic plasticity," *The Journal of Neuroscience*, vol. 20, pp. 1129–1141, 2000.

[31] E. S. Fortune and G. J. Rose, "Short-term synaptic plasticity as a temporal filter," *Trends in Neurosciences*, vol. 24, pp. 381–385, 2001.

[32] T. Natschläger, W. Maass, and A. Zador, "Efficient temporal processing with biologically realistic dynamic synapses," *Network: Computation in Neural Systems*, vol. 12, pp. 75–87, 2001.

[33] G.-Q. Bi and M.-M. Poo, "Activity-induced synaptic modifications in hippocampal culture: Dependence on spike timing, synaptic strength and cell type," *Journal of Neuroscience*, vol. 18, pp. 10464–10472, 1998.

[34] Sen Song, Kenneth D. Miller, and L. F. Abbott, "Competitive hebbian learning through spike-timing-dependent synaptic plasticity," *Nature Neuroscience*, vol.

3, pp. 919–926, 2000.

[35] C. W. Eurich, K. Pawelzik, U. Ernst, A. Thiel, J. D. Cowan, and J. G. Milton, "Delay adaptation in the nervous system," *Neurocomputing*, vol. 32-33, pp. 741–748, 2000.

[36] F. W. Fröhlich, "Über die messung der empfindungszeit," *Zeitschrift für Sinnesphysiologie*, vol. 54, pp. 57–78, 1923.

[37] D. H. Arnold, S. Durant, and A. Johnston, "Latency differences and the flash-lag effect," *Vision Research*, vol. 43, pp. 1829–1835, 2003.

[38] M. V. Baldo, "Extrapolation or attention shift?," *Nature*, vol. 378, pp. 565–566, 1995.

[39] B. Krekelberg and M. Lappe, "A model of the perceived relative positions of moving objects based upon a slow averaging process," *Vision Research*, vol. 40, pp. 201–215, 2000.

[40] D. Eagleman and T. J. Sejnowski, "Motion integration and postdiction in visual awareness," *Science*, vol. 287, pp. 2036–2038, 2000.

[41] B. Krekelberg and M. Lappe, "Neural latencies and the position of moving objects," *Trends Neurosciences*, vol. 24, pp. 335–339, 2001.

[42] J. Liaw and T. W. Berger, "Dynamic synapse: Harnessing the computing power of synaptic dynamics," *Neurocomputing*, vol. 26-27, pp. 199–206, 1999.

[43] H. Markram, "Elementary principles of nonlinear synaptic transmission," in *Computational Models for Neuroscience: Human Cortical Information Processing*, Robert Hecht-Nielsen and Thomas McKenna, Eds., chapter 5, pp. 125–169. Springer, London, UK, 2002.

[44] M. Tsodyks, K. Pawelzik, and H. Markram, "Neural networks with dynamic synapses," *Neural Computation*, vol. 10, pp. 821–835, 1998.

[45] G. Silberberg, C. Wu, and H. Markram, "Synaptic dynamics control the timing of neuronal excitation in the activated neocortical microcircuit," *The Journal of Physiology*, vol. 556, pp. 19–27, 2004.

[46] W. H. Press, B. P. Flannery, S. A. Teukolsky, and W. T. Vetterling, *Numerical Recipes in FORTRAN: The Art of Scientific Computing*, Cambridge University Press, Cambridge, UK, 2nd edition, 1992.

[47] A. E. Bryson and Y. Ho, *Applied Optimal Control*, Blaisdell Publishing Company, Waltham, MA, 1975.

[48] R. E. Kalman, "A new approach to linear filtering and prediction theory," *Journal of Basic Engineering*, vol. 82, pp. 35–45, 1960.

[49] R. Nijhawan, "Neural delays, visual motion and the flash-lag effect," *Trends in Cognitive Sciences*, vol. 6, pp. 387–393, 2002.

[50] W. Maass and H. Markram, "Synapses as dynamic memory buffers," *Neural Networks*, vol. 15, pp. 423–431, 2002.

[51] R. Legenstein, C. Naeger, and W. Maass, "What can a neuron learn with spike-timing-dependent plasticity?," *Neural Computation*, vol. 17, pp. 2337–2382, 2005.

[52] F. Gabbini and C. Koch, "Principles of spike train analysis," in *Methods in Neural Modeling*, C. Koch and I. Segev, Eds., pp. 313–360. MIT Press, Cambridge, MA, 1999.

[53] S. L. Macknik and M. S. Livingstone, "Neuronal correlates of visibility and invisibility in the primate visual system," *Nature Neuroscience*, vol. 1, pp. 144–149, 1998.

[54] M. Tanaka and S. G. Lisberger, "Role of arcuate frontal cortex of monkeys in smooth pursuit eye movements. i. basic response properties to retinal image motion and position," *Journal of Neurophysiology*, vol. 87, pp. 2684–2699, 2002.

[55] S. Grossberg and E. Mingolla, "Neural dynamics of form perception: Boundary completion, illusory figures, and neon color spreading," *Psychological Review*, vol. 92, pp. 173–211, 1985.

[56] S. Grossberg and E. Mingolla, "Neural dynamics of perceptual grouping: Textures, boundaries, and emergent segmentations," *Perception and Psychophysics*, vol. 38, pp. 141–171, 1985.

[57] G. Francis, "Cortical dynamics of lateral inhibition: Metacontrast masking," *Psychological Review*, vol. 104, pp. 572–594, 1997.

[58] G. Francis, "Developing a new quantitative account of backward masking," *Cognitive Psychology*, vol. 46, pp. 198–226, 2003.

[59] B. G. Breitmeyer and H. Ogmen, "Recent models and findings in visual backward masking: A comparison, review, and update," *Perception and Psychophysics*, vol. 62, pp. 1572–1595, 2000.

[60] M. Kinoshita and H. Komatsu, "Neural representation of the luminance and brightness of a uniform surface in the macaque primary visual cortex," *Journal of Neurophysiology*, vol. 86, pp. 2559–2570, 2001.

[61] A. F. Rossi, C. D. Rittenhouse, and M. A. Paradiso, "The representation of brightness in primary visual cortex," *Science*, vol. 273, pp. 1104–1107, 1996.

[62] B. Berninger and G.-Q. Bi, "Synaptic modifiction in neural circuits: a timely action," *BioEssays*, vol. 24, pp. 212–222, 2002.

[63] G. Purushothaman, S. S. Patel, H. E. Bedell, and H. Öğmen, "Moving ahead through differential visual latency," *Nature*, vol. 396, pp. 424, 1998.

[64] C. W. Anderson, "Learning to control an inverted pendelum using neural networks," *IEEE Control Systems Magazine*, vol. 9, pp. 31–37, 1989.

[65] K. O. Stanley and R. Miikkulainen, "Efficient reinforcement learning through evolving neural network topologies," in *Proceedings Genetic and Evolutionary Computation Conference (GECCO)*. 2002, pp. 1757–1762, IEEE.

[66] F. Gomez and R. Miikkulainen, "2-D pole balancing with recurrent evolutionary networks," in *Proceeding of the International Conference on Artificial Neural Networks (ICANN)*. 1998, pp. 758–763, Elsevier.

[67] F. Gomez and R. Miikkulainen, "Incremental evolution of complex general behavior," *Adaptive Behavior*, vol. 5, pp. 317–342, 1997.

[68] F. Gomez and R. Miikkulainen, "Active guidance for a finless rocket through neuroevolution," in *Proceedings of the Genetic and Evolutionary Computation Conference (GECCO)*, Chicago, IL, 2003, pp. 2084–2095, Springer.

[69] Richard S. Sutton, "Learning to predict by the methods of temporal differences," *Machine Learning*, vol. 3, pp. 9–44, 1988.

[70] S. Schaal, "Learning from demonstration," in *The Proceedings of the Advances in Neural Information Processing Systems (NIPS 1997)*, M. C. Mozer,

M. Jordan, and T. Petsche, Eds., Cambridge, MA, 1997, pp. 1040–1046, MIT Press.

[71] K. Doya, "Reinforcement learning in continuous time and space," *Neural Computation*, vol. 12, pp. 219–245, 2000.

[72] J. Si and Y.-T. Wang, "On-line learning control by association and reinforcement," *IEEE Transactions on Neural Networks*, vol. 12, pp. 264–276, 2001.

[73] X. Yao, "Evolving articifial neural networks," *Proceedings of the IEEE*, vol. 87, pp. 1423–1447, 1999.

[74] D. E. Moriarty, "Efficient reinforcement learning through symbiotic evolution," *Machine Learning*, vol. 22, pp. 11–32, 1997.

[75] J. Hawkins and S. Blakeslee, *On Intelligence*, Times Books, Hency Holt and Company, New York, 1st edition edition, 2004.

[76] A. Pellionisz and R. Llinas, "Brain modeling by tensor network theory and computer simulation, the cerebellum: Distributed processor for predictive coordination," *Neuroscience*, vol. 4, pp. 328–348, 1979.

[77] A. Kataria, H. Özbay, and H. Hemani, "Controller design for natural and robotic systems with transmission delays," *Journal of Robotic Systems*, vol. 19, pp. 231–244, 2002.

[78] D. M. Wolpert and J. R. Flanagan, "Motor prediction.," *Current Biology*, vol. 11(18), pp. R729–R732, 2001.

[79] C. W. Eurich, K. Pawelzik, U. Ernst, J. D. Cowan, and J. G. Milton, "Dynamics of self-organized delay adaptation," *Physical Review Letters*, vol. 82, pp. 1594–1597, 1999.

[80] A. P. Shon and R. P. Rao, "Learning temporal patterns by redistribution of synaptic efficacy," *Neurocomputing*, vol. 52-54, pp. 13–18, 2003.

[81] Y. Choe, "The role of temporal parameters in a thalamocortical model of analogy," *IEEE Transactions on Neural Networks*, vol. 15, pp. 1071–1082, 2004.

[82] W. Gerstner, "Hebbian learning of pulse timing in the barn owl auditory system," in *Pulsed Neural Networks*, W. Maass and C. M. Bishop, Eds., chapter 14, pp. 353–377. MIT Press, 1998.

[83] D. Wang, "Temporal pattern processing," in *The Handbook of Brain Theory and Neural Networks (2nd edition)*, M. A. Arbib, Ed., pp. 1163–1166. MIT Press, Cambridge, MA, 2003.

[84] S. George, A. Dibazar, V. Desai, and T. W. Berger, "Using dynamic synapse based neural networks with wavelet preprocessing for speech applications," in *Proceedings of the International Joint Conference on Neural Networks (IJCNN)*. 2003, pp. 666–669, IEEE.

[85] R. Derakhshani, "Biologically inspired evolutionary temporal neural circuits," in *Proceedings of the International Joint Conference on Neural Networks (IJCNN)*. 2002, pp. 1357–1361, IEEE.

[86] M. Salami, C. Itami, T. Tsumoto, and F. Kimura, "Change of conduction velocity by regional myelination yields constant latency irrespective of distance between thalamus and cortex," in *Proceedings of the National Academy of Sciences, USA*, 2003, vol. 100, pp. 6174–6179.

[87] S. P. Vecera and M. J. Farah, "Is visual image segmentation a bottom-up or an interactive process?," *Perception&psychophysics*, vol. 59, pp. 1280–1296, 1997.

[88] A. Delorme, G. A. Rousselet, J.-M. Marc, and M. Fabre-Thorpe, "Interaction of top-down and bottom-up processing in the fast visual analysis of natural scenes," *Cognitive brain research*, vol. 19, pp. 103–113, 2004.

[89] Sander M. Bohte and Michael C. Mozer, "Reducing spike train variability: A computational theory of spike-timing dependent plasticity," in *Advances in Neural Information Processing Systems 17*, pp. 201–208. MIT Press, Cambridge, MA, 2005.

[90] C. Panchev and S. Wermter, "Hebbian spike-timing dependent self-organization in pulsed neural networks," in *World Congress on Neuroinformatics: Part II, Proceedings*, Frank Rattay, Ed., Vienna, 2001, pp. 378–385, ARGESIM/ASIM-Verlag.

[91] H. Yao, Y. Shen, and Y. Dan, "Intracortical mechanism of stimulus-timing-dependent plasticity in visual cortical orientation tuning," in *Proceedings of the National Academy of Sciences, USA*, 2004, vol. 101, pp. 5081–5086.

[92] R. P. Rao and T. J. Sejnowski, "Predictive sequence learning in recurrent neocortical circuits," in *Advances in Neural Information Processing Systems 12*, Todd K. Leen, Thomas G. Dietterich, and Volker Tresp, Eds., Cambridge, MA, 2000, pp. 164–170, MIT Press.

[93] R. Guyonneau, R. VanRullen, and S. J. Thorpe, "Neurons tune to the earliest spike through stdp," *Neural Computation*, vol. 17, pp. 859–879, 2005.

[94] H. Lim and Y. Choe, "Compensating for neural transmission delays using

extrapolatory neural activation in evolutionary neural networks," *Neural Information Processing–Letters and Reviews*, 2006, In press.

[95] D. M. Wolpert, "Computational approaches to motor control," *Trends in Cognitive Sciences*, vol. 1, pp. 209–216, 1997.

[96] Ralf Möller, "Perception through anticipation: An approach to behavior-based perception," in *Proceedings of New Trends in Cognitive Science*, 1997, pp. 184–190.

[97] H.-M. Gross, A. Heinze, T. Seiler, and V. Stephan, "Generative character of perception: A neural architecture for sensorimotor anticipation," *Neural Networks*, vol. 12, pp. 1101–1129, 1999.

[98] Rodolfo R. Llinás, *I of the Vortex*, MIT Press, Cambridge, MA, 2001.

[99] R. C. Miall and D. M. Wolpert, "Forward models for physiological motor control," *Neural Networks*, vol. 9, pp. 1265–1285, 1996.

[100] E. Oztopa, D. Wolpert, and M. Kawato, "Mental state inference using visual control parameters," *Cognitive Brain Research*, vol. 22, pp. 129–151, 2005.

[101] S-J. Blakemore, D. M. Wolpert, and C. D. Frith, "Central cancellation of self-produced tickle sensation," *Nature Neuroscience*, vol. 1, pp. 635–640, 1998.

[102] M. Desmurget and S. Grafton, "Forward modeling allows feedback control for fast reaching movements," *Trends in Cognitive Sciences*, vol. 4, pp. 423–431, 2000.

[103] M. R. Mehta, "Neural dynamics of predictive coding," *The Neuroscientist*, vol. 7, pp. 490–495, 2001.

[104] B. Webb, "Neural mechanisms for prediction: do insects have forward models?," *Trends in Neurosciences*, vol. 27, pp. 278–282, 2004.

[105] E. Milne, J. Swettenham, P. Hansen, R. Campbell, H. Jefferies, and K. Plaisted, "Visual motion coherence thresholds in people with autism," *Journal of Child Psychology and Psychiatry*, vol. 43, pp. 255–263, 2002.

[106] B. Gepner, C. Deruelle, and S. Grynfeltt, "Motion and emotion: A novel approach to the study of face processing by young autistic children," *Journal of Autism and Developmental Disorders*, vol. 31, pp. 37–45, 2001.

[107] B. Gepner, "Rapid visual-motion integration deficit in autism," *Trends in Cognitive Sciences*, vol. 6, pp. 455, 2002.

[108] R. Hari and H. Renvall, "Impaired processing of rapid stimulus sequences in dyslexia," *Trends in Cognitive Sciences*, vol. 5, pp. 525–532, 2001.

[109] S. Grossberg and D. Seidman, "Neural dynamics of autistic behaviors: Cognitive, emotional, and timing substrates," *Psychological Review*, vol. in press, 2006.

[110] E. Courchesne, R. Carper, and N. Akshoomoff, "Evidence of brain overgrowth in the first year of life in autism," *Journal of American Medical Association*, vol. 290, pp. 337–344, 2003.

[111] M. R. Herbert, D. A. Ziegler, N. Makris, P. A. Filipek, T. L. Kemper, J. J. Normandin, H. A. Sanders, D. N. Kennedy, and V. S. Caviness, "Localization of white matter volume increase in autism and developmental language disorder," *Annals of Neurology*, vol. 55, pp. 530–540, 2004.

[112] C. V. Hess, "Untersuchungen über den erregungsvorgang in sehorgan bei kurz und bei länger dauernder reizung," *Pflügers Arch. Gesamte Physiol.*, vol. 101, pp. 226–262, 1904.

[113] A. Rozov, N. Burnashev, B. Sakmann, and E. Neher, "Transmitter release modulation by intracellular $ca^{2+}$ buffers in facilitating and depressing nerve terminals of pyramidal cells in layer 2/3 of the rat neocortex indicates a target cell-specific difference in presynaptic calcium dynamics," *Journal of Physiology*, vol. 531, pp. 807–826, 2001.

# Vita

Heejin Lim was born in Seoul, Korea on December 22, 1967, the daughter of Kwangkil Lim and Haeja Lee. She received her Bachelor of Science degree in Computer Science and Master of Science in Computer Science from Keimyung University in 1991 and 1993 respectively. After graduation, she worked at Electronics and Telecommunication Research Institute in Daejon, Korea. She entered Texas A&M University for her Ph.D. in the fall of 2000.